NBS TECHNICAL NOTE

360

On the Selection of the Intermolecular Potential Function: Application of Statistical Mechanical Theory to Experiment

U.S. DEPARTMENT OF COMMERCE
National Bureau of Standards

THE NATIONAL BUREAU OF STANDARDS

The National Bureau of Standards[1] provides measurement and technical information services essential to the efficiency and effectiveness of the work of the Nation's scientists and engineers. The Bureau serves also as a focal point in the Federal Government for assuring maximum application of the physical and engineering sciences to the advancement of technology in industry and commerce. To accomplish this mission, the Bureau is organized into three institutes covering broad program areas of research and services:

THE INSTITUTE FOR BASIC STANDARDS . . . provides the central basis within the United States for a complete and consistent system of physical measurements, coordinates that system with the measurement systems of other nations, and furnishes essential services leading to accurate and uniform physical measurements throughout the Nation's scientific community, industry, and commerce. This Institute comprises a series of divisions, each serving a classical subject matter area:

—Applied Mathematics—Electricity—Metrology—Mechanics—Heat—Atomic Physics—Physical Chemistry—Radiation Physics—Laboratory Astrophysics[2]—Radio Standards Laboratory,[2] which includes Radio Standards Physics and Radio Standards Engineering—Office of Standard Reference Data.

THE INSTITUTE FOR MATERIALS RESEARCH . . . conducts materials research and provides associated materials services including mainly reference materials and data on the properties of materials. Beyond its direct interest to the Nation's scientists and engineers, this Institute yields services which are essential to the advancement of technology in industry and commerce. This Institute is organized primarily by technical fields:

—Analytical Chemistry—Metallurgy—Reactor Radiations—Polymers—Inorganic Materials—Cryogenics[2]—Materials Evaluation Laboratory—Office of Standard Reference Materials.

THE INSTITUTE FOR APPLIED TECHNOLOGY . . . provides technical services to promote the use of available technology and to facilitate technological innovation in industry and government. The principal elements of this Institute are:

—Building Research—Electronic Instrumentation—Textile and Apparel Technology Center—Technical Analysis—Center for Computer Sciences and Technology—Office of Weights and Measures—Office of Engineering Standards Services—Office of Invention and Innovation—Clearinghouse for Federal Scientific and Technical Information.[3]

---

[1] Headquarters and Laboratories at Gaithersburg, Maryland, unless otherwise noted; mailing address Washington, D. C., 20234.

[2] Located at Boulder, Colorado, 80302.

[3] Located at 5285 Port Royal Road, Springfield, Virginia, 22151.

UNITED STATES DEPARTMENT OF COMMERCE
Alexander B. Trowbridge, Secretary
NATIONAL BUREAU OF STANDARDS • A. V. Astin, Director

NBS TECHNICAL NOTE 360

ISSUED NOVEMBER 20, 1967

ON THE SELECTION OF THE INTERMOLECULAR POTENTIAL FUNCTION: APPLICATION OF STATISTICAL MECHANICAL THEORY TO EXPERIMENT

H. J. M. HANLEY

Cryogenics Division
Institute for Materials Research
National Bureau of Standards
Boulder, Colorado

MAX KLEIN

Heat Division
Institute of Basic Standards
National Bureau of Standards
Washington, D. C.

For sale by the Superintendent of Documents, U.S. Government Printing Office, Washington, D.C., 20402
Price 50 cents.

CONTENTS

ABSTRACT

We have developed a method here to evaluate quantitatively the relationship between model intermolecular potential functions and macroscopic experimental properties. Specifically, we have studied the function families: m-6, Kihara, exp:6, and Morse, and the properties: viscosity coefficient, diffusion coefficient, second virial, and Joule-Thomson coefficient. Our method is not restricted to these functions and properties; it is valid for any function and any property provided the appropriate theoretical expressions are available.

The principal conclusions from this work are: 1. A temperature range exists (around room temperature for most substances) in which data are completely insensitive to the potential function. This range makes it possible to quantitatively define what is meant by "high" or "low" temperatures. These definitions are most important when extrapolation of data arises. 2. The function families studied are essentially equivalent. 3. More than one function is required to represent data over a range of about 1000°K. 4. We have estimated the experimental error which can be tolerated if experimental data are to be used to select a potential function. The conclusions are experimentally verified for both transport and equilibrium properties.

Key words: Intermolecular potential function, experimental data, theory, correlation, transport properties, equilibrium properties.

1. INTRODUCTION

One describes a natural phenomenon by methods that are appropriate to the level that one wants to understand it. The levels of understanding range from the most empirical to the most fundamental.

If we wished to classify methods in terms of levels we might list, in order of rigor:

1. Curve fitting empirical methods which merely serve to correlate experimental data. Examples are the least square fits to empirical multi-parameter equations of state.
2. Macroscopic theories which are soundly based on verifiable macroscopic arguments and postulates. Thermodynamics and hydrodynamics are examples.
3. Theories, such as statistical mechanics and kinetic theory, which try to understand and derive the laws of nature and the properties of materials from molecular considerations. These theories explain the fundamentals and results of the macroscopic theories of the previous level. We must have, however, a knowledge of the intermolecular potential function to translate formal expressions into working equations.
4. The most rigorous theories which try to explain natural phenomena from first principles. Quantum mechanics is the example here.

The choice of the level to work with is obviously a matter of convenience. The pure scientist would be at home at level 4, whereas the laboratory worker might prefer levels 1 or 2.

One can argue that the theories at level 3 are the most rewarding in the long run. Quite apart from the academic satisfaction of describing a natural process in terms of molecular properties, the theories provide very powerful methods to correlate and predict experi-

ment. An empirical theory cannot do this. The rigorous theories, on the other hand, involve much too much detail with which present-day computing and analytic tools cannot cope.

Naturally, application of the 3rd level theories is limited to phenomena which can be described in terms of molecular properties. But there is another limitation about which we are concerned here. As we said above, the 3rd level requires the intermolecular potential function to get results from experiment. Unfortunately, quantum mechanics has not yet derived a complete function from first principles. One is therefore left with only model functions which approximate to the real potential as far as it is known. The testing and choice of the most realistic model function must come from experiment.

This point has long been realized and numerous authors have tested model function with experimental data. The explosive use of the computer has enormously increased the output of this type of work. Although most authors are aware of the overall relation between model functions and experiment, most of the knowledge is intuitive rather than quantitative. All too often the computer has been abused with the result that much of the work published is at best repetitious and at worst incorrect and misleading.

We shall examine here exactly what requirements have to be satisfied if one is to obtain sensible conclusions when a given function is inserted into statistical mechanical theories and the result compared with experiment. In particular we will see what experimental properties and what temperature ranges are most likely to give us information on the function. We will also investigate just how accurate experimental data must be, so that this information is not obscured by random error.

To emphasize the conclusions that come from this study we state them here in advance. However, first the following definitions are required:

a) results are given in terms of reduced temperatures, T^*. A reduced temperature is defined by the relation $T^* = T/(\epsilon/k)$, where T is the absolute temperature, ϵ is the value of the maximum energy of attraction between two molecules for a given potential function, and k is Boltzmann's constant. We most frequently refer to the temperature reduced with respect to the 12-6 (Lennard-Jones) potential, T^*_{12-6}; this choice is a matter of convenience because values of $(\epsilon/k)_{12-6}$ are known for most common substances, at least to a first approximation†.

b) We will use the terms two- and three-parameter potential functions. A two-parameter function is a function described by ϵ/k and R, with R a distance parameter. A three-parameter function is described by ϵ/k and R together with a third parameter which designates the family of which the function is a member. The functions are completely specified when values are assigned to the parameters.

Keeping in mind the above definitions, the conclusions that result from this work are as follows:

1. It is difficult to distinguish between one reasonable intermolecular potential function and another in the reduced temperature range of about $2.0 < T^*_{12-6} < 5.0$.

† There is nothing magic about the choice of the 12-6 function here. At this point in our discussion we are using the parameters for the 12-6 function merely as a convenient means for reducing certain of the experimental quantities.

2. If a potential function in one three-parameter family correlates data in a particular manner, it appears that a potential of another such family can always be chosen to correlate the data in a similar manner. This is especially true for the temperature range $1.5 < T^*_{12-6} < 10.0$. This conclusion obviously includes the result of 1 (above).

3. It seems that it is impossible to find a three-parameter function that will satisfactorily correlate experimental data over the temperature range of approximately $1.0 < T^*_{12-6} < 20.0$. This is a very wide range; for argon, for example, it is $125°K < T < 2500°K$.

4. More information on the behavior of a potential function results from a study of experimental transport data (e.g., viscosity coefficients) than results from a study of experimental equilibrium data (e.g., second virial coefficients).

5. Calculations have indicated that the possibility of distinguishing between one function and another, which is already negligible between $2.0 < T^*_{12-6} < 5.0$, is further reduced over a wider temperature range if the data have a certain random error. For viscosity data, this error is about 0.5%. For second virial data the error is a constant which is about $0.03\ (b_0)_{12-6}$ [where $(b_0)_{12-6} = \frac{2}{3}\pi N R^3_{12-6}$, N = Avogadros number, and R_{12-6} = the distance parameter for the 12-6 function].

We work with the properties: viscosity, diffusion, second virial, and Joule-Thomson effect, and with the functions: the m-6, the Kihara, the exp:6, and the Morse. We limit ourselves to these properties and intermolecular potential functions only because they are the most frequently discussed in the literature. In principle, the procedure described can be applied to <u>any</u> property and function.

Our discussion will necessarily contain material covered in an earlier publication [1]‡ (hereafter referred to as I). The present work contains a more complete and slightly more accurate discussion than found there, although the basic conclusions previously reached remain unchanged.

2. THE INTERMOLECULAR POTENTIAL FUNCTION

The potential functions available at this time can be divided into families, each with a family parameter. The discussion will be restricted to the four most commonly used families of functions: the m-6, the Kihara, the exp:6, and the Morse. These have all been described in the literature so it will suffice to define these functions without explanation.

If $U(r)$ is the interaction potential of two molecules separated by a distance r and if ϵ is the maximum energy of attraction (i.e., the energy minimum), one writes the functions as follows:

The m-6 [2, 3] :

$$U(r) = \frac{\epsilon}{\left(\frac{6}{m}\right)^{\frac{6}{m-6}} - \left(\frac{6}{m}\right)^{\frac{m}{m-6}}} \left\{\left(\frac{\sigma}{r}\right)^m - \left(\frac{\sigma}{r}\right)^6\right\}$$

where σ is that value of r for which $U(r) = 0$. The family parameter m denotes the repulsive exponent of the potential.

The Kihara [4, 5] :

$$U(r) = \infty \,, \quad r \leq a$$

$$U(r) = 4\epsilon \left[\left(\frac{\sigma - a}{r - a}\right)^{12} - \left(\frac{\sigma - a}{r - a}\right)^6\right], \quad r > a \,.$$

Here the finite size of the molecule is taken into account by means of a hard core diameter a; σ is again that value of r for which

‡ Numbers in brackets refer to references.

$U(r) = 0$. It is convenient to define a reduced core diameter by $\gamma = a/\sigma$, which is the family parameter.

The exp:6 [6] :

$$U(r) = \frac{\epsilon}{1 - 6/\alpha} \left[\frac{6}{\alpha} \exp \left\{ \alpha \left(1 - \frac{r}{r_m} \right) \right\} - \left(\frac{r_m}{r} \right)^6 \right] .$$

Here r_m is the value of r at the energy minimum and α is the family parameter which represents the steepness of the repulsive part of the potential.

The Morse [7, 8] :

$$U(r) = \epsilon \left\{ \exp \left[-\frac{2c}{\sigma} \left(r - r_m \right) \right] - 2 \exp \left[-\frac{c}{\sigma} \left(r - r_m \right) \right] \right\} ,$$

where r_m is again the value of r at the minimum and the family parameter c is related to the curvature of $U(r)$ at $r = r_m$.

3. THE STATISTICAL MECHANICAL EXPRESSIONS FOR THE PROPERTIES

Statistical mechanics and kinetic theory provide microscopic descriptions of equilibrium and nonequilibrium thermodynamics. As such, their use generally results in expressions relating macroscopic experimental properties to theoretical microscopic intermolecular potentials. These expressions are central to our work.

3.1 Equilibrium Properties

According to the Uisell-Mayer density expansion of the equation of state, the experimental second virial coefficient of Kamerlingh-Onnes is related to the intermolecular potential [9] by

$$B(T) = b_o B^*(T^*) = - b_o \int_o^\infty \left[\exp \left(- \frac{U^*(r^*)}{T^*} \right) - 1 \right] r^{*2} \, dr^* ,$$

where

$$b_o = \frac{2\pi N R^3}{3}, \quad T^* = kT/\epsilon, \quad U^* = U/\epsilon, \text{ and } r^* = r/R.$$

Here R is the characteristic length associated with the potential U(r) (i.e., $R = \sigma$ or $R = r_m$, as the case may be), N is Avogadro's number, ϵ the depth of the potential well, and k is Boltzmann's constant.

With the aid of this same theory, one can derive the expression for the Joule-Thomson coefficient at zero density, μ_o,

$$\mu_o = \frac{b_o}{C_p^{(o)}} \left[B'^* - B^* \right]$$

where $C_p^{(o)}$ is the zero pressure molar heat capacity and $B'^* = T^* dB^*/dT^*$. We shall actually work with the quantity $\mu_o C_p^{(o)}$.

3.2 Transport Properties

The Chapman-Enskog solution of the Boltzmann equation provides one with a formally complete solution of the problem of describing the transport properties of dilute gases. In particular, one obtains expressions which relate the transport coefficients appearing in the experimental phenomonological flow equations to the intermolecular potential function. The expressions for the properties of particular interest to us are, to a first approximation [9, 10] :

Viscosity (η):

$$10^7 \eta = \frac{266.93 (MT)^{\frac{1}{2}}}{R^2 \Omega^{(2,2)*}(T^*)} \qquad g\ cm^{-1}\ sec^{-1} .$$

Thermal Conductivity (λ):

$$10^7 \lambda = \frac{1989.1\ (T/M)^{\frac{1}{2}}}{R^2 \Omega^{(2,2)*}(T^*)} \qquad J\ cm^{-1}\ sec^{-1}\ deg^{-1} \ .$$

Self-diffusion coefficient (D):

$$10^4 D = \frac{26.28\ (T^3/M)^{\frac{1}{2}}}{p\ R^2\ \Omega^{(1,1)*}(T^*)} \qquad cm^2\ sec^{-1} \ .$$

Here M is the molecular weight, R the characteristic distance associated with the potential, T the absolute temperature, p the gas pressure, and $\Omega^{(\ell, s)*}(T^*)$ the reduced collision integral at the reduced temperature $T^* = kT/\epsilon$. As we will discuss in the next section, we only require the collision integral part of the above expressions. Thus, the expressions for λ and η are equivalent.

The intermolecular potential function is contained in the reduced collision integrals $\Omega^{(\ell, s)*}(T^*)$. This quantity is given by

$$\Omega^{(\ell, s)*}(T^*) = \frac{2}{(s+1)!\ T^{*(s+2)}} \int_0^\infty \exp(-g^{*2}/T^*)\ g^{*(2s+3)}\ Q^{(\ell)*}(g^*) dg^* \ ,$$

where $Q^{(\ell)*}(g^*)$ is a scattering cross section at a reduced energy g^* defined by

$$Q^{(\ell)*}(g^*) = \frac{2}{1 - \frac{1}{2}\frac{(1+(-1)^\ell}{1+\ell}} \int_0^\infty (1 - \cos^\ell \chi)\ b^*\ db^* \ .$$

The scattering angle $\chi(g^*, b^*)$ for reduced energy g^* and impact parameter b^* is related to the intermolecular potential function $U^*(r^*)$ through

$$\chi(g^*, b^*) = \pi - 2b^* \int_{r_m^*}^\infty \frac{dr^*/r^{*2}}{\left(1 - \frac{b^{*2}}{r^{*2}} - \frac{U^*(r^*)}{g^{*2}}\right)^{\frac{1}{2}}} \ .$$

Here r_m^* is the reduced distance between a pair of molecules at the point of closest approach.

4. METHOD

4.1 Background

The method which we have used to determine the sensitivity of a particular experimental property with respect to changes in the potential function has been described in I for the second virial coefficient. For the sake of completeness we shall repeat the discussion, only this time using the viscosity coefficient as an example. As in I, the discussion will be limited to two-parameter potential functions. This results in no loss of generality since a three-parameter function can be considered to generate a family of two-parameter functions, one function being associated with each value of the third parameter.

At a given experimental temperature, T, one obtains an experimental value of the viscosity, $\eta(T)$, for the dilute gas in question. For a given potential function, which we shall designate by the subscript 1, this value of the viscosity is predicted by the relation

$$\eta(T) = \frac{\text{const. } T^{\frac{1}{2}}}{R_1^2 \, \Omega_1^{(2,2)*}(T_1^*)} \quad ,$$

which, in terms of the experimental temperature, is

$$\eta(T) = \frac{\text{const. } T^{\frac{1}{2}}}{R_1^2 \, \Omega_1^{(2,2)*}(kT/\epsilon_1)} \quad ,$$

given the proper values of the potential parameters R_1 and ϵ_1/k. In fact, given the experimental value at the temperature T and having chosen the potential function this constitutes an equation in the two unknowns R_1 and ϵ_1/k. The loci of pairs of points $(R_1, \epsilon_1/k)$ which satisfy this equation lie on a curve in a plane determined by R, ϵ/k as axes. This is illustrated in Fig. 1 for the case of argon at 123°K [11].

Had we chosen to use a second potential function, designated by subscript 2, this same experimental value would have been predicted by

$$\eta(T) = \frac{\text{const. } T^{\frac{1}{2}}}{R_2^2 \, \Omega_2^{(2,2)*}(T_2^*)} \quad . \tag{1}$$

Our method is based on the requirement that the same value be predicted by both potentials. Thus these two expressions must be equated. After so doing one obtains

$$\frac{\Omega_2^{(2,2)*}(T_2^*)}{\Omega_1^{(2,2)*}(T_1^*)} = \left(\frac{R_1}{R_2}\right)^2 \quad .$$

But

$$T = \frac{\epsilon_1 T_1^*}{k} = \frac{\epsilon_2 T_2^*}{k} \quad ,$$

so that we have

$$\frac{T_2^*}{T_1^*} = \frac{\epsilon_1}{\epsilon_2} \quad .$$

Thus, the requirement that the single experimental point $\eta(T)$ be predicted simultaneously by both potential functions also requires that the equation

$$\frac{\Omega_2^{(2,2)*}\left(\frac{\epsilon_1}{\epsilon_2} T_1^*\right)}{\Omega_1^{(2,2)*}\left(T_1^*\right)} = \left(\frac{R_1}{R_2}\right)^2 \tag{2}$$

be satisfied. This relationship connects the two potential functions through the collision integrals $\Omega^{(2,2)*}$. Note that the experimental $\eta(T)$ has disappeared. For each value of T_1^*, Eq (2) is a relationship between the parameter ratios ϵ_1/ϵ_2 and R_1/R_2 such that the viscosity predicted using $\Omega^{(2,2)*}(T_1^*)$ is exactly given by the viscosity obtained using $\Omega^{(2,2)*}(T_2^*)$. Clearly, having chosen a particular pair of potential functions as 1 and 2, Eq (2) constitutes, for each value of T_1^*, a single equation in the two unknowns ϵ_1/ϵ_2, R_1/R_2. A plot of the loci of solutions to this equation will look like Fig. 1 with the axes

now being labeled ϵ_1/ϵ_2 and $(R_1/R_2)^2$. It should be noted that Eq (2) can be written in terms of T_2^* merely by substituting $T_1^* = \epsilon_2/\epsilon_1\ T_2^*$.

Equation (2) has been derived here for the viscosity. It is easy to verify that corresponding equations for the other properties are:

a) the second virial coefficient

$$(b_0)_1\ B_1^*\ (T_1^*) = (b_0)_2\ B_2^*\ (T_2^*) \tag{2a}$$

b) the Joule-Thomson coefficient

$$(b_0)_1\ [B_1^{*\prime}\ (T_1^*) - B_1^*\ (T_1^*)] = (b_0)_2\ [B_2^{*\prime}\ (T_2^*) - B_2^*\ (T_2^*)] \tag{2b}$$

c) the self-diffusion coefficient

$$R_1^2\ \Omega_1^{(1,1)*}\ (T_1^*) = R_2^2\ \Omega_2^{(1,1)*}\ (T_2^*)\ . \tag{2c}$$

Returning to Eq (2): This single equation in two unknowns becomes two equations in two unknowns if one requires that, for some property other than the viscosity, a single datum point also be predicted simultaneously for the same pair of potentials. Suppose that we take as this property the first derivative of the viscosity with respect to the logarithm of the temperature. Now, in terms of unreduced collision integrals, for potential 1 we have [9, 10]

$$\eta = \frac{5}{8}\ \frac{kT}{\Omega_1^{(2,2)}\ (T)}\ .$$

It follows then that

$$T\frac{d\eta}{dT} = \frac{5}{8}\ \frac{kT}{\Omega^{(2,2)}(T)} + \frac{5}{8}\ \frac{kT^2}{[\Omega^{(2,2)}\ (T)]^2}\ \frac{d\Omega^{(2,2)}}{dT}$$

$$= \eta(T)\left[\ 1 + \frac{d\ell n\ \Omega^{(2,2)}}{d\ell nT}\ \right]\ .$$

It is easily shown that [1]

$$\frac{d\ell n\ \Omega^{(2,2)}}{d\ell n\ T} = \frac{\Omega^{(2,2)}}{\Omega^{(2,2)}} - \frac{5}{2}\ ,$$

so that

$$T\frac{d\eta}{dT} = \eta(T)\left[\frac{\Omega^{(2,3)}}{\Omega^{(2,2)}} - \frac{3}{2}\right] .$$

In terms of reduced collision integrals this becomes

$$T\frac{d\eta}{dT} = \eta(T)\left[4\frac{\Omega_1^{(2,3)*}(T_1^*)}{\Omega_1^{(2,2)}(T_1^*)} - \frac{3}{2}\right] .$$

For potential 2, this is written

$$T\frac{d\eta}{dT} = \eta(T)\left[4\frac{\Omega_2^{(2,3)*}(T_2^*)}{\Omega_2^{(2,2)*}(T_2^*)} - \frac{3}{2}\right] . \qquad (1a)$$

Equating these two and remembering that we also require the equality of the viscosity itself for the two potentials we see that we, in effect, have to solve the equation

$$\frac{\Omega_1^{(2,3)*}(T_1^*)}{\Omega_1^{(2,2)}(T_1^*)} = \frac{\Omega_2^{(2,3)*}(T_2^*)}{\Omega_2^{(2,2)*}(T_2^*)} .$$

In terms of T_1^* this becomes

$$\frac{\Omega_1^{(2,3)*}(T_1^*)}{\Omega_1^{(2,2)*}(T_1^*)} = \frac{\Omega_2^{(2,3)*}(T_1^* \ \epsilon_1/\epsilon_2)}{\Omega_2^{(2,2)*}(T_1^* \ \epsilon_1/\epsilon_2)} .$$

For each T_1^* and for a particular choice of potentials 1 and 2, this is a single equation in the ratio ϵ_1/ϵ_2. This equation is solved as previously described [1]. That is, one calculates for each function, a table of values of the function

$$S^*(T^*) = \frac{\Omega^{(2,3)*}(T^*)}{\Omega^{(2,2)*}(T^*)} .$$

The equation to be solved is then

$$S_1^*(T_1^*) = S_2^*(T_2^*) . \qquad (3)$$

An equation (3) can be derived for each of the other properties of interest. In each case, however, the function $S^*(T^*)$ will have a different definition. These definitions are as follows:

a) the second virial coefficient

$$S^*(T^*) = \frac{T^*}{B^*(T^*)} \frac{dB^*}{dT^*} \tag{3a}$$

b) the Joule-Thomson coefficient

$$S^*(T^*) = \frac{(T^*)^2 \frac{d^2 B^*}{dT^{*2}}}{T^* \frac{dB^*}{dT^*} - B^*} \tag{3b}$$

c) the self-diffusion coefficient

$$S^*(T^*) = \frac{\Omega^{(1,2)*}}{\Omega^{(1,1)*}} \quad . \tag{3c}$$

Our approach is equivalent to taking the properties calculated for potential 1 as "experimental" data and attempting to fit them by properties calculated for potential 2. In other words, we take our "experimental" system to be that system whose molecular interactions are described by potential 1. Our entire discussion could have proceeded with no mention of experiment. In particular, the left hand side of Eq (1) could contain the viscosity calculated for potential 1 instead of that determined from experiment. The same description would apply to Eq (1a). Among other things, our method enables us to deal with exact "experimental" data and to control the effect of error. In what follows we shall use quotation marks to set off the words "experimental" and "data" from their counterparts for a real laboratory system.

4.2 Graphical Procedure

Our method can be illustrated graphically. This is most simply done with the second virial coefficient and its first derivative as described in I. We write Eq (2a) in terms of T_1^*,

$$B_1^*(T_1^*) = \frac{(b_0)_2}{(b_0)_1} B_2^*(\epsilon_2/\epsilon_1 \; T_1^*) \quad . \tag{4}$$

Equation (4) is a single equation in the two ratios $(b_0)_2/(b_0)_1$ and ϵ_2/ϵ_1. For each value of T_1^*, this is a relationship between the parameter ratios ϵ_1/ϵ_2 and $(b_0)_1/(b_0)_2$ such that the second virial coefficient predicted using $B_1^*(T_1^*)$ is exactly equal to the second virial coefficient predicted using $B_2^*(T_2^*)$. Figure 2 contains the loci of solutions to Eq (4) for several values of T_1^* when the two potentials are the 12-6 and the exp:6 for $\alpha = 12$. That is, we denote function 1 as the m-6 with $m = 12$ and function 2 as the exp:6 with $\alpha = 12$ and write T_1^* as T_{12-6}^*. For graphical purposes we define $P_{21} \equiv (b_0)_2/(b_0)_1$.

By equating the first derivatives of the second virial coefficient one obtains the equation

$$B_1^{*\prime}(T_1^*) = \frac{(b_0)_2}{(b_0)_1} B_2^{*\prime}(T_1^* \ \epsilon_2/\epsilon_1) \qquad (5)$$

where $B^{*\prime} = T^* dB^*/dT^*$. This is again a relationship connecting the two parameter ratios. Figure 3 contains the loci of solutions to Eq (5) for several reduced temperatures.

The two relationships hold simultaneously, at a given reduced temperature, only for those parameter pairs which are simultaneously on corresponding isotherms of Figs. 2 and 3, i. e., those parameter pairs which are at the intersections of corresponding isotherms. Figure 4 contains some of the curves of Figs. 2 and 3 with the intersection points indicated. Clearly, these intersection points define the loci of solutions of Eq (3).

4. 3 Computer Procedure

There is obviously no point to solving these equations graphically except for purpose of illustration as we have just done. It is far quicker to give the entire task to the computer. Returning to the viscosity example: In the general case, we solve Eq (3) by inverse interpolation.

That is, given T_1^*, one has a value $S_1(T_1^*)$ in the table associated with function 1. The value of T_2^* associated with this value is then found in the $S_2(T_2^*)$ table associated with function 2 by interpolation. The ratio ϵ_1/ϵ_2 can then be calculated simply from

$$\epsilon_1/\epsilon_2 = T_2^*/T_1^* \quad .$$

The corresponding value of the second unknown R_1^2/R_2^2 can be calculated from the relation (2) corresponding to the same pair of values T_1^* and T_2^*, e.g., for the viscosity

$$\frac{R_1^2}{R_2^2} = \frac{\Omega^{(2,2)*}(T_2^*)}{\Omega^{(2,2)*}(T_1^*)} \quad .$$

At a given T_1^*, one now has the pair of values, ϵ_1/ϵ_2 and $(R_1/R_2)^2$, such that $\Omega_1^{(2,2)*}$ and its first derivative are exactly reproduced by $\Omega_2^{(2,2)*}$ and its first derivative for the second potential at the reduced temperature T_2^*. It follows that the theoretical values of $\eta(T)$ and $Td\eta/dT$, predicted by potential 1 when the parameters ϵ_1, R_1 are used, will be exactly reproduced with potential 2 when the parameters $\epsilon_2(=\epsilon_1/(\epsilon_1/\epsilon_2))$, $R_2(=R_1/(R_1/R_2))$ are used.

These equations can be solved as functions of T_1^*. Having done this, one has the ratios ϵ_1/ϵ_2 and R_1^2/R_2^2 as functions of the reduced temperature T_1^*. With these ratios one can, for each T_1^*, determine the temperature T_2^* and scale factor $(R_2)^2$ such that both η and $d\eta/dT$ as calculated for potential 1 will be duplicated for potential 2. In the particular trivial case that occurs when we choose to take potential 2 identical with potential 1, each of these ratios is a constant equal to unity for all T_1^*. In particular, the ratios are then independent of T_1^*. One expects that, in the more general case where potential 2 is taken different from potential 1, these ratios will not be independent of T_1^*.

Suppose, however, that, after solving Eq (3) as a function of T_1^* with potential 2 different from potential 1, the ratios are found to be constant over a range of values of T_1^*. This would mean that potentials 1 and 2 are equivalent over that range of temperature, as far as the viscosity is concerned, since both η and $Td\eta/dT$ as obtained from one of the functions (e. g., potential 1 with the parameters ϵ_1, R_1) are exactly reproduced by a calculation using the second function (e. g., potential 2 with a single pair of parameters ϵ_2, R_2).

In this work we are concerned with solving Eq (3) for the ratios ϵ_1/ϵ_2, $(R_1/R_2)^2$ as functions of T_1^* for various pairs of potentials. For simplicity we take potential 1 to be the 12-6 function. In this sense we take as our "experimental" system that system whose molecular interactions are described by the 12-6 function and try to fit that system's properties with those predicted for other potentials. This enables us to deal with exact properties and to control the effect of error. A number of conclusions will result from this "experimental" system. We show later that our results do not depend on this particular choice for potential 1. Any function could have been taken to be potential 1. We will show that our results are valid for a real system.

Collision integrals and reduced second virial coefficients were taken from the references indicated in Table I.

Table I

Function	Collision integral refs.	Second virial refs.
m-6	[2]	[12]
Kihara	[4]	[12]
exp:6	[6, 9]	[12]
Morse	[12]	[12]

4.4 Effect of Experimental Error

It should be noted that our discussions have been based on the requirement that the property ($\eta(T)$ in our example) predicted by one potential be exactly equal to that predicted by a second potential†. The same has been true for the first derivative. So Eq (3) represents, in principle, precise equivalence between the two potentials as far as the property being discussed is concerned. We cannot expect precise equivalence when working with real experimental data. But as pointed out in I, results which indicate a lack of uniqueness between two potentials are thereby strengthened. Thus, if two potentials yield the same property in an exact fit, they will, a fortiori, continue to do so when experimental error is introduced and one accepts a more approximate fit as exact. On the other hand, any ability to distinguish between two potentials which we may have found applies strictly only to the conditions of the calculation, namely, the exact equality of the property for the two potentials. It is quite possible that this ability to distinguish between potentials might disappear entirely on the introduction of any uncertainty in the property. Clearly it disappears when one introduces complete uncertainty.

An exact fit is obviously experimentally unrealistic. Before we can relate our results to experimental situations we must introduce

† Actually, the exactness is limited by the accuracy of the tables used. These are estimated as better than one part per thousand for the transport properties and one part per ten thousand for the equilibrium properties. These accuracies can be called exact when compared with the precision of the corresponding experimental data. We note, in this context, that the correction factors have not been included in Eq (2). A calculation has shown that the correction factors f_η and f_λ and their derivatives can be neglected as contributing less than one part per thousand in the transport part of the calculations.

a model of the experimental uncertainty into our calculation.

We only need to describe how experimental error affects the relationship between a potential function and a macroscopic property. It is not necessary in the discussion to include the effect of error on the second equality, i. e., the equality of the first derivatives for the two potentials.

Suppose, for a given temperature, we estimate that an uncertainty $\pm\Delta$ exists in the experimental property. That is, the experimental value can lie anywhere in the range $\eta(T) \pm \Delta$. The left-hand side of Eq (1) can be replaced by any value in the range $\eta(T) \pm \Delta$. Any such value will have associated with it a curve in the $(\epsilon/k, R^2)$ plane describing the loci of solutions to Eq (1) for that experimental value. Let us consider the extreme values. Figure 5 contains curves for fixed extreme values for a single datum point (the same one used for Fig. 1) for a particular experimental system. Clearly, the curves for values intermediate to $\eta(T) \pm \Delta$ must lie within the area defined by the pair of curves of Fig. 5. The shaded area of Fig. 5, therefore, corresponds to those pairs of values $(\epsilon/k, R^2)$ which satisfy Eq (1) within the confidence limits assigned to the datum $\eta(T)$.

This same method for introducing uncertainty can be applied when, instead of an experimental datum point, the left-hand side contains the value of this property predicted by a second potential function. In this case the experimental temperature T in Eq (2) would be replaced by T_1^*. Figure 5 will still apply except that the axes will be labeled ϵ_1/ϵ_2 and R_1^2/R_2^2 rather than ϵ/k and R^2. In the discussion to follow we shall always be considering this latter case (the equality for two potentials).

Suppose now that we were to add to Fig. 5, the pair of curves associated with a second value of T_1^*. This would add a second shaded area to Fig. 5 as indicated in Fig. 6. The common intersection of the two shaded areas now represents the loci of pairs of ratios ϵ_1/ϵ_2, R_1^2/R_2^2 such that the values of the property for one potential can be replaced by those for the other simultaneously for the two values of T_1^* within the confidence limits assigned. The addition of curves corresponding to other values of T_1^* leads to the introduction of still more such areas. In general, every T_1^* curve added reduces the common area of intersection. This is illustrated in Fig. 6 for three temperatures. Potentials are entirely equivalent for a given property for given assigned confidence limits when there remains an area of overlap, no matter how many values of T_1^* are added in this way. That is, there will be ϵ_1/ϵ_2, R_1^2/R_2^2 pairs so that, within the confidence limits assigned, the property predicted for one potential can be predicted for the other simultaneously for all of the values of T_1^* considered. The absence of a net area of overlap means that the property under discussion can be used to distinguish between the two potentials, provided the data covers the same range of T_1^* shown and provided the confidence limits for the data are the same as that used here.

We have used the method just described to introduce the effect of experimental error. This has enabled us to get a good idea of the accuracy required of the experimental properties considered in order to distinguish between potential functions. The results will be given below.

5. RESULTS

We have obtained results which are conveniently divided into two categories. First, there are our results for the exact fit to an individual property and its first derivative. Second, we have results for the fit to the individual properties within assigned confidence limits.

5.1 Exact Fit to a Property and Its First Derivative

As mentioned earlier, we have always taken the 12-6 intermolecular potential function as the reference function. In what follows we shall always use the subscript 1 to refer to the 12-6 function, the subscript 2 designating the potential which is compared with it. We are thus taking the system whose molecular interactions are described by the 12-6 function as our "experimental" system.

Representative results from our method are depicted by Figs. 7 - 10. Figures 7 and 8 contain plots of the ratio ϵ_1/ϵ_2 versus the reduced temperature T^*_{12-6} for some members of the exp:6 family for the viscosity and second virial coefficients. Figures 9 and 10 contain the corresponding plots of the ratio P_{12}, where $P_{12} \equiv (b_0)_1/(b_0)_2$ for equilibrium properties and $P_{12} \equiv R_1^2/R_2^2$ for transport properties. Similar plots were done for the other properties and other families. These plots are fully described in I and do not have to be discussed at length here.

In examining these curves one should remember that a potential function is equivalent to the reference function if the ratios ϵ_1/ϵ_2 and P_{12} are independent of T^*_{12-6}. Independence of T^*_{12-6} means that the corresponding graphs are parallel to the abscissa. Examination of Figs. 7 - 10 (and the other curves which are not reproduced here) showed most of the curves to be essentially flat in the temperature

range of about $2.0 < T^*_{12-6} < 5.0$[†]. It therefore follows that, for the properties considered, all potentials are equivalent in that temperature range. Conversely, one cannot possibly choose any of the potential functions if one has data only in this range[‡]. Such data are insensitive to the potential function.

Such data are, therefore, entirely of no use for the selection of one potential function over another.

We can define "high" and "low" temperature ranges according to this sensitivity. We define T^*_{12-6} as a low temperature if $T^*_{12-6} < 2.0$ and T^*_{12-6} as a high temperature if $T^*_{12-6} > 5.0$. According to Figs. 7 - 10, however, the second virial coefficient provides no discrimination over the larger temperature range $2.0 < T^*_{12-6} < 10.0$. Therefore the definitions of high and low temperatures need to be altered as follows:

a) for transport properties we define T^*_{12-6} as a low temperature if $T^*_{12-6} < 2.0$, and T^*_{12-6} as a high temperature if $T^*_{12-6} > 5.0$.

---

† For the transport properties (Figs. 7 and 9), the $\alpha = 12$ curve shows a rapid variation between $T^* = 4.0$ and 5.0, indicating that a value of 4.0 might be preferred over 5.0. Experience with applying our results to real experimental systems (see section 6 below) showed the range $2.0 < T^*_{12-6} < 5.0$ to be the best rule of thumb definition, however.

‡ While the temperature range has a precise definition here, it should be taken as only approximate when applied to a real experimental system. Experimental error and uncertainty in the value of $(\epsilon/k)_{12-6}$ might alter it to, say, $1.5 < T^*_{12-6} < 4.5$ or $3.0 < T^*_{12-6} < 6.0$. Considerable uncertainty in $(\epsilon/k)_{12-6}$ can be introduced when the 12-6 function is far from adequate. This results in a considerable degree of arbitrariness in the choice of a best fit to the data.

b) for equilibrium properties we define T^*_{12-6} as a low temperature if $T^*_{12-6} < 2.0$, and T^*_{12-6} as a high temperature if $T^*_{12-6} > 10.0$.

We note that the temperature range is beyond the reach of experiment for most substances while $T^*_{12-6} = 5.0$ is not. For this reason the transport properties are much more useful as probes of the potential function.

This result, i. e., the proof of the existence of temperature ranges in which the properties are insensitive to the potential function, has a very important corollary. That is, one can always extrapolate properties over the entire insensitive region (i. e., $2.0 < T^*_{12-6} < 5.0$ for transport properties and $2.0 < T^*_{12-6} < 10.0$ for equilibrium properties) based on potential functions determined by data in a sensitive region. This corollary is most usefully applied to substances for which $(\epsilon/k)_{12-6}$ is quite large. Thus, for example, one can safely extrapolate the second virial coefficient of xenon ($(\epsilon/k)_{12-6} \cong 224$) to temperatures up to 2240°K based on fits to data which can be at temperatures entirely below 448°K.

5.1.1 General Results

Our results can be presented much more concisely by plotting the ϵ ratios against the P_{12} ratios. These curves contain all the necessary information. Figure 11 contains curves for the exp:6 family of functions for the simultaneous equality of the second virial coefficient and its first derivative. Note that the curves are made up from the intersection points of corresponding isotherms for a property and its first derivative. These are intersection points similar to those of Fig. 4. In fact, the $\alpha = 12$ curve of Fig. 11 is precisely that curve which follows from Fig. 4. (Note that the abscissae and ordinates of Fig. 11 are the reciprocals of Fig. 4).

In each curve of Figs. 11 - 26, the reduced temperature T^*_{12-6} appears as a parameter signifying distance along the curve. In other words, each point on a curve corresponds to a different value of T^*_{12-6}. If ξ represents the distance along the curve, then $d\xi/dT^*$ represents the rate of change along the curve. Clearly, then, both the ϵ and P_{12} ratios are slowly varying functions of T^*_{12-6} near a point where $d\xi/dT^*$ is small. On the other hand, the property being examined is sensitive to the difference between the two potential functions when $d\xi/dT^*$ is large. With the manner of presentation of Fig. 11, one needs to look at only one curve to determine sensitivity with respect to the potential function. The advantage of a one curve presentation is more apparent in Fig. 12 which contains curves for the Kihara function. In Fig. 12, the P_{12} ratios are seen to depend much more strongly on T^*_{12-6} than do the ϵ ratios at the low temperature end of the curves while the opposite is true at the highest temperatures. Thus, the curves are mainly vertical at low temperatures and mainly horizontal at high temperatures. Both ratios are insensitive to the potential function in the intermediate temperature region. For this reason, a large temperature range is crowded into a small distance along the curve in this intermediate region, making $d\xi/dT^*$ small.

Figure 11 illustrates, in an interesting way, another of the results discussed in I, namely, that a three-parameter function is not sufficiently flexible to replace a two-parameter function like the 12-6 as far as the thermodynamic properties predicted by each is concerned. Consider, first, the data at low temperatures. At such temperatures, the curves have opposite slopes for $\alpha = 13$ and $\alpha = 15$. Presumably, $d\xi/dT^*$ approaches zero over the entire low temperature range for a value of α between these. The high temperature ends of the curves, on the other hand, change very little in this same α

range. At the high temperature end of the curves, a similar change takes place between $\alpha = 15$ and $\alpha = 17$ in which range the low temperature behavior is not much affected. Thus, while there exists a value of α such that the second virial coefficient for the 12-6 potential can be replaced by the exp:6 at low temperatures and there exists another value of α which allows a similar replacement at high temperatures, a single value of α does not exist for which this can be done simultaneously at high and low temperatures. This makes the requirement of the simultaneous fit of high and low temperature data (high and low being quantitatively defined) a potentially sensitive probe of the potential function. It should be noted (Fig. 11) that the high temperature direction change occurs at $T^*_{12-6} = 10.0$. Thus, unfortunately, the high temperature part of this sensitivity for the second virial coefficient occurs at temperatures which are beyond the laboratory range for many substances (i.e., 2240°K for xenon and 1200°K for argon).

Figures 13 and 14 contain results for the second virial coefficient and its first derivative for the Morse and m-6 families, respectively. In each case, the behavior is similar to that observed for the exp:6 family of functions. Thus, for the Morse family there is a change in the direction of the curves at low temperature between $c = 4.0$ and 5.0. Presumably, there is a value of c in that interval for which $d\xi/dT^* \cong 0$, for the low temperature range. The high temperature part of the curve changes very little in that region. A similar change of direction occurs at high temperatures between $c = 6.0$ and 8.0 in which interval the low temperature data change very little.

Figure 14 is particularly instructive. Here an exact fit occurs for $m = 12$. In this case, as expected, the curves change direction

as m goes through 12 at both high and low temperatures simultaneously. The sensitivity to the repulsive exponent, m, seen at low temperatures in Fig. 14 seems to contradict the argument which states that only the long range part of the potential is important at low temperatures.

Figures 15 - 18 contain similar curves for the viscosity. Results obtained for these properties are essentially the same as obtained for the second virial coefficient except that the temperature scale is somewhat different. Here again, the low temperature end of the curve changes direction between $\alpha = 12$ and $\alpha = 15$ where the high temperature end of the curve remains unchanged. The high temperature end, on the other hand, changes direction between $\alpha = 15$ and $\alpha = 17$. In this latter range the low temperature end of the curve does not change character. This high temperature sensitivity occurs at a reduced temperature $T^*_{12-6} = 5.0$ as can be seen in Fig. 15 where the direction change occurs at $T^*_{12-6} = 5.0$. This is an accessible experimental temperature for most substances. The application of this result to viscosity data for argon will be discussed below.

We have also examined the Joule-Thomson and diffusion coefficients. Results for the Joule-Thomson coefficient are essentially the same as those for the second virial coefficient while those for the diffusion coefficient repeat our results for viscosity. The Joule-Thomson coefficient results are presented in Figs. 19 - 22 while the results for the diffusion coefficients are shown in Figs. 23 - 26. It should be noted that these properties (the Joule-Thomson and diffusion coefficients) are slightly more sensitive than their counterparts (second virial and viscosity coefficients).

The figures contain important additional information. We can learn from them that these three parameter functions are equivalent. All figures show the same reduction in sensitivity as the third potential parameter approaches the value associated with the best representation of the 12-6 function. Hence, this best representation for one family is equivalent to that for another family. This is actually a general result since the choice of the 12-6 function for the reference function was entirely arbitrary. The choice of another reference function would have led to a best fit for some other member of each family and so to another set of equivalent functions. Proceeding in this manner, from one reference function to another, one could "map out" the equivalence of entire families.

This result can also be illustrated in a different manner. One need not concentrate on the best fits to the reference function. Since, for a given property, all of the figures have essentially the same character, one can find a curve for each family all of which fit the "data" in essentially the same way. This is quite apart from the best fit mentioned above. The potentials corresponding to these curves are equivalent. We can illustrate this for the second virial coefficient (Figs. 11 - 14). The curves for the 15-6, $\gamma = 0.1$, and $c = 8.0$ are very similar when superimposed. We have since found these to behave equivalently when fitting real data.

5.2 Fit to a Given Property Within Assigned Confidence Limits

Our second group of results have to do with the fits of individual properties within assigned confidence limits.

5.2.1 Equilibrium properties

We will work with the second virial coefficient and with the $\alpha = 12$ member of the exp:6 family representing potential 2.

Since our purpose in this section is to emulate the effect of experimental error, the method of assigning the confidence limits must have some relation to the usual error associated with experimental data. Experience indicates that the uncertainty in the second virial coefficient should be essentially independent of temperature. Therefore, we have replaced the second virial coefficient for the 12-6 function (our "experimental" system) by $B^*_{12-6} + \Delta$, where Δ is a constant equal to a percentage of the B^*_{12-6} value for $T^* = 2.0$. This was done for $\Delta = 0$, 1, 5, and 10% of the $T^* = 2.0$ value.

When $\Delta = 0$, as illustrated by Fig. 2, there is only a single curve associated with each reduced temperature. Two potentials are equivalent in this case if all curves have a single common intersection point. Now, according to Fig. 2, there is no common intersection point for the temperature range $1.0 < T^*_{12-6} < 20.0$. The curves associated with the isotherms $T^* = 1.0$ and 20.0 do not intersect near the area where the others intersect. This illustrates the sensitivity of precise data to the potential function at high and low temperatures. Let us now examine the accuracy with which data must be taken in order to preserve this sensitivity. Figure 27 contains results for the case $\Delta = 10\%$ of the B^*_{12-6} value at $T^*_{12-6} = 2.0$. There being a net area of overlap, it is clear that the sensitivity available with $\Delta = 0$ cannot be depended on, given an experimental uncertainty which is this large. Figure 28, on the other hand, contains results for $\Delta = \pm 1\%$ of the B^*_{12-6} value at $T^*_{12-6} = 2.0$. There being no net area of overlap, it is clear that one can use second virial coefficient data with this amount of experimental uncertainty to distinguish

between potential functions. Figure 29 contains the data for $\Delta = \pm 5\%$ of the B^*_{12-6} value at $T^*_{12-6} = 2.0$. Since there is just barely a net overlap, it is clear that this case represents an upper limit on the error allowed.

Naturally, the precision required increases as one approaches the best fit with respect to α. Thus, the 5% obtained here represents an upper limit only when the potential function being examined is as far off from the best choice as is the $\alpha = 12$ from that value of α which gives the best fit to the 12-6. Clearly, the error allowed decreases for a function which is closer to the real function.

These error limits can very easily be converted into experimental error for a given system as soon as the value of b_0 for that system is known. Thus,

$$B(T) = b_0 \, B^*(T^*) \, ,$$

so that if

$$B^*(T^*) = B^*_0(T^*) + \Delta \, ,$$

it follows that

$$B(T) = b_0 B^*_0(T^*) + b_0 \Delta \, .$$

Now, if $\Delta = aB^*_{12-6}(T^*)$ for $T^*_{12-6} = 2.0$ then, since $B^*_{12-6} = -.62763$ for $T^* = 2.0$ [12], it follows that $\Delta = -.62763\, ab_0$. For argon, b_0 is approximately 50 cm^3/mole for the 12-6 function so that $\Delta = -(31.4a)$ cm^3/mole. If we take 4% of the $T^*_{12-6} = 2.0$ value as the appropriate upper limit of the uncertainty, it follows that one can have an experimental uncertainty of approximately 1.4 cm^3/mole and still distinguish between potential functions, to the extent that the $\alpha = 12$ function is not an appropriate representation of the 12-6

function as far as the second virial is concerned. The statistical uncertainty in the argon measurements of Levelt, for example [13], are well within these limits.

We have also found the limiting experimental error allowed for the zero density Joule-Thomson coefficient to determine the potential function. We again worked with the exp:6, $\alpha = 12$ function. Our experience indicates that, when the Joule-Thomson coefficient is obtained from experimental P-V-T data, its uncertainty is independent of temperature and is given approximately by five times the uncertainty in the second virial coefficient. Our experience with more direct measurement of the Joule-Thomson coefficient is somewhat limited mainly as a result of the paucity of such data. In this latter case we have used a percentage of the value as a model of the error.

Error calculations based on the P-V-T experiments show that the added uncertainty (i. e., the factor 5) over that for the second virial coefficient more than overcomes the extra sensitivity of the Joule-Thomson coefficients as a probe of the potential function. Thus, the increase in sensitivity apparent when Figs. 19 - 22 are compared with Figs. 11 - 14 is not attainable in an actual experimental situation when the Joule-Thomson coefficients are obtained from P-V-T data. For the direct measurements we found that an error of 1% was the limiting error required to mask the sensitivity.

5.2.2 Transport properties

There are two sensitive regions to consider for the transport properties as opposed to effectively one region for the equilibrium properties. Therefore three kinds of error limits need to be described here. These are: a) the experimental uncertainty needed to mask the sensitivity of the property at the low temperatures (i. e., $T^*_{12-6} < 2.0$),

b) that needed to mask it at high temperatures (i. e., $T^* > 5.0$), and c) that needed for removing the sensitivity simultaneously at both high and low temperatures. We shall first describe these for the viscosity and as before, shall use the viscosity calculated for the 12-6 function as our "experimental" system. How close these data fit to that calculated for the $\alpha = 12$ member of the exp:6 will again serve as the criterion for determining the limits of experimental uncertainty.

We found that an uncertainty of 0.5% in the low temperature data will mask the sensitivity at low temperatures. In the temperature range $5.0 < T^*_{12-6} < 20.0$, on the other hand, an uncertainty of approximately 3% was required. In order to lose complete sensitivity over the entire range $1.0 < T^*_{12-6} < 20.0$ it was necessary to introduce an uncertainty of 5%†. It is thus clear that, given viscosity data simultaneously at both high ($T^*_{12-6} > 5.0$) and low ($T^*_{12-6} < 2.0$) temperatures, high and low being quantitatively defined, one can learn something about the intermolecular potential function even when such data are highly inaccurate. This is a powerful result. Generally speaking, the same experiment will not cover both of these ranges because of the different temperature control techniques required. One is, therefore, almost always required to use data from different laboratories.

† The juxtaposition of the values 0.5% and 3% can be misleading. It will be recalled (see Fig. 23 for diffusion) that the high temperature range is best fit by a value of α equal approximately to 16 while the low temperature range is best fit by α equal approximately to 13.5. The error limits of the fit to the function $\alpha = 12$ therefore do not have the same meaning at the two ends of the temperature scale considered separately. The 5% limit placed on the simultaneous fit to both ends of the temperature range retains its full meaning, however.

Our results show that such data can be highly inconsistent and still yield a moderate amount of information on the potential function.

As already stated, this sensitivity in the simultaneous fit of high and low temperature data is not available for the second virial coefficient because the high temperature region ($T^*_{12-6} > 10.0$) is not amenable to experiment for most systems.

6. EXPERIMENTAL VERIFICATION

As stated earlier, our approach has been, in effect, to take an idealized system with a known intermolecular potential (i.e., the 12-6) as our "experimental" system and fit its properties to those calculated for other potential functions. It might be argued that the behavior which we have found should not be typical of a real experimental system simply because the 12-6 function is not a suitable function for real systems. We have, therefore, investigated some real experimental systems, looking specifically for the behavior which we found in our idealized "experimental" system.

6.1 Equivalence of Potential Functions

We examined the equivalence of three-parameter families of functions by fitting the experimental second virial coefficient data for argon to five families of potential functions. These fits are presented in Table II. The method was to determine, for each potential, the pair of parameters ϵ/k, b_0, such that the mean square deviation of experiment from theory was a minimum. This was done to four figures. Such precision is reasonable for our purposes since we are interested in obtaining the same degree of fit to all potential functions. The resulting parameters should not, however, be taken as the precise parameters for argon since other pairs near them would also fit the data within experimental precision.

TABLE II

Best fits, including mean least square derivations ($\overline{\Delta}$), for the second virial of Argon. Data from Ref. 13.

Family		Potential	ϵ/k	b_o	$\overline{\Delta}$
m - 6	m =	9	84.16	66.36	.392
		12	115.06	54.76	.223
		15	140.10	47.76	.110
		16	147.50	45.96	.103
		17	154.53	44.34	.118
		18	161.22	42.87	.145
		21	179.57	39.19	.252
		24	195.79	36.28	.363
		27	210.25	33.93	.471
		30	223.14	32.04	.576
		40	254.82	28.35	.895
Kihara	γ =	.1	140.76	47.34	.102
		.15	154.72	43.74	.142
		.2	169.67	40.28	.245
		.25	185.82	36.78	.377
		.3	203.31	33.35	.539
		.4	238.05	27.93	.985
		.5	262.36	25.82	1.589
		.6	279.96	25.11	2.252
exp:6	α =	12	99.90	61.15	.271
		13	110.71	56.99	.220
		14	120.44	53.73	.173
		15	129.35	51.05	.134
		17	145.33	46.78	.102
		19	159.46	43.47	.144
12-n	n =	4	36.84	90.03	.723
		5	76.71	68.83	.499
		6	115.06	54.76	.223
		7	153.58	43.50	.166
		8	195.16	33.75	.539
Morse	c =	4	91.77	64.97	.207
		5	152.03	42.53	.270
		6	269.73	27.34	1.125
		7	300.04	24.64	2.554
		8	349.24	24.00	3.996
		10	504.80	23.19	6.421

Figure 30 dramatically illustrates the equivalence of the various families of potential functions used. In this diagram, we have taken ϵ/k for the abscissa and b_o for the ordinate, each best fit then corresponding to a point on the graph. Figure 30 contains our results for five families of functions. It is seen immediately that all points fall on essentially the same curve†. Given a point on this curve, one can, for each family of functions, find a member of that family which corresponds to it. All families, therefore, appear to be equivalent as far as the second virial coefficient is concerned. It should be noted that the 12-n family has been added to the four families previously described. This was done in order to study the sensitivity of the experimental data to the exponent of the dispersion term in the potential function.

In order to make certain that these produce the same fits, we have plotted the root mean square deviation of theory from experiment versus the parameter ϵ/k for each member of each family. This is presented in Fig. 31. The data for the m-6, Kihara, 12-n, and exp:6 families all fall on essentially the same curve. While deviations do occur for large values of ϵ/k these are less striking than are the similarities between the curves. The deviations of the Morse function data from the rest are not understood at this time, particularly in light of the behavior of the Morse function data in Fig. 30 and in the light of the behavior of the 12-n family of functions. In both Fig. 30 and 31, the 12-n family shows no peculiar behavior with respect to those functions having a $1/r^6$ attraction term. It would seem, then, that the absence of such a term in the Morse function is not responsible for the deviations in Fig. 31.

† We have also verified that a corresponding curve exists for viscosity data.

We can see the equivalence from Figs. 12 and 14 for example. From these figures we predicted that, for the second virial coefficient, the 15-6 function should be essentially equivalent to the $\gamma = 0.1$ function of the Kihara family. We then calculated, for these two functions, the second virial coefficients and the deviations of these calculated coefficients from the experimental argon data. The results are contained in Fig. 32 where the equivalence of the two potentials with respect to the second virial coefficient is strikingly clear. We have also included deviation plots for the 12-6 and 18-6 functions in Fig. 32 in order to establish the sensitivity of the deviation plot to the potential function. It is clear that a small change in the potential function results in a rather large change in the deviation plot so that the equivalence of the 15-6 and $\gamma = 0.1$ functions, as demonstrated in Fig. 32, is a very real thing. This equivalence is, in fact, much stronger than that demonstrated by the essential superposition in Fig. 30 of the points associated with these functions. Fig. 30 is based on comparisons of the sums of the deviations of theory from experiment. The requirement of equivalence based on sums of deviations is much less stringent than that based on detailed deviations such as shown in Fig. 32.

The same approach was used to construct Fig. 33 for the viscosity coefficient of argon. In this case, Figs. 16 and 18 were examined and the 15-6 predicted to be equivalent to the $\gamma = 0.1$. Figure 33 contains the corresponding deviation plots. Here, again, the equivalence is striking.

This experimental verification of the equivalence of the three-parameter functions is very important. It experimentally verifies two results:

1. That we may choose any of the functions as a reference; there is nothing special about the 12-6.

2. It verifies our conclusions that if a member of one three-parameter family fits data in a certain manner, then a member of another three-parameter family can be chosen to fit the data in the same manner.

6.2 The sensitivity of the simultaneous fit of the high and low temperature viscosity data to the potential function.

We examine the sensitivity of the fit of high and low temperature viscosity data to the potential function by fitting experimental data for argon and nitrogen. Sufficient data exist at both extremes of temperature for both substances. We used the very sensitive method of plotting ϵ/k versus T at constant σ as our method of determining the best fit [22]†. Parameters thus obtained were then used to calculate theoretical viscosities and the deviations of these from experiment determined. These deviations are plotted in Figs. 34 and 35. The m-6 family was used exclusively.

Results for argon are contained in Fig. 34. These were obtained as follows. The argon viscosity data of the several workers were combined. These were then divided into three groups according

† The method of plotting ϵ/k versus T at constant σ was rendered somewhat more sensitive as a result of our understanding of Fig. 13. Note that the direction of the change of ϵ/k with T^* changes in going from $\alpha = 12$ and $\alpha = 15$ with the best fit lying between these values. A similar direction change in the fit of the low temperature experimental data for argon was found in the ϵ/k versus T^* at constant σ plots for $m = 18$ and 21 indicating a best fit for m approximately equal to 20. Similar behavior was seen in the low temperature fit of nitrogen. This method for the determination of the potential thus becomes a most sensitive one. Similar behavior was not found in the high temperature fits to the published data although, according to Fig. 13, it should have been present.

Note added while in press: It is encouraging that such behavior is found at high temperatures if we use some new unpublished data. See note after acknowledgement, page 42.

to temperature. All low temperature data ($T^*_{12-6} < 2.0$ i. e., $T < 240°K$) were placed in one group, all intermediate temperature data ($2.0 < T^*_{12-6} < 5.0$, i. e., $240°K < T < 600°K$) in a second group, and the high temperature data ($T^*_{12-6} > 5.0$, i. e., $T > 600°K$) placed in a third group. Plots of ϵ/k versus T at constant σ were done for each of the m-6 potential functions for both the high and low temperature data, the middle temperature data being ignored completely. The choice of a best value of m turned out to be a relatively simple matter at both high and low temperatures. The parameters obtained are listed in Table III. These parameters, along with the appropriate collision integrals, were used to calculate a theoretical viscosity at each experimental data point.

According to Fig. 34a, the low temperature parameters give an excellent representation of the data at both low and intermediate temperatures even though the data at the intermediate temperatures were not included in the parameter determination. The fit is, in fact, good even to a reduced temperature $T^*_{12-6} = 10.0$, indicating that our definition for the beginning of the high temperature range might need to be revised upward for a real system. The theoretical viscosities calculated at high temperatures using these low temperature parameters deviate from experiment. These deviations are outside the range of estimated experimental accuracy and show a tendency to deviate further from experiment as the temperature increases.

Figure 34b is based on the use of parameters obtained from the fit of the high temperature data only. There is an excellent fit over both the high and intermediate temperature ranges even though the latter data were not included in the determination of the parameters. In this case, the fit at low temperatures is very poor and again is

TABLE III

Best values of m, ϵ/k and σ which fit high and low temperature viscosity data.

Gas	m	ϵ/k °K	σ Å
	Low Temperature		
Ar	21	170.5	3.26
N_2	18	113.2	3.56
	High Temperature		
Ar	40	224.1	3.15
N_2	50	189.6	3.34

outside the range of estimated accuracy. That these two fits are irreconcilable is apparent in Table III. Radically different values of m were required in each case.

From Fig. 35 we see that we get essentially the same results for nitrogen. The same remarks apply to nitrogen as to argon.

6.3 The Insensitivity of Intermediate Range Data to the Potential Function

According to Figs. 34 and 35, the intermediate range data are fitted quite well using either of the radically different high and low temperature potentials. Clearly, data in this middle range of temperatures cannot contribute any sensitivity in a determination of the potential function. Since they do contribute the experimental uncertainty associated with their measurement, these data can only serve to mask the choice of a potential. Obviously, such data are less than useless in this respect and should be ignored in the initial stages of a determination of the intermolecular potential function as we have done.

This insensitivity has been present, implicitly, in previous work, for both transport and equilibrium properties. For example, it was quite obvious in previous correlations of argon [34] and oxygen and nitrogen [35] . We reproduce Fig. 2 of reference 34 as Fig. 36 here.

Figures 34 and 35 also very clearly demonstrate the corollary which we attached to the existence of insensitive temperature ranges. Thus, we stated that it is always safe to extrapolate a potential function from a sensitive temperature range over the entire insensitive range. The potential functions of Figs. 34a and 34b, each, more than adequately describe the data in the intermediate range even

though the intermediate range data were not included in the determination of the parameters. This extrapolation is good in spite of the fact that the two potentials are radically different.

7. CONCLUSIONS

We have made a study of the information on the potential function which one obtains from fitting theoretically calculated viscosity, diffusion, second virial, and Joule-Thomson coefficient data to experimental data. In order to avoid the masking effect of experimental error, we took an ideal "experimental" system whose interaction potential is known and drew our conclusions from it. This also enabled us to study the effect of experimental error in a carefully controlled fashion. Conclusions resulting from this study of our idealized system were then specifically sought and found in the behavior of actual experimental systems. We have thus substantiated the points made in the introduction.

We have found that it is impossible to distinguish between one reasonable intermolecular potential function and another if one uses experimental viscosity data in the reduced temperature range of about $2.0 < T^*_{12-6} < 5.0$, the upper limit being increased to 10.0 for the second virial coefficient. It follows, therefore, that potential functions chosen as a result of the correlation of data entirely in that temperature range should be used with extreme caution in applications other than the data correlation itself†. Furthermore, where data exist both inside and outside the temperature range $2.0 < T^*_{12-6} < 5.0$

† Unfortunately the literature is full of such applications. One example is the use of the 12-6 potential and parameters for argon based on the correlation of Michels 1948 data [36].

(the latter being replaced by 10.0 for the second virial coefficient), the data inside this range should be removed and not used until the final correlation. Such data, as we have stated, do not provide information on the potential function but do add to the overall statistical uncertainty, thus spuriously reducing the difference in standard deviation between the best fit and other fits. By reversing these arguments we concluded that it is perfectly safe to cover the insensitive temperature range by means of an extrapolation based on a potential function determined from data outside such a range.

We have also seen that all three-parameter families are essentially equivalent in fitting experimental data for the quantities studied here. This means that the introduction of a new three-parameter function will rarely (if at all) result in an improvement in the fit of such data. Such fitting to additional functions is then unnecessary once a fit has been made to a reasonable three-parameter function.

The simultaneous fit of high ($T^*_{12-6} > 5.0$) and low ($T^*_{12-6} < 2.0$) temperature viscosity data has been found to be potentially a sensitive probe of the potential function. A corollary of these results is that potentials determined for systems for which only low or (in rare cases) only high temperature data exist should be used with caution in applications other than the correlation itself since such functions, in general, would not even fit data at the other end of the temperature scale if such data existed.

The main part of our effort has gone into the study of "exact" fits of data, i.e., we have dealt with precise data from an ideal "system". Our results might easily be masked by error in the application to real systems. By studying the effect of controlled

amounts of error, we have found, however, that present day experimental errors will not mask these results. In particular it was found that the sensitivity at low temperatures will remain, provided viscosity data have a precision of better than 0.5% and second virial data of better than 4% of the value of the second virial coefficient at $T^*_{12-6} = 2.0$ (this latter is equivalent to $0.03\ (b_0)_{12-6}$ for each system). The sensitivity of viscosity data to the potential function in the simultaneous fit of high and low temperatures was found to remain even when errors of 3% were introduced.

We have shown our idealized experimental system to emulate real experimental systems sufficiently so that the conclusions drawn from its study can be expected to be found in experimental systems. Further use of our method is, therefore, clearly indicated. In progress are studies of the thermal diffusion factor and the simultaneous fit of pairs of the properties studied here.

We have also shown that systems for which high and low temperature viscosity data exist should be studied with an aim to finding a four- (or more) parameter potential function which fits such data. In particular, our results would appear to indicate that the inability to properly fit such data in the past is not only due to systematic errors at high temperature as has been suggested by some workers.

8. ACKNOWLEDGEMENT

We acknowledge the grants supporting this work: (For H. J. M. H.) The National Aeronautics and Space Administration, Contract Number R-06-006-046, and (for M. K.) the Air Force Systems Command, Arnold Engineering Development Center, Tullahoma, Tenn., Delivery Order Number (40-600) 66-22 Program Element 61445014, AF Project 8951.

We are also grateful to G. E. Childs for his assistance with the computing, and to R. D. Weekley and Mrs. M. Birchfield for their help with the preparation of the manuscript.

NOTE

While this manuscript was in preparation for publication, we reassessed the high temperature viscosity data. We now feel that the data largely represented by the work of Trautz and Vasilesco are most probably erroneous. Recent measurements for argon [37] for example, lead to a value of $m = 13$ for the high temperature correlation [38]. This value is more compatible with independent scattering experiments than $m = 40$.

We emphasize, however, that all conclusions noted here are upheld with the new data.

9. REFERENCES

1. M. Klein, Determination of Intermolecular Potential Functions from Macroscopic Measurements, J. Res. Natl. Bur. Std. 70A, No. 3, 259-69 (1966).

2. M. Klein and F. J. Smith, to be published in the J. Natl. Bur. Std. (1968).

3. J. H. Dymond, M. Rigby and E. B. Smith, Two-Parameter Intermolecular Potential Energy Functions for Simple Molecules, Phys. Fluids 9, 1222-9 (1966).

4. J. P. O'Connell and J. M. Prausnitz, Applications of the Kihara Potential to Thermodynamic and Transport Properties of Gases, ADVANCES IN THERMOPHYSICAL PROPERTIES AT EXTREME TEMPERATURES AND PRESSURES, 19-31, Am. Soc. Mech. Engr., New York (1965).

5. J. A. Barker, W. Fock, and F. Smith, Calculation of Gas Transport Properties and the Interaction of Argon Atoms, Phys. Fluids 7, 897-903 (1964).

6. E. A. Mason and W. E. Rice, The Intermolecular Potentials for Some Simple Non-polar Molecules, J. Chem. Phys. 22, 843-51 (1954).

7. S. E. Lovell and J. O. Hirschfelder, Tables of Collision Integrals for Gases Obeying the Morse Potential, University of Wisconsin Theoretical Chemistry Laboratory, WIS-AF-21 (June 1962).

8. D. D. Konowalow and S. Carra, Determination and Assessment of Morse Potential Functions for Some Nonpolar Gases, Phys. Fluids 8, 1585-9 (1965).

9. J. O. Hirschfelder, C. F. Curtiss, and R. B. Bird, MOLECULAR THEORY OF GASES AND LIQUIDS, John Wiley & Sons, New York (1964) Second Printing.

10. S. Chapman and T. G. Cowling, THE MATHEMATICAL THEORY OF NON UNIFORM GASES, Cambridge (1964) 7th Printing.

11. H. L. Johnston and E. R. Grilly, Viscosities of Carbon Monoxide, Helium, Neon, and Argon Between 80° and 300°K Coefficients of Viscosity, J. Phys. Chem. 46, 948-63 (1942).

12. M. Klein. Unpublished data. We remark that the second virial coefficients of Klein hardly differ from those from other sources.

13. A. Michels, J. M. Levelt and W. De Graaff, Compressibility Isotherms of Argon at Temperatures Between - 25°C and - 155°C and at Densities up to 640 Amagats, Physica 24, 659 (1958).

14. A. L. Gosman, Thermodynamic Properties of Argon in the Liquid and Gaseous State for Temperatures from the Triple Point to 300°K and Pressures to 1000 Atmospheres, State Univ. of Iowa, Iowa City, Ph. D. Thesis (1965).

15. A. Michels, A. Botzen, and W. Schuurman, The Viscosity of Argon at Pressures up to 2000 Atmospheres, Physica 20, 1141-48 (1954).

16. A. Van Itterbeek and O. Van Paemel, Measurements on the Viscosity of Argon Gas at Room Temperature and Between 90° and 55°K, Physica 5, 1009-11 (1938).

17. M. Trautz and R. Zink, Die Reibung, Wärmeleitung und Diffusion in Gasmischungen. XII. Gasreibung bei höheren Temperaturen, (The Viscosity, Heat Conduction and Diffusion of Gas Mixtures. XII. The Viscosity of Gases at Higher Temperatures), Ann. Physik 7, 427-52 (1930).

18. V. Vasilesco, Recherches Experimentales sur la Viscosite des Gaz aux Temperatures Elevees, (Experimental Research on the Viscosity of Gas at Elevated Temperatures), Ann. Phys. (Paris) 20, 137-76 (1945).

19. G. P. Filippova and I. P. Ishkin, The Viscosity of Air, Nitrogen, and Argon at Low Temperatures and at Pressures up to 150 Atmospheres, Inzh. Fiz. Zh. Akad. Nauk Belorussk SSR 4, 105-9 (1961).

20. R. Wobser and F. Müller, Die innere Reibung von Gasen und Dämpfen und ihre Messung im Höppler-Viskosimeter, (The Viscosity of Gases and Vapors and their Measurement with the Hoppler Viscometer), Kolloid-Beih. 52, 165-276 (1941).

21. F. G. Keyes, The Heat Conductivity, Viscosity, Specific Heat and Prandtl Numbers for Thirteen Gases, Mass. Inst. of Techol., Cambridge, Proj. Squid, Tech. Rept. No. 37 (1952), DDC ATI 167 173.

22. H. J. M. Hanley, Comparison of the Lennard-Jones, Exp:6, and Kihara Potential Functions from Viscosity Data of Dilute Argon, J. Chem. Phys. 44, 4219-22 (1966).

23. C. F. Bonilla, S. J. Wang and H. Weiner, The Viscosity of Steam, Heavy-water Vapor, and Argon at Atmospheric Pressure up to High Temperatures, Trans. ASME 78, 1285-9 (1956).

24. K - L. Yen, An Absolute Determination of the Coefficients of Viscosity of Hydrogen, Nitrogen, and Oxygen, Phil. Mag. (6) 38, 582-96 (1919).

25. M. Trautz and P. B. Baumann, Die Reibung, Wärmeleitung und Diffusion in Gasmischungen. II. Die Reibung von H_2 - N_2 und H_2 - CO - Gemischen, (The Viscosity, Heat Conductivity, and Diffusion in Gas Mixtures. II. The Viscosities of H_2 - N_2 and H_2 - CO Mixtures), Ann. Physik 2, 733-36 (1929).

26. M. Trautz and A. Melster, Die Reibung, Wärmeleitung und Diffusion in Gasmischungen, XI. Die Reibung von H_2, N_2, CO, C_2H_4, O_2, und ihren binaren Gemischen, (The Viscosity, Heat Conduction, and Diffusion in Gas Mixtures. XI. The Viscosities of H_2, N_2, CO, C_2H_4, O_2, and their Binary Mixtures), Ann. Physik 7, 409-26 (May 1930).

27. M. Trautz and R. Heberling, Die Reibung, Wärmeleitung und Diffusion in Gasmischungen. XVII. Die Reibung von NH_3 und seinen Gemischen mit H_2, N_2, O_2, C_2H_4, (The Viscosity, Thermal Conductivity, and Diffusion of Gas Mixtures. XVII. Viscosity of NH_3 and its Mixtures with H_2, N_2, O_2, C_2H_4), Ann. Physik 10, 155-77 (1931).

28. P. J. Rigden, Viscosity of Air, Oxygen, and Nitrogen, Phil. Mag. (7) 25, 961-81 (1938).

29. H. L. Johnston and K. E. McCloskey, Viscosity of Several Common Gases between 90°K and Room Temperature, J. Phys. Chem. 44, 1038-58 (1940).

30. H. L. Johnston, W. R. Mattox, and R. W. Powers, Viscosities of Air and Nitrogen at Low Pressures, Natl. Advisory Comm. Aeronaut. Tech. Note No. 2546 (1951), NASA N62 54546.

31. C. F. Bonilla, R. D. Brooks, and P. L. Walker, Jr., The Viscosity of Steam and Nitrogen at Atmospheric Pressure and High Temperatures, Proc. General Discussion on Heat Transfer, London, Sept. 1951, Inst. Mech. Engrs., 167-73 (1952).

32. L. Andrussow, Conductibilite Thermique, Viscosite et Diffusion en Phase Gazeuse. Memoire 10. -Relation entre les Coefficients de ces phenomenes et l'Equation de Maxwell, (Thermal Conductivity, Viscosity and Diffusion in the Gas Phase. Report 10. Relation between the Coefficients of these Phenomena and the Equation of Maxwell), J. Chim. Phys. 52, 295-306 (1955).

33. F. Lazarre and B. Vodar, Measurement of the Viscosity of Compressed Nitrogen up to 3000 Atmospheres, Proc. Conf. Thermodynamic and Transport Properties Fluids, London, July 1957, Inst. Mech. Engrs., 159-62 (1958).

34. H. J. M. Hanley, The Viscosity and Thermal Conductivity Coefficients of Dilute Argon between 100 and 2000°K, Natl. Bur. Std. Tech. Note No. 333 (March 1966).

35. G. E. Childs and H. J. M. Hanley, The Viscosity and Thermal Conductivity Coefficients of Dilute Nitrogen and Oxygen, Natl. Bur. Std. Tech. Note No. 350 (October 1966).

36. A. Michels, Hub. Wijker and HK. Wijker, Isotherms of Argon Between 0°C and 150°C and Pressures up to 2900 Atmospheres, Physica 15, 627-33 (1949).

37. F. A. Guevara, B. B. McInteer and W. E. Wageman, Private Communication: R. DiPippo, An Absolute Determination of the Viscosity of Seven Gases to High Temperatures, Brown Univ., Providence, Ph. D. Thesis (1966).

38. H. J. M. Hanley, Discrepancies Between Viscosity Data for Simple Gases, to be published. An account of this work will also be published in the Proc. of the 7th Conference on Thermal Conductivity, Natl. Bur. Stds. (1967).

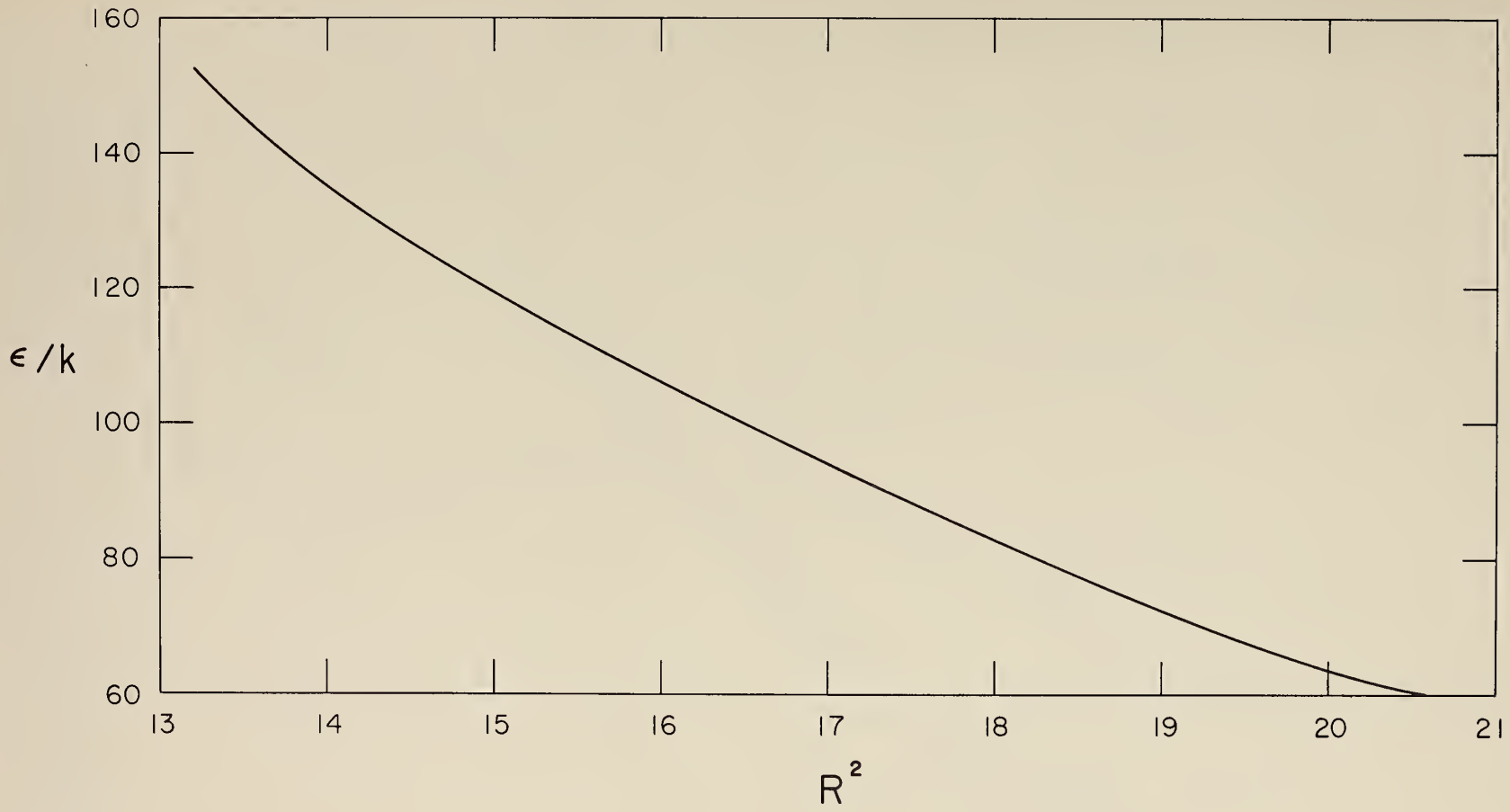

Fig. 1. The loci of potential parameters for the 12-6 potential function which give an exact fit to the viscosity of argon at T = 123°K.

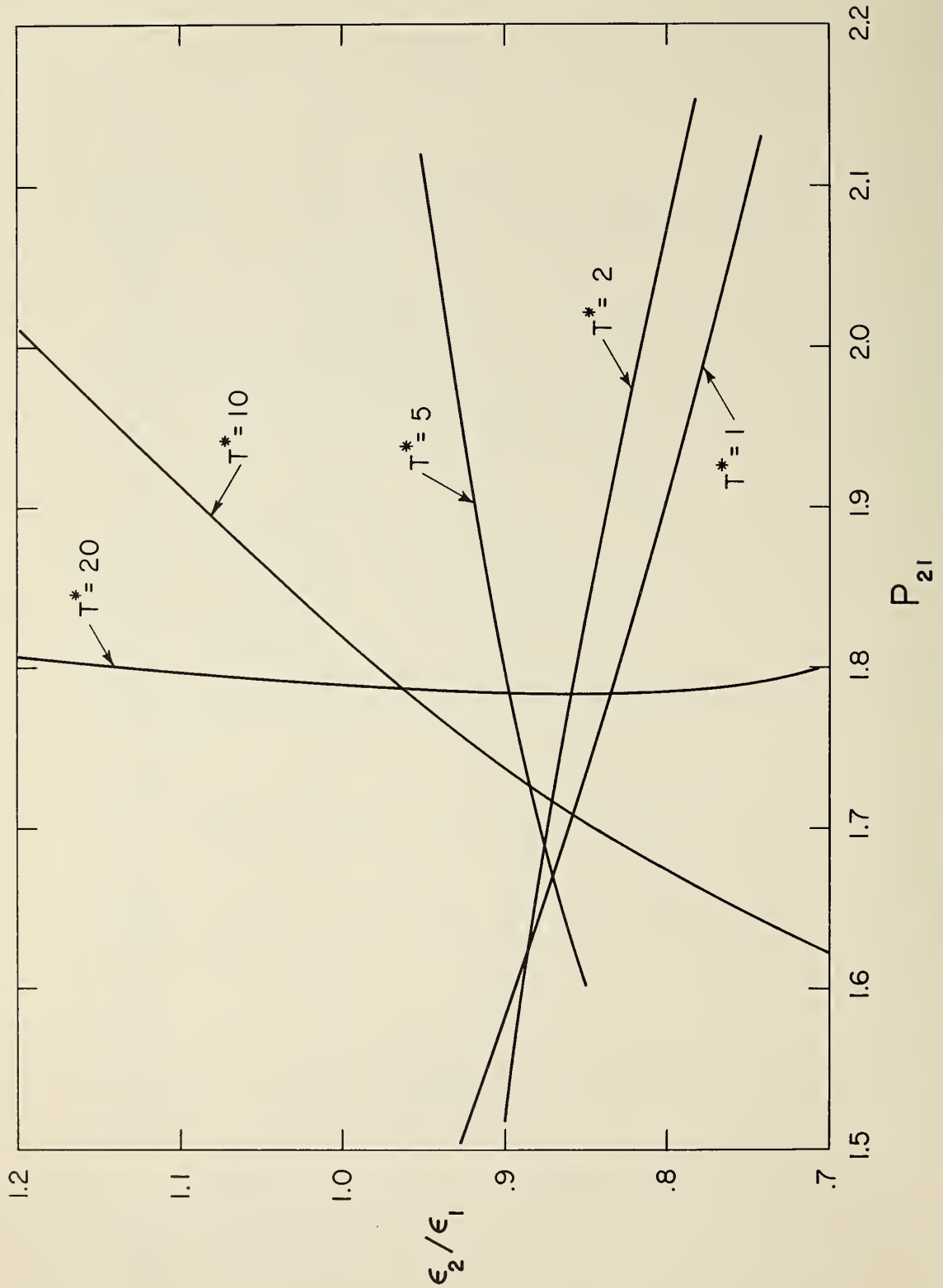

Fig. 2. The loci of potential parameter ratios which give a precise conversion of several values of the second virial coefficient from the 12-6 potential function to the exp:6 function with $\alpha = 12$.

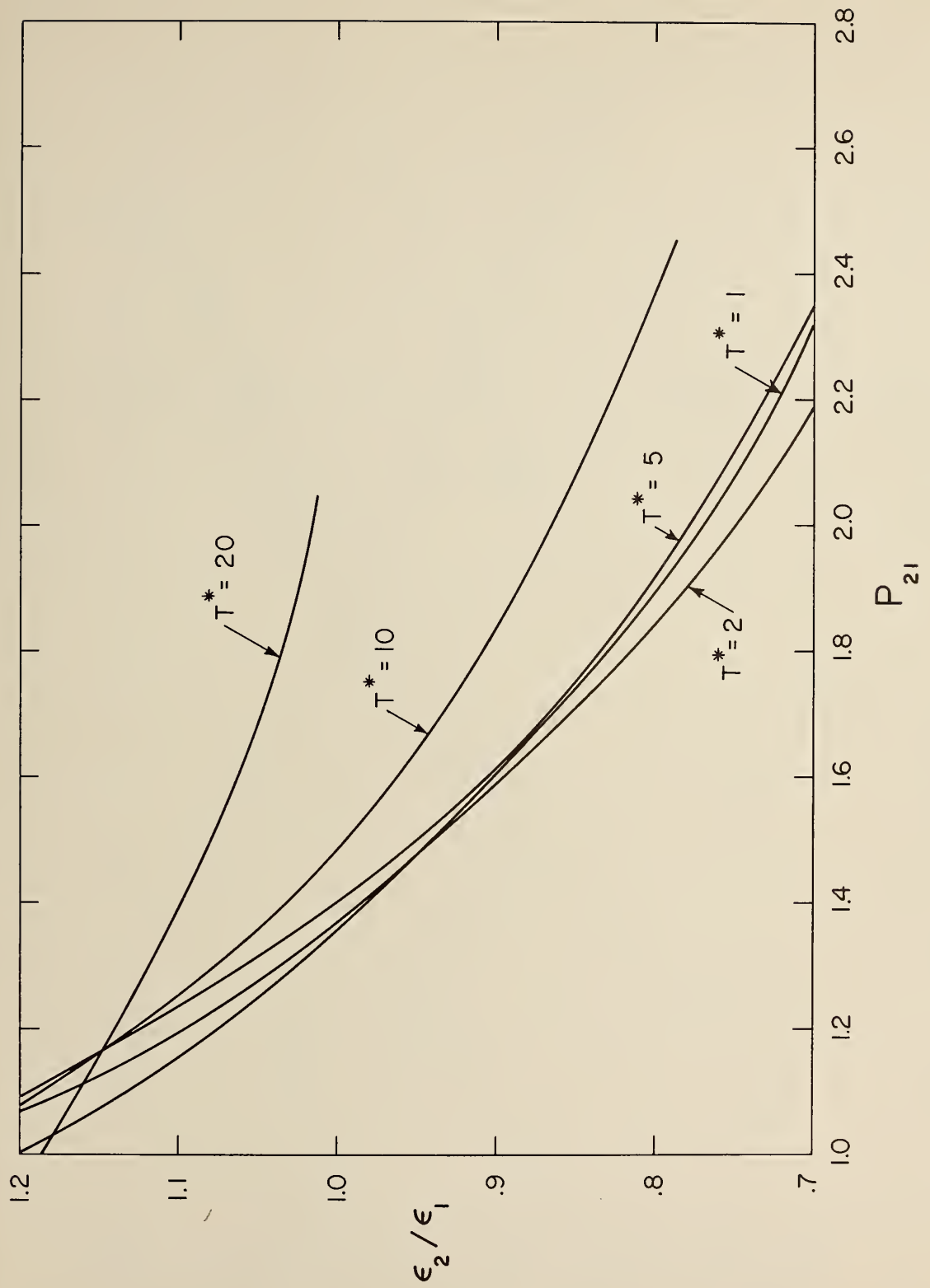

Fig. 3. The loci of potential parameter ratios which give a precise conversion of several values of the first derivative of the second virial coefficient from the 12-6 potential function to the exp:6 function with $\alpha = 12$.

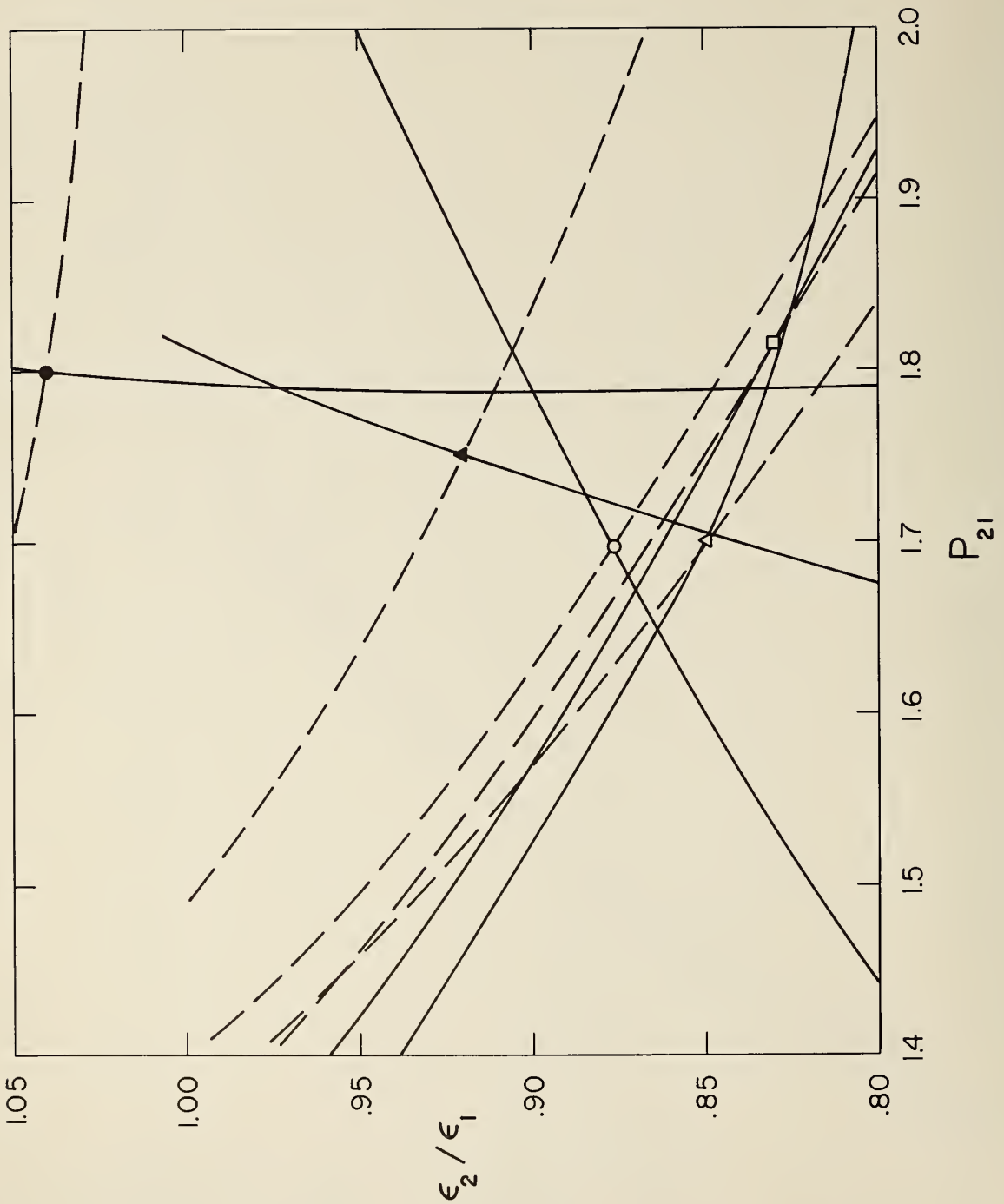

Fig. 4. The loci of potential parameter ratios which give a precise conversion from the 12-6 potential function to the exp:6 function with $\alpha = 12$. Both the second virial and its first derivative are included. Each intersection point gives the ratio for the simultaneous conversion of both properties. The solid curve represents B^*, the broken curve B'^*. The following T^*_{12-6} are included □ , 1.0; △ , 2.0; ○ , 5.0; ▲ , 10.0; ● , 20.0.

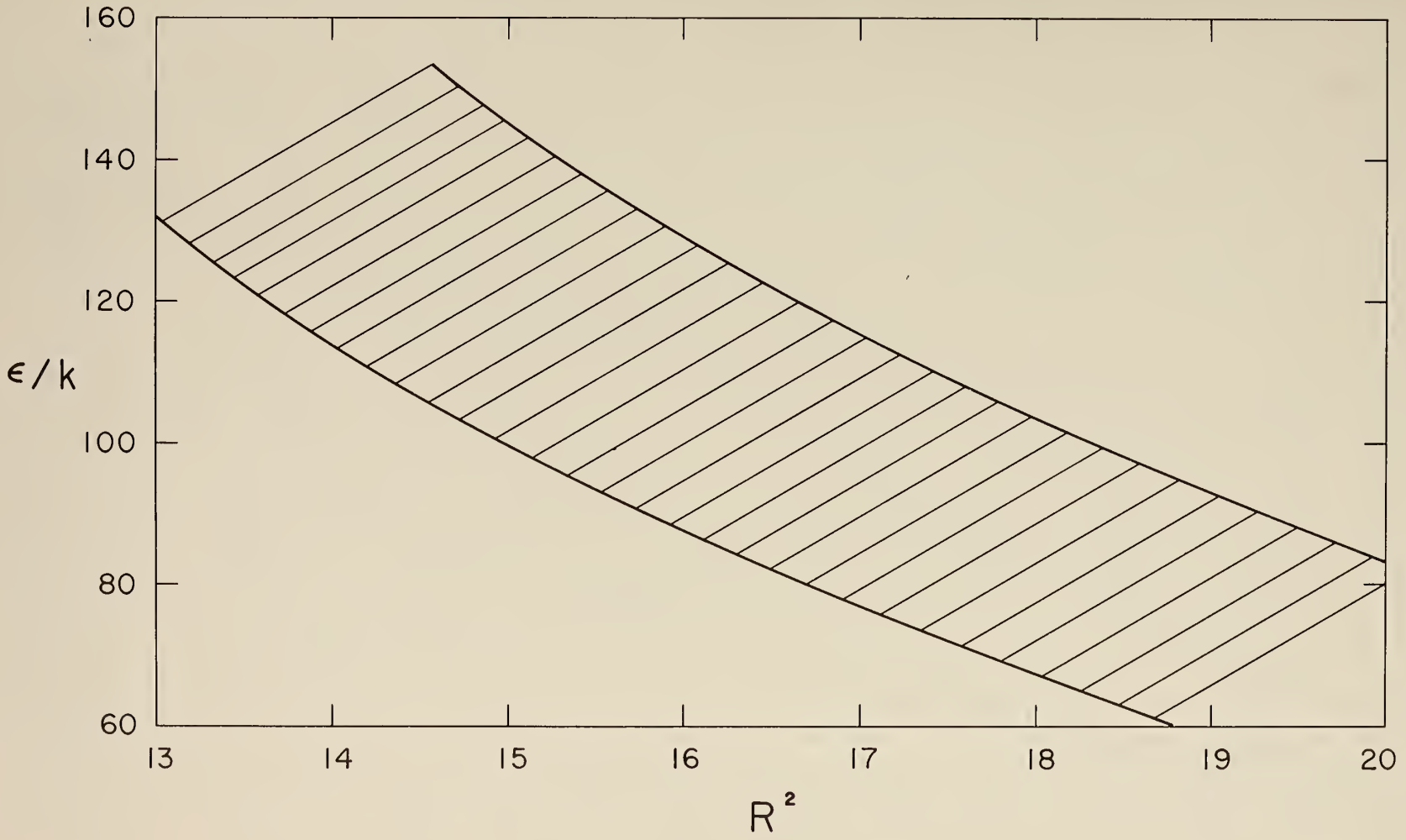

Fig. 5. The loci of potential parameters, for the 12-6 potential function, which fit the viscosity of argon at T = 123°K within an assigned tolerance.

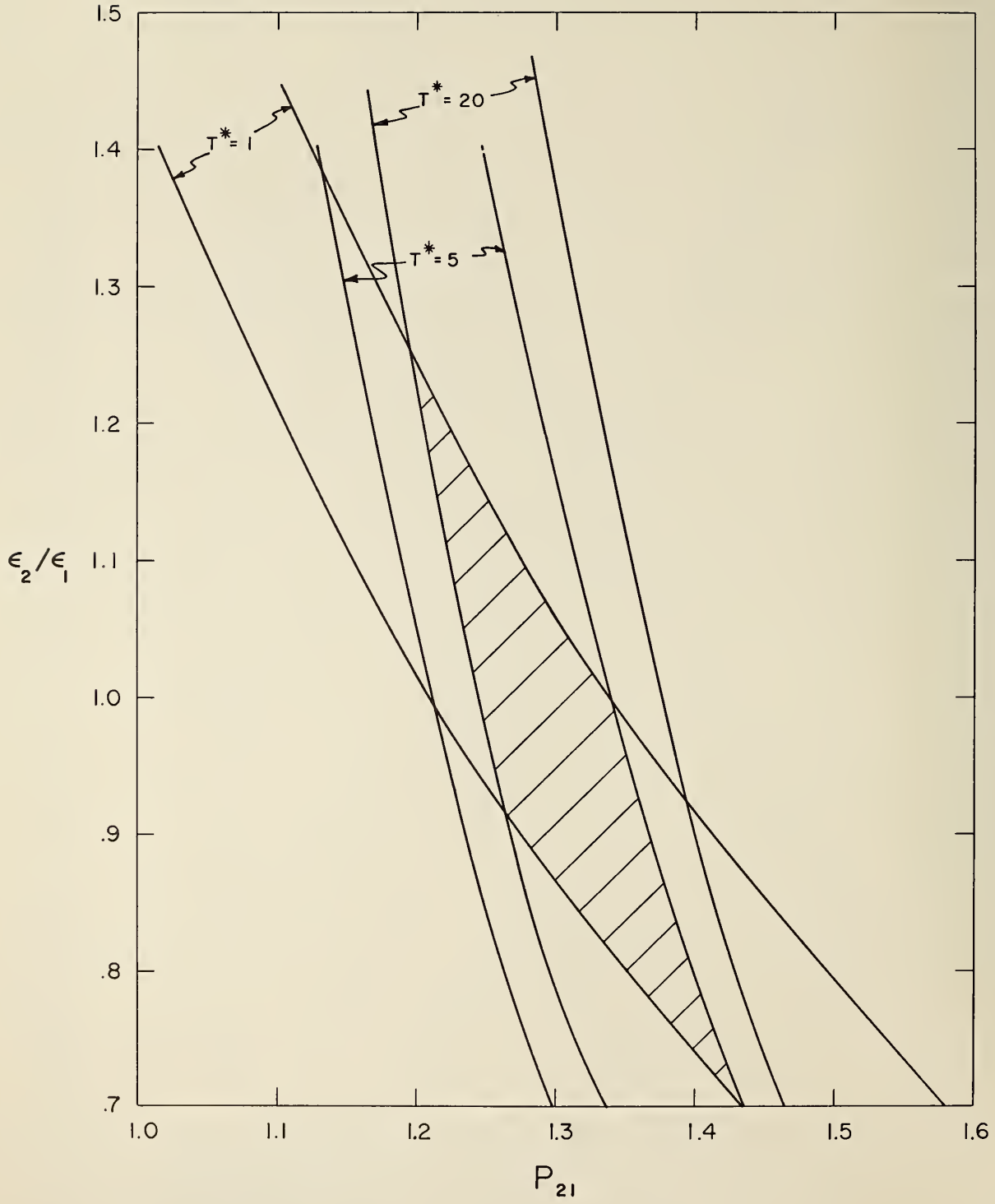

Fig. 6. The loci of potential parameter ratios which, within assigned tolerances, convert the second virial coefficients of the 12-6 potential function into those for the exp:6 function with $\alpha = 12$ at three temperatures.

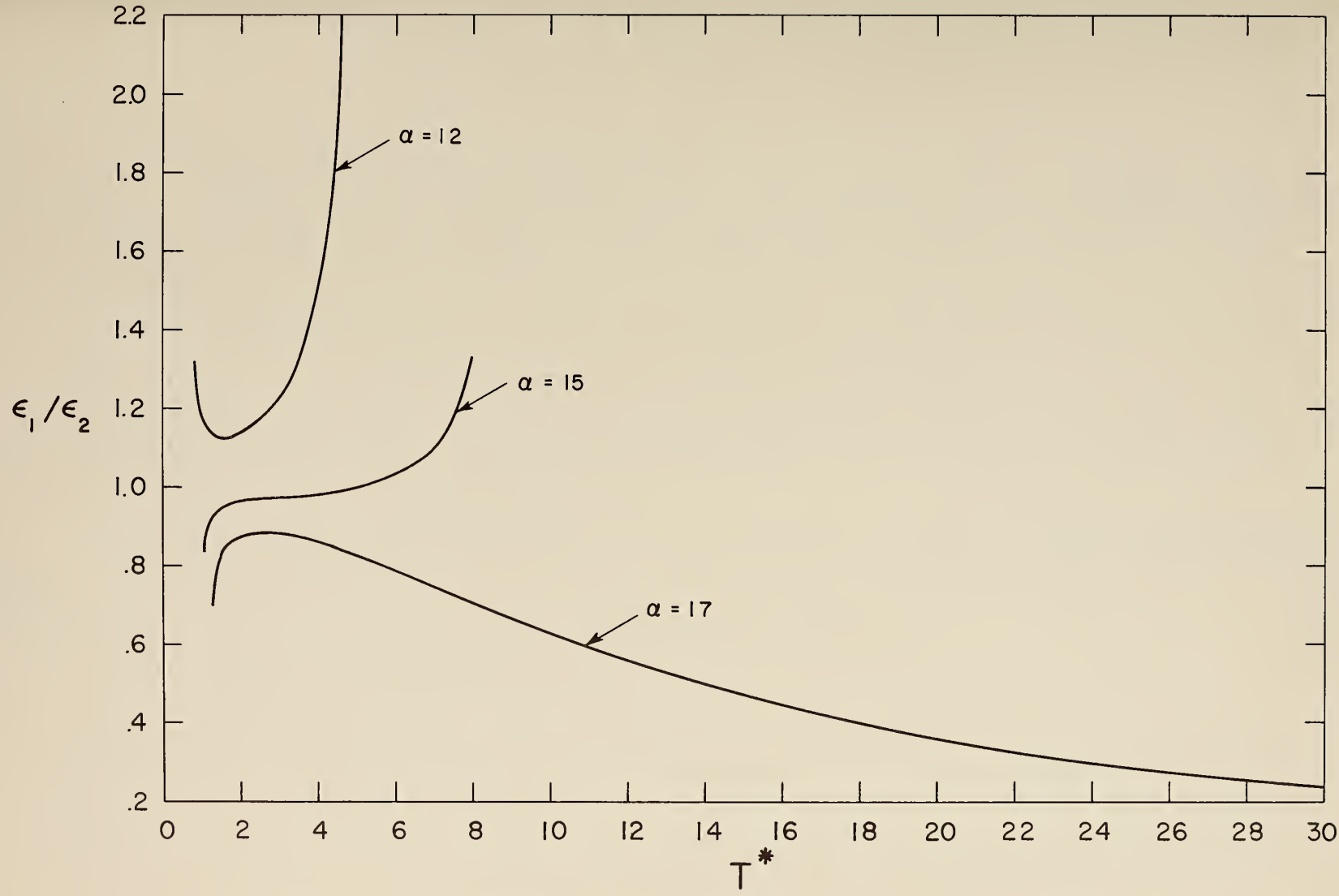

Fig. 7. The ratios of the well depths, ϵ_1/ϵ_2, versus T^*_{12-6} by means of which one can replace the viscosity calculated for the 12-6 potential function by that calculated for the exp:6 function. These ratios go with the P_{12} of Fig. 9. Note that the ratios are most nearly constant in the T^*_{12-6} range 2.0 - 4.0.

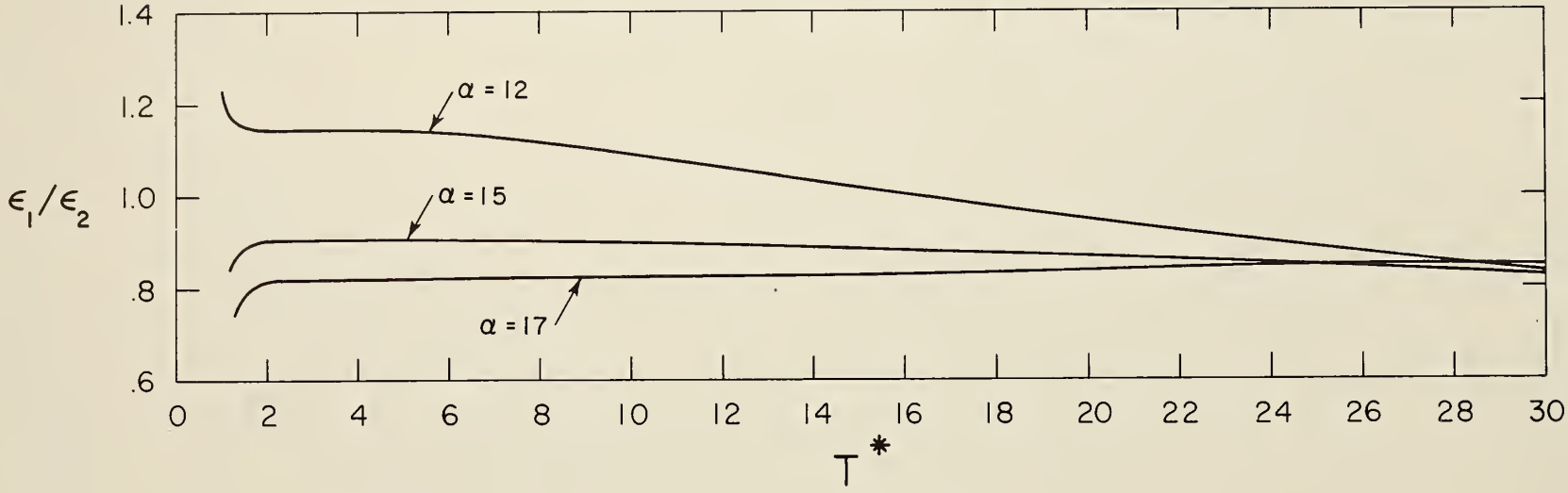

Fig. 8. The ratio of the well depths, ϵ_1/ϵ_2, versus T^*_{12-6} by means of which one can replace the second virial coefficients calculated for the 12-6 potential function by that calculated for the exp:6 function. These ratios go with the P_{12} of Fig. 10. Note that these ratios are quite constant above $T^*_{12-6} = 2.0$.

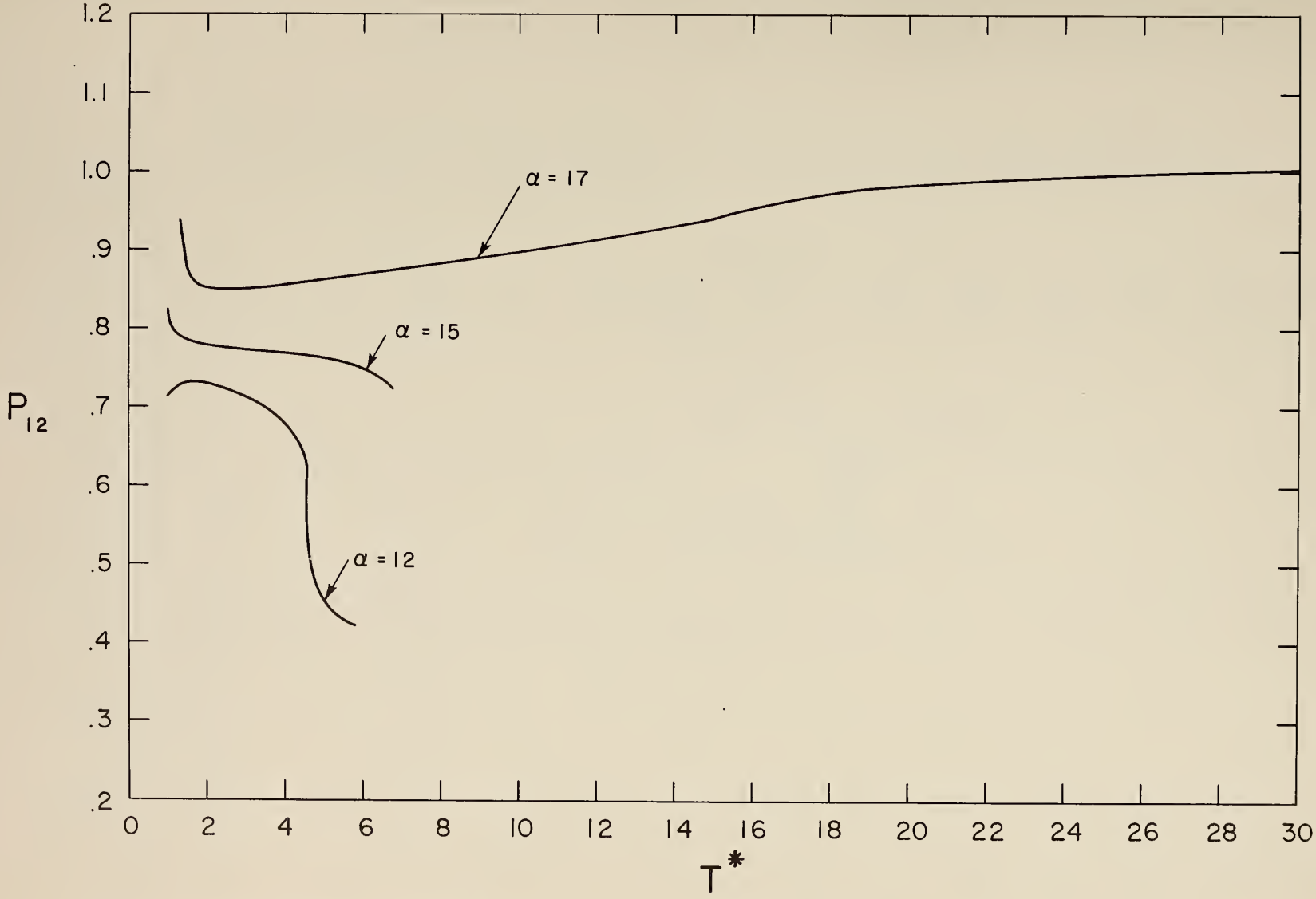

Fig. 9. The ratio of potential parameters, P_{12}, versus T^*_{12-6} by means of which one can replace the viscosity calculated for the 12-6 potential function by that calculated for the exp:6 function.

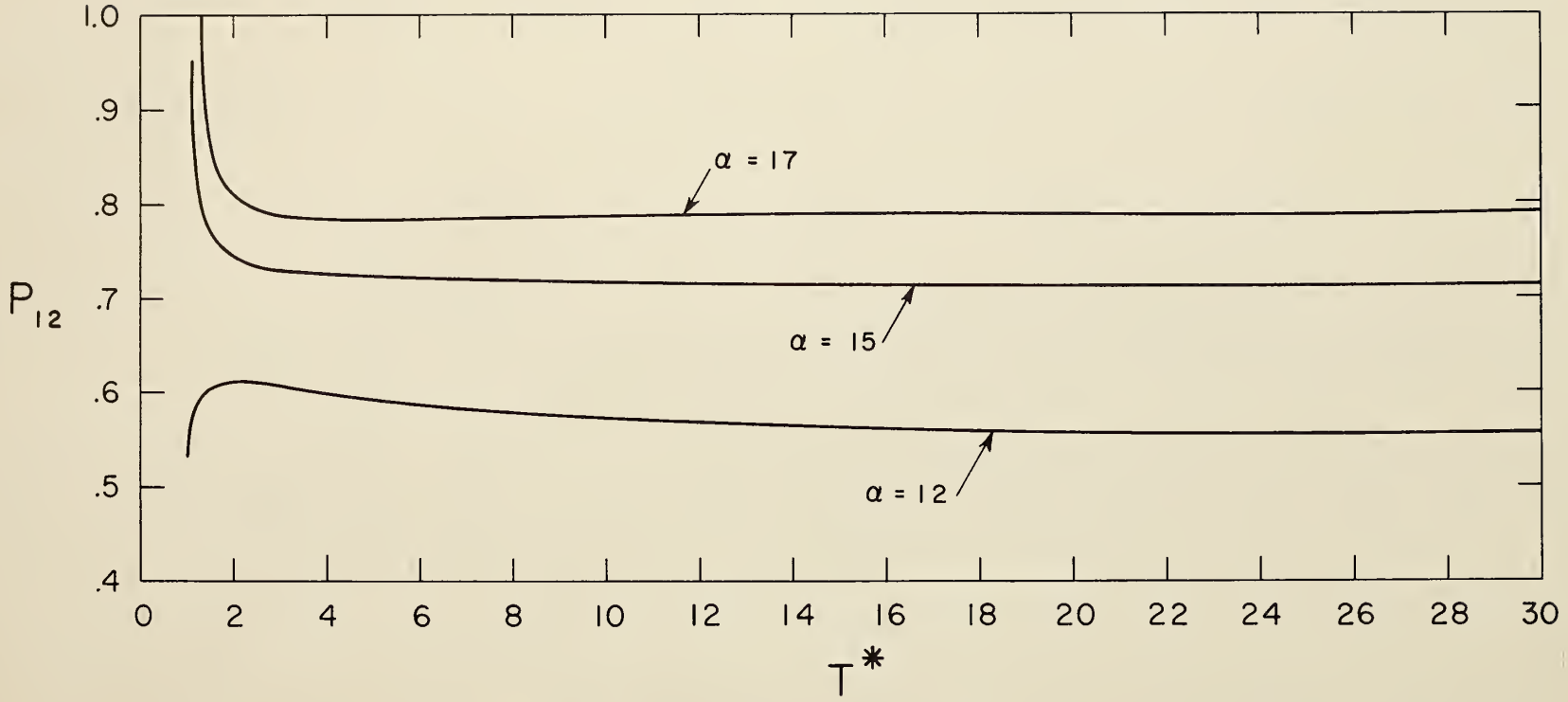

Fig. 10. The ratio of the potential parameters P_{12} versus T^*_{12-6} by means of which one can replace the second virial coefficients calculated for the 12-6 potential function by that calculated for the exp:6 function.

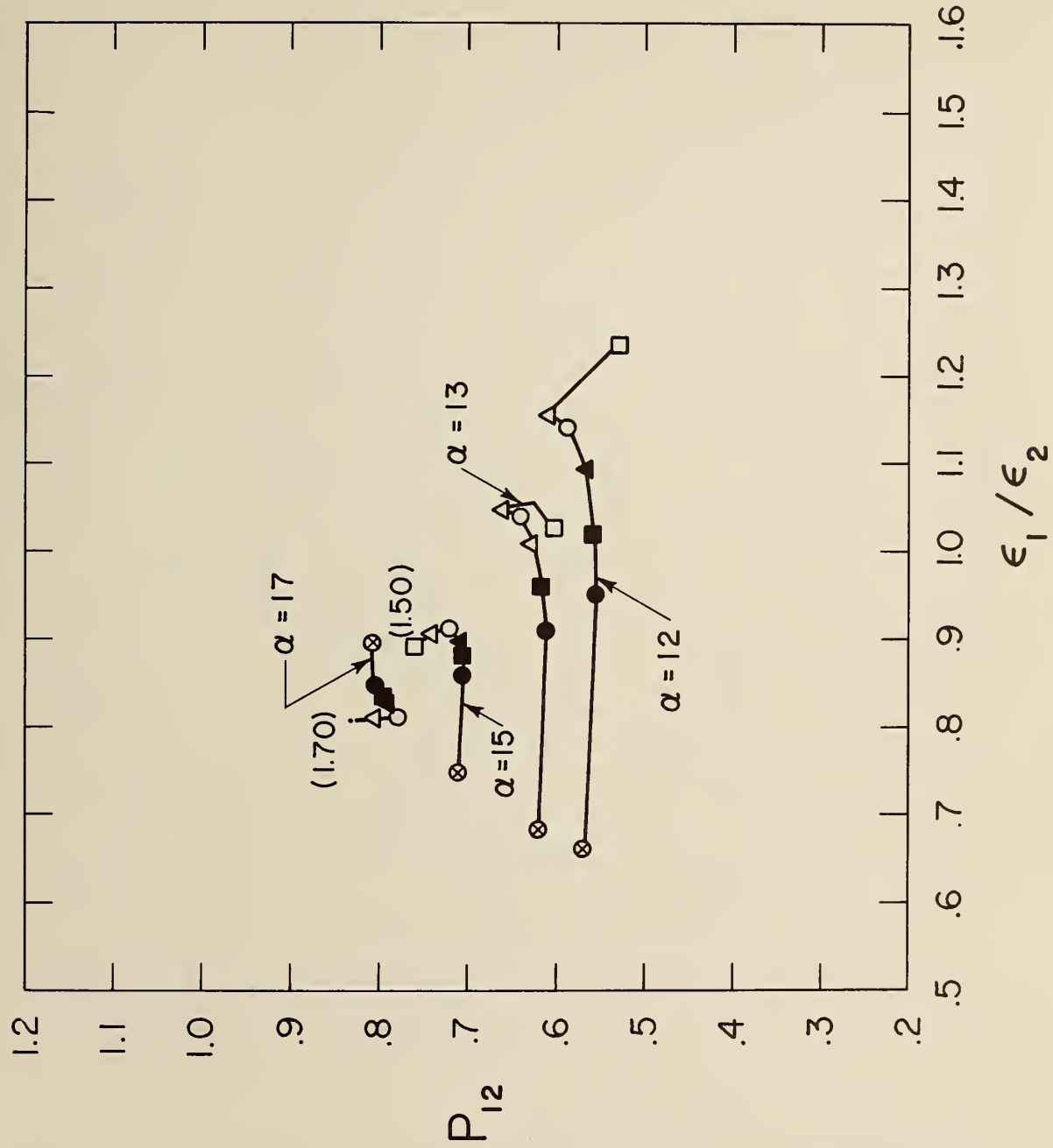

Fig. 11. ϵ ratios versus P_{12} ratios for the replacement of the second virial coefficients calculated for the 12-6 potential function by that calculated for the exp:6 function. Note that each point on a given curve refers to a different temperature. The following values of T^*_{12-6} are included □ , 1.0; △ , 2.0; ○ , 5.0; ▲ , 10.0; ■ , 15.0; ● , 20.0; ⊗ , 50.0.

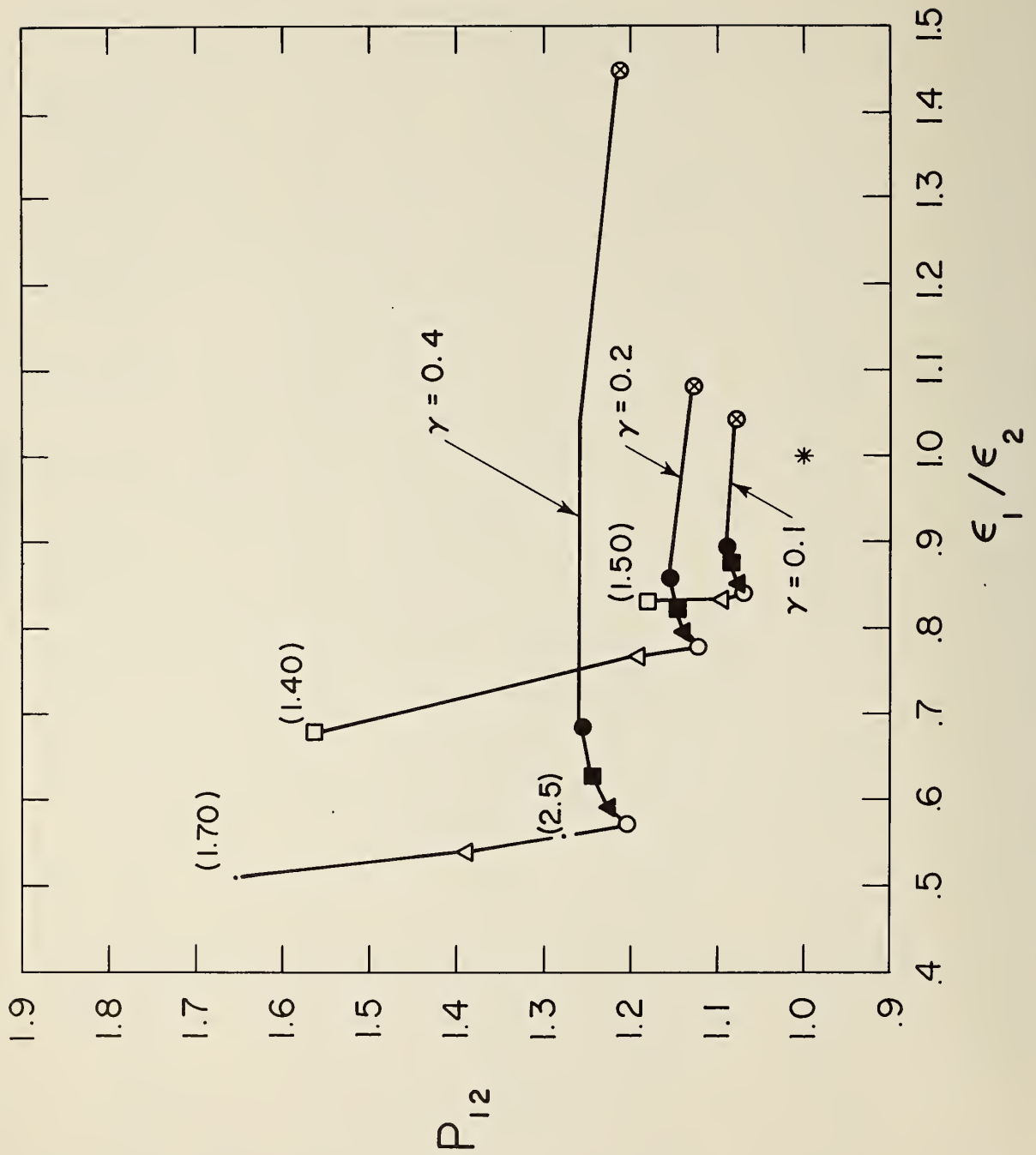

Fig. 12. ϵ ratios versus P_{12} ratios for the replacement of the second virial coefficients calculated for the 12-6 potential function by that calculated for the Kihara function. The key to temperatures along the curve is as in Fig. 11. Note that an exact fit reduces a curve to a point as demonstrated by the point at (1.0, 1.0) for $\gamma = 0$.

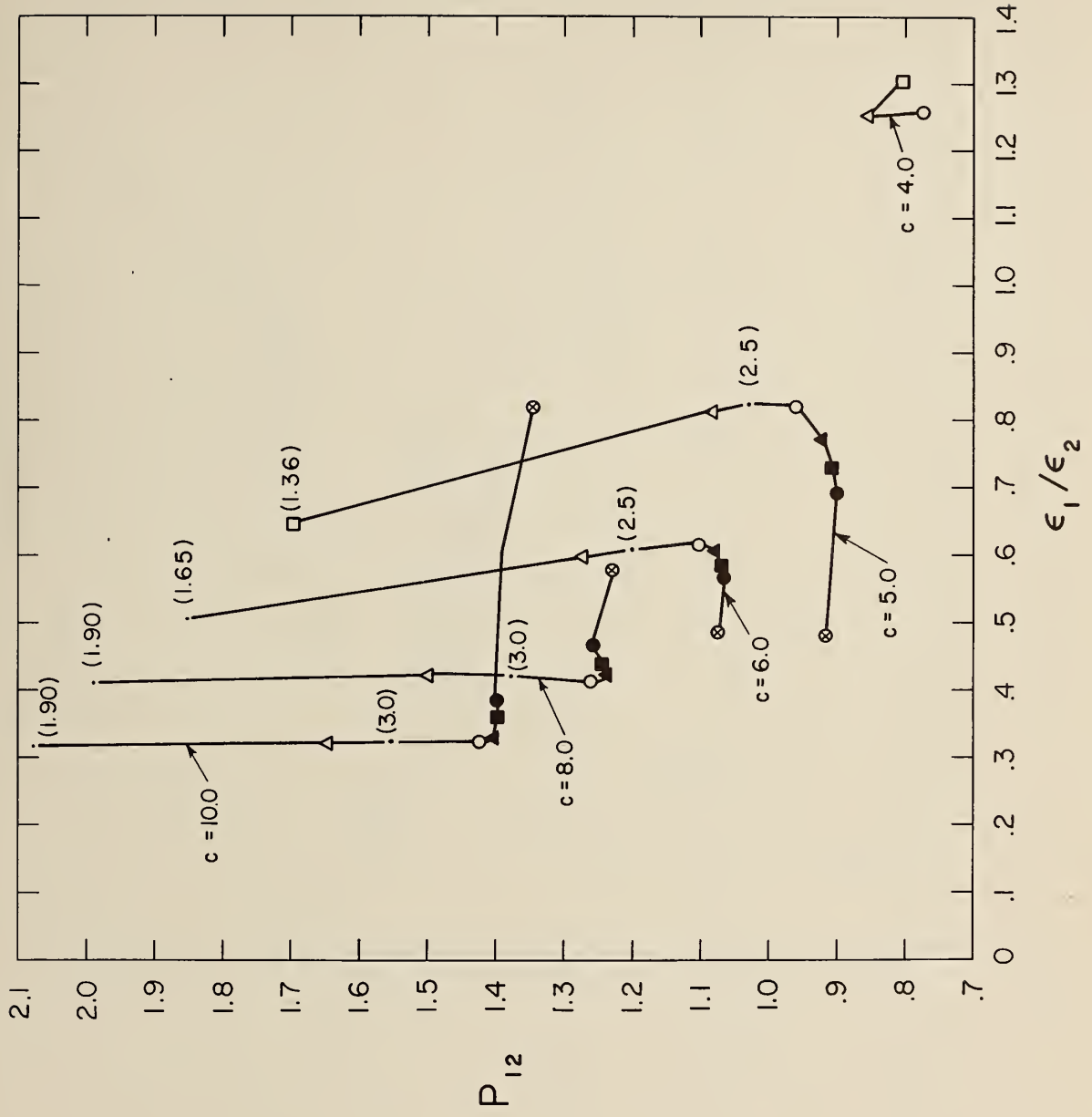

Fig. 13. ϵ ratios versus P_{12} ratios for the replacement of the second virial coefficients calculated for the 12-6 potential function by that calculated for the Morse function. The key to temperatures along the curve is as in Fig. 11.

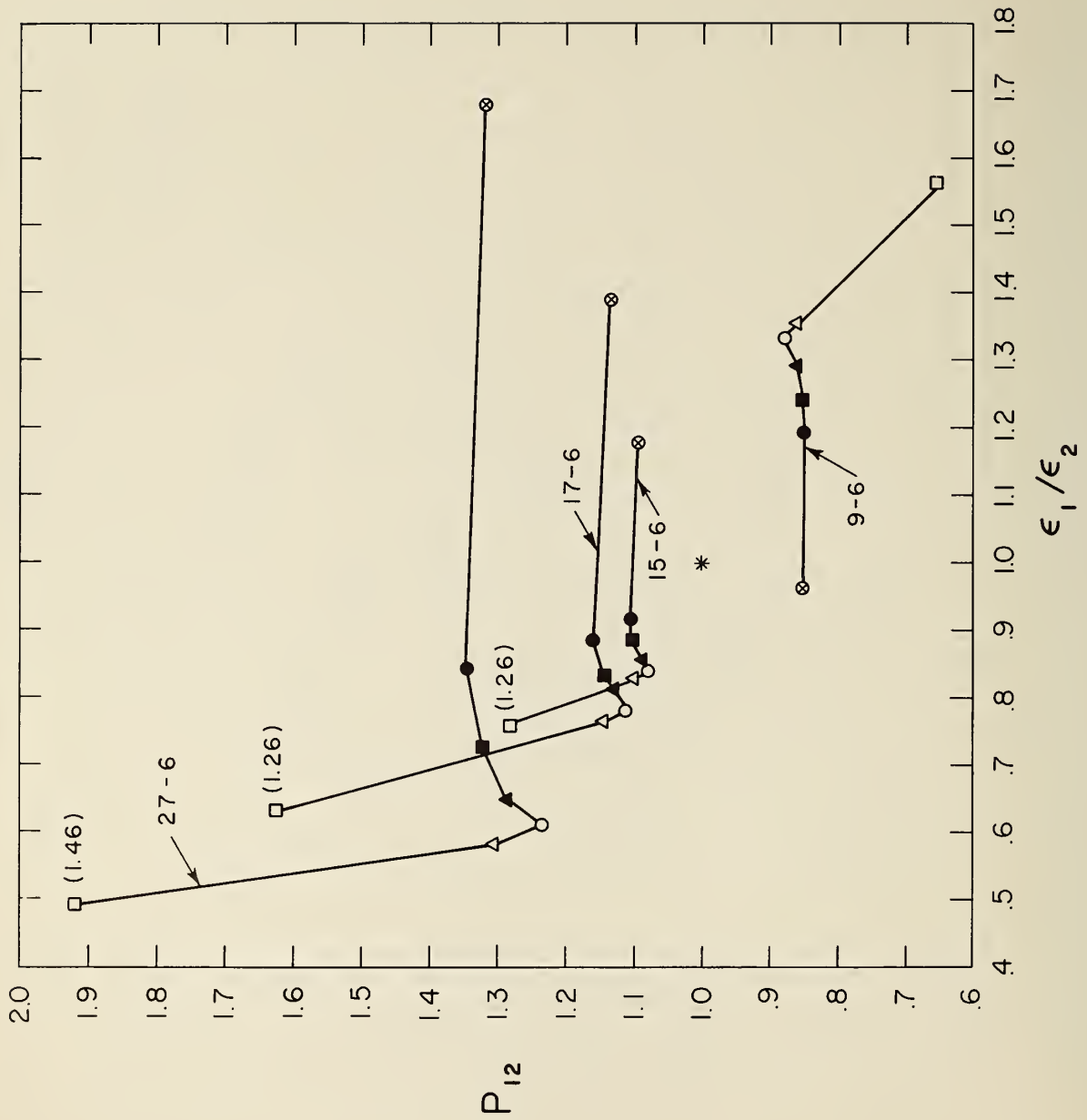

Fig. 14. ϵ ratios versus P_{12} ratios for the replacement of the second virial coefficients calculated for the 12-6 potential function by that calculated for the m-6 potential function. The key to temperatures along the curve is as in Fig. 11.

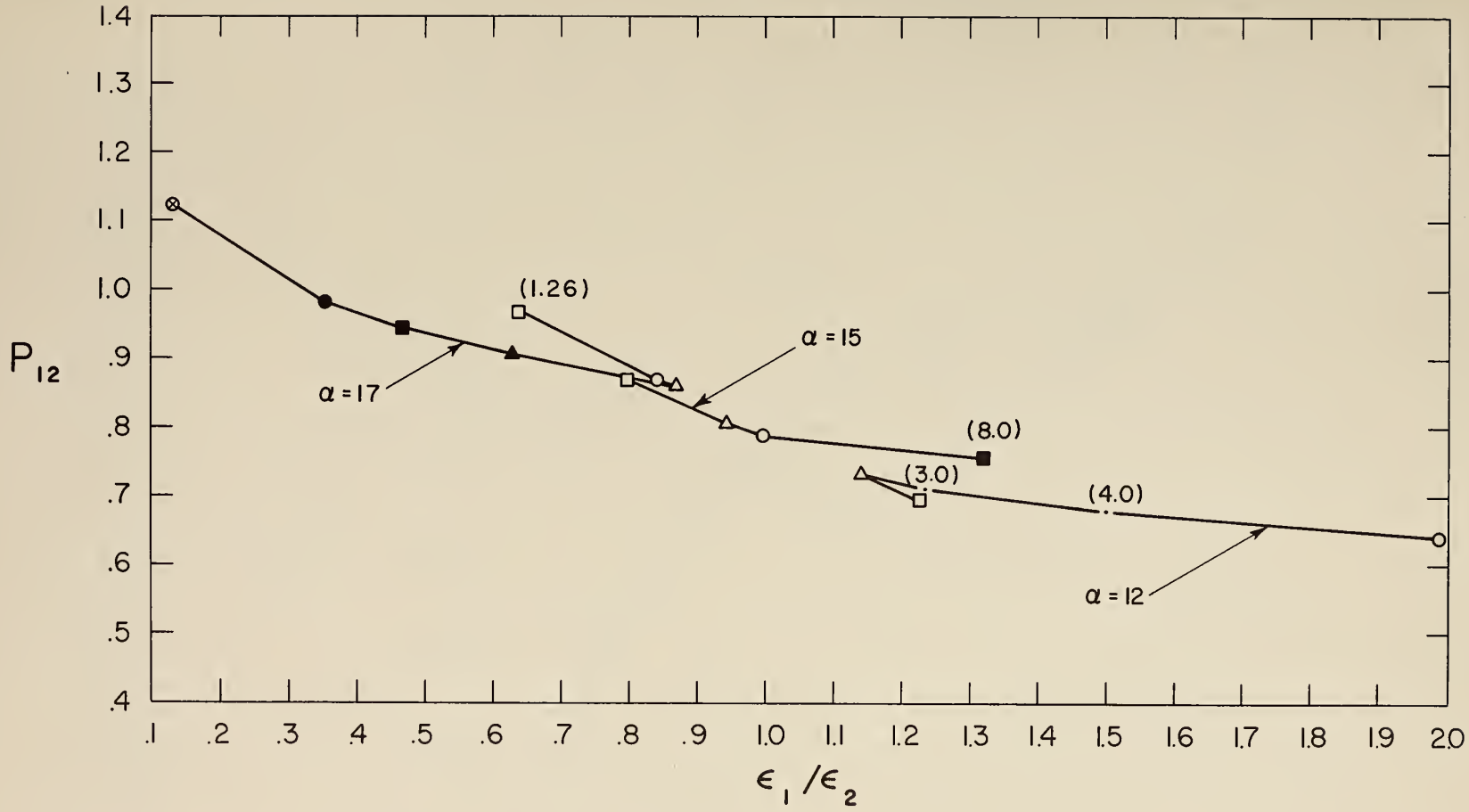

Fig. 15. ε ratios versus P_{12} ratios for the replacement of the viscosity calculated for the 12-6 potential function by that calculated for the exp:6 function. Except where indicated to the contrary, the key to temperatures along the curve is as in Fig. 11.

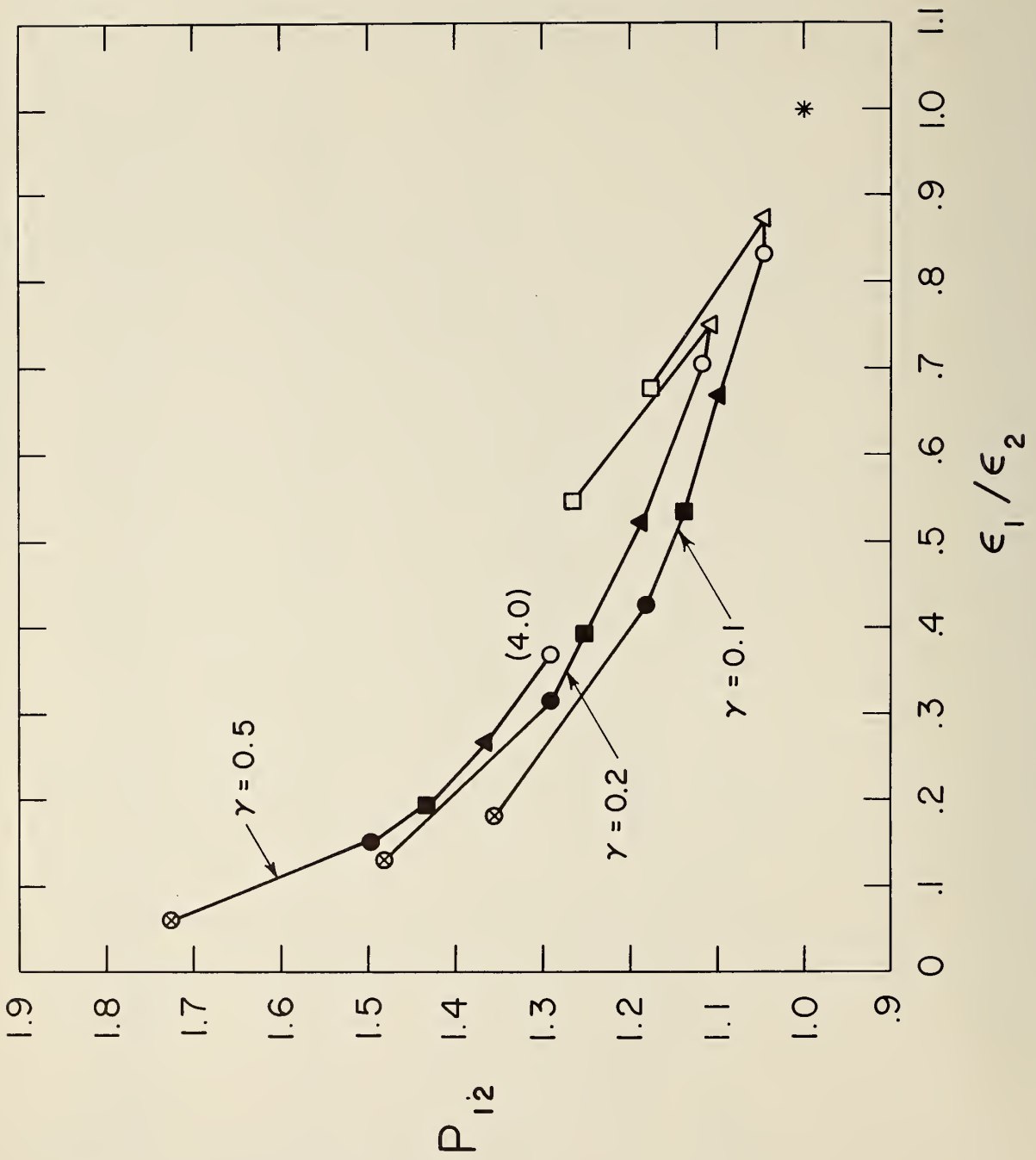

Fig. 16. ϵ ratios versus P_{12} ratios for the replacement of the viscosity calculated for the 12-6 potential function by that calculated for the Kihara potential. The key to temperatures along the curve is as in Fig. 11.

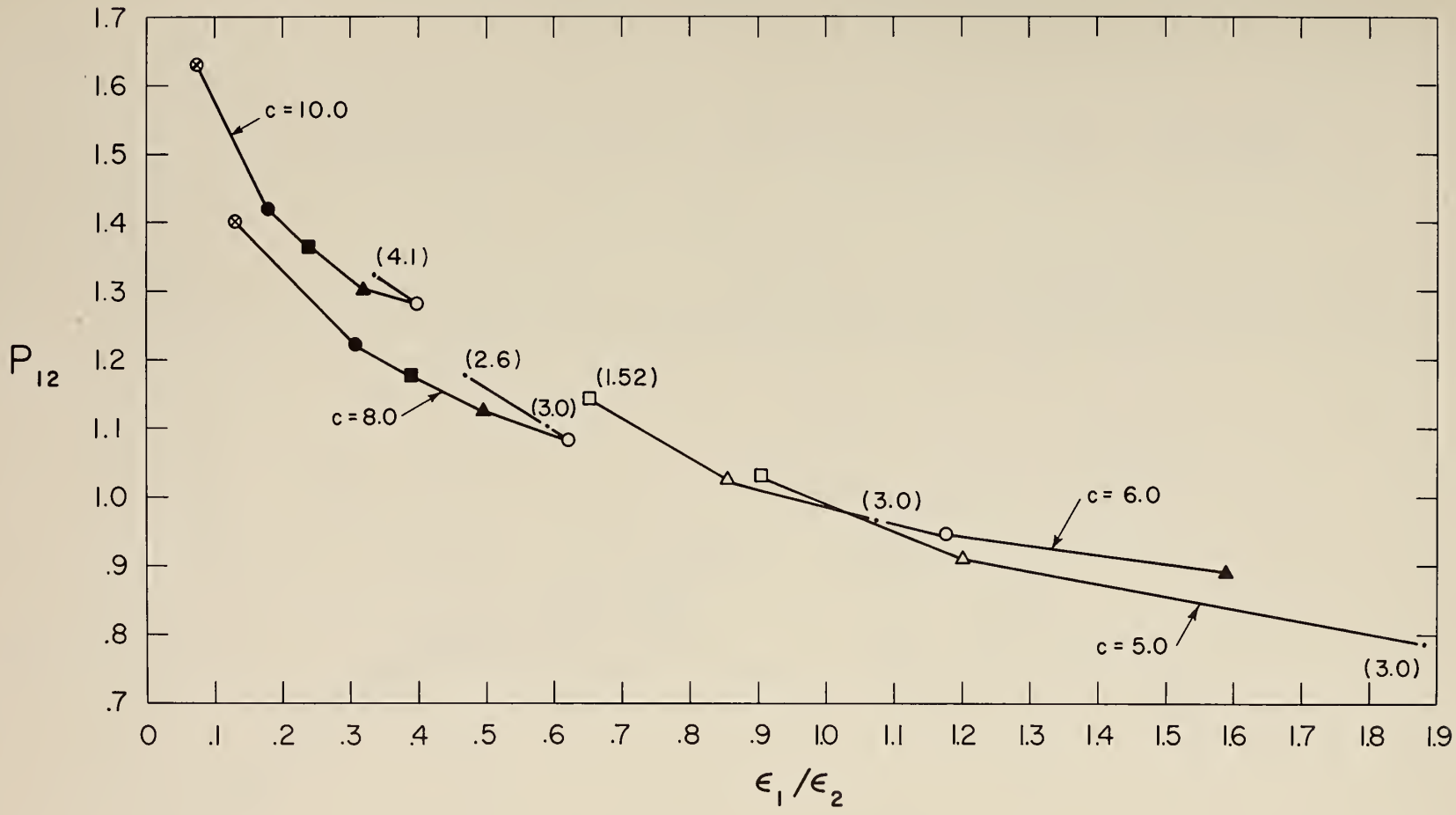

Fig. 17. ϵ ratios versus P_{12} ratios for the replacement of the viscosity calculated for the 12-6 potential function by that calculated for the Morse function. The key to temperatures along the curves is as in Fig. 11.

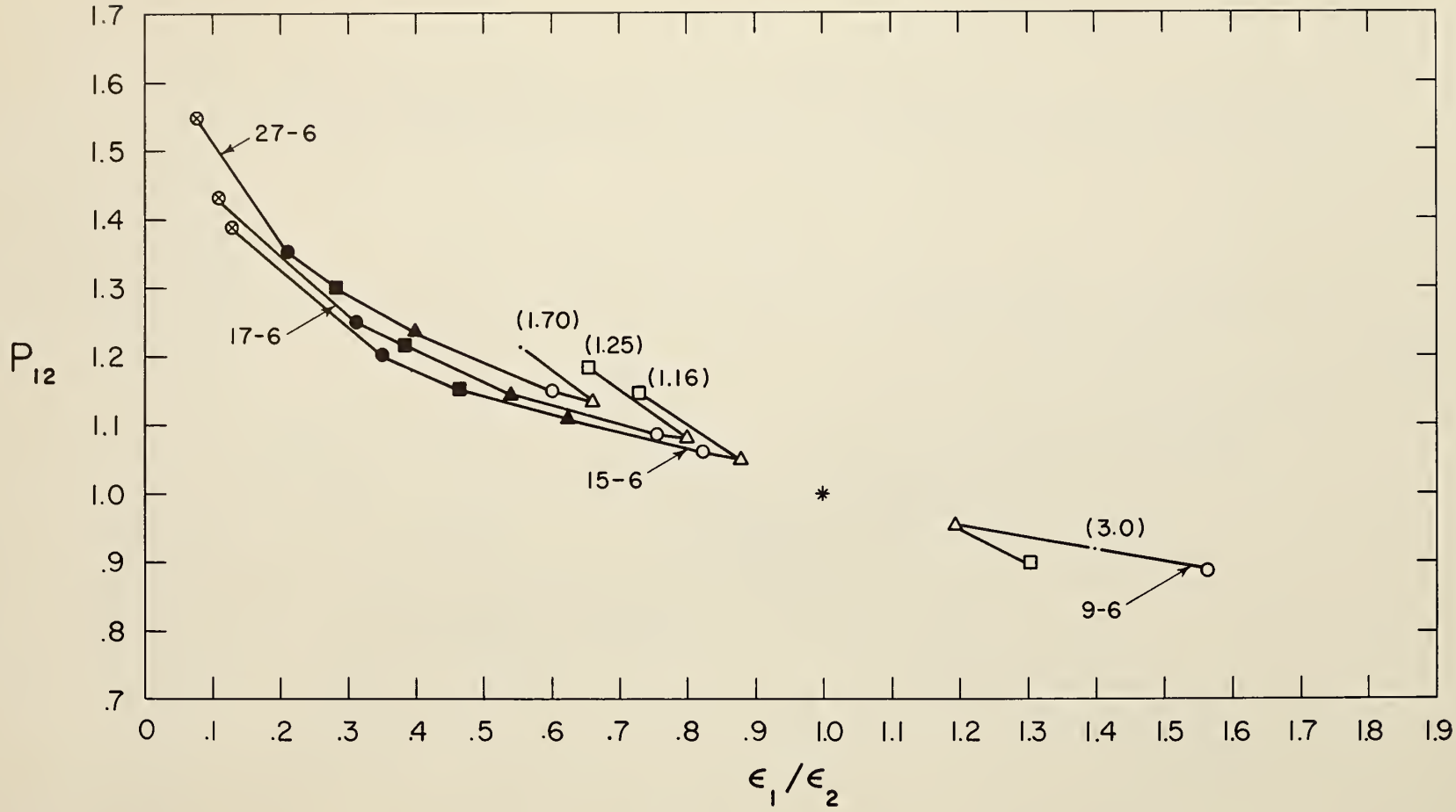

Fig. 18. ϵ ratios versus P_{12} ratios for the replacement of the viscosity calculated for the 12-6 potential function by that calculated for the m-6 function. Except where indicated to the contrary, the key to temperatures along the curves is as in Fig. 11.

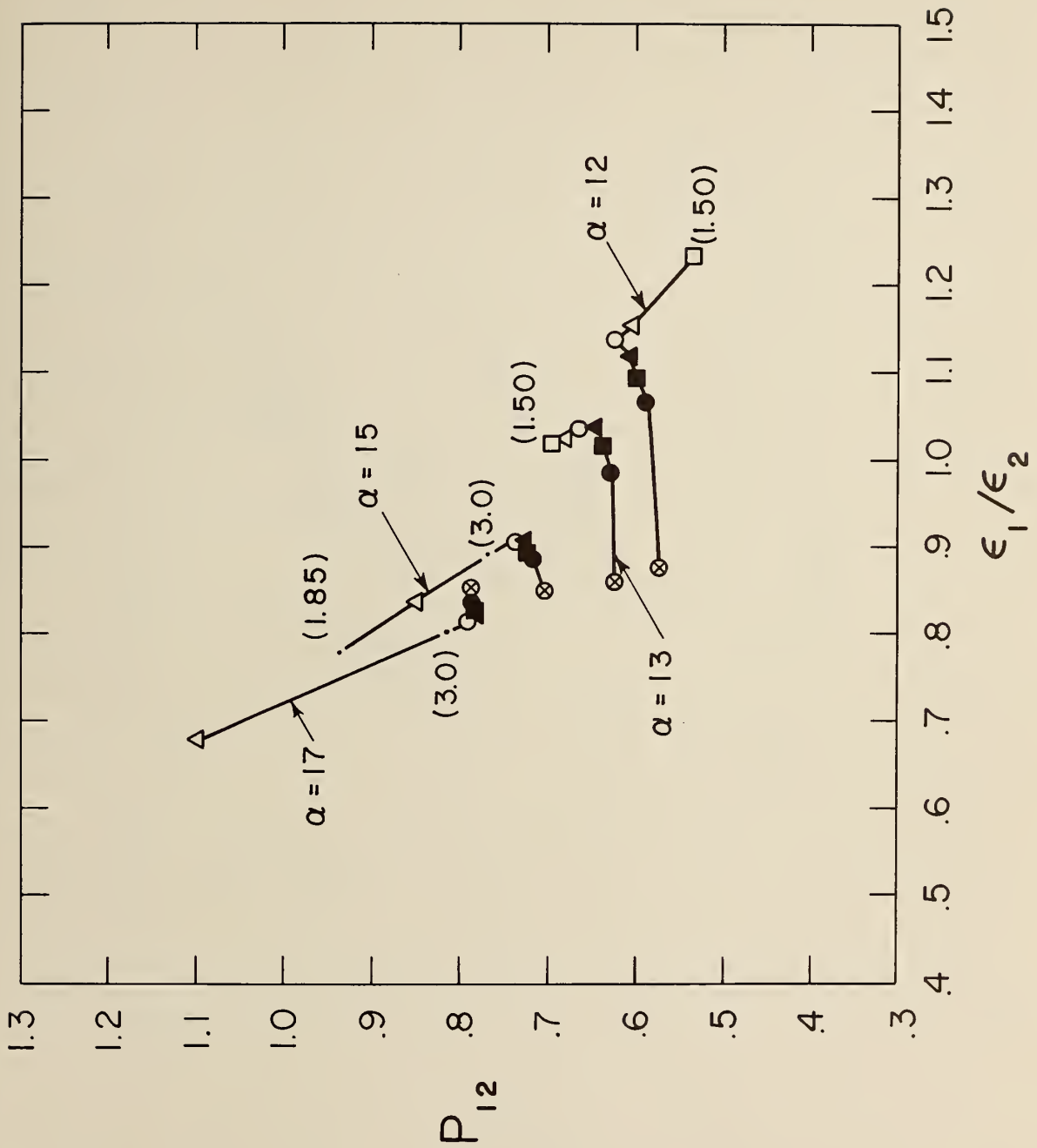

Fig. 19. ϵ ratios versus P_{12} ratios for the replacement of the zero density Joule-Thomson coefficient calculated for the 12-6 potential function by that calculated for the exp:6 function. The key to temperatures along the curves is as in Fig. 11, unless otherwise indicated.

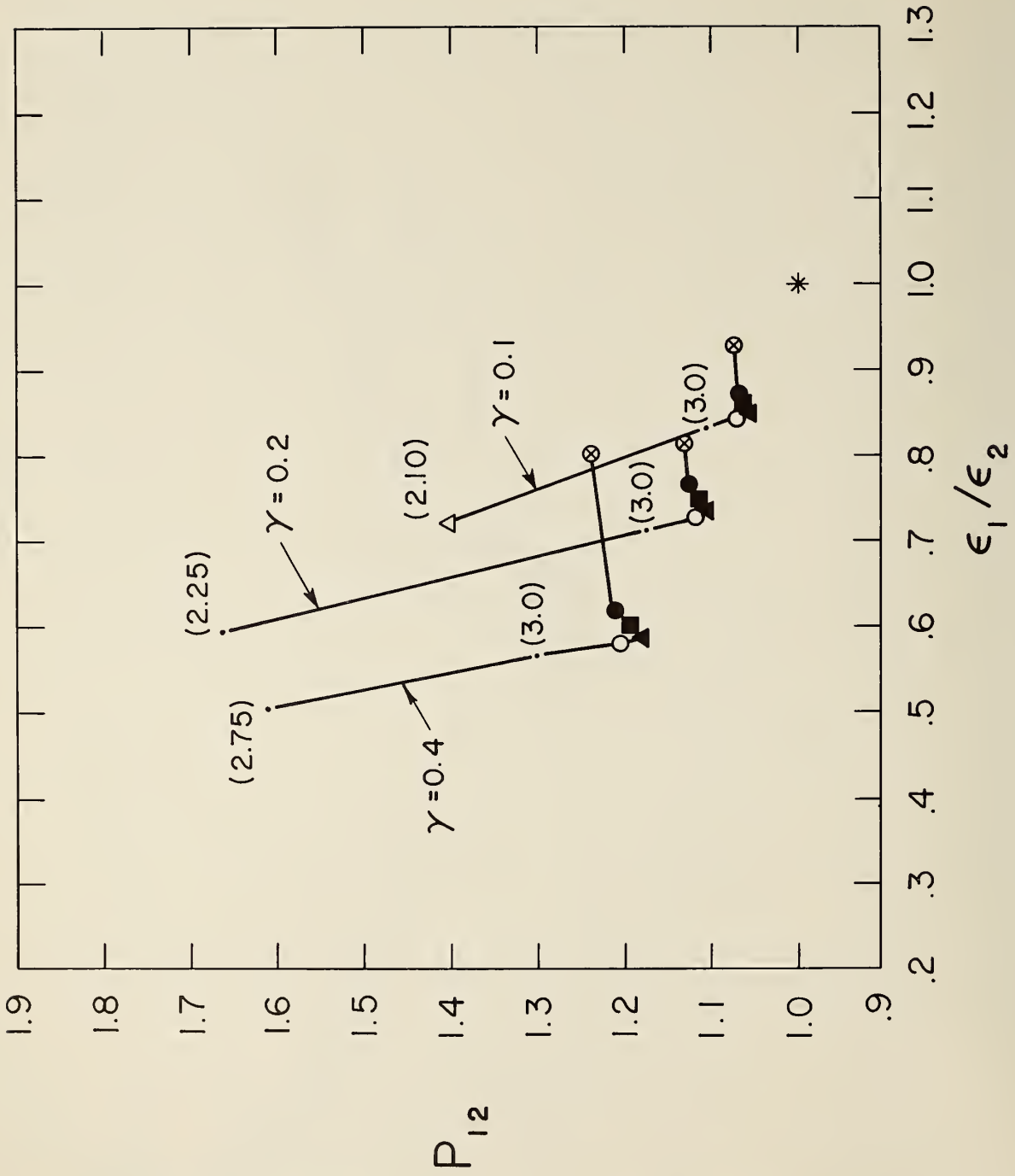

Fig. 20. ε ratios versus P_{12} ratios for the replacement of the zero density Joule-Thomson coefficient calculated for the 12-6 potential function by that calculated for the Kihara function. Unless otherwise indicated, the key to temperatures along the curves is as in Fig. 11.

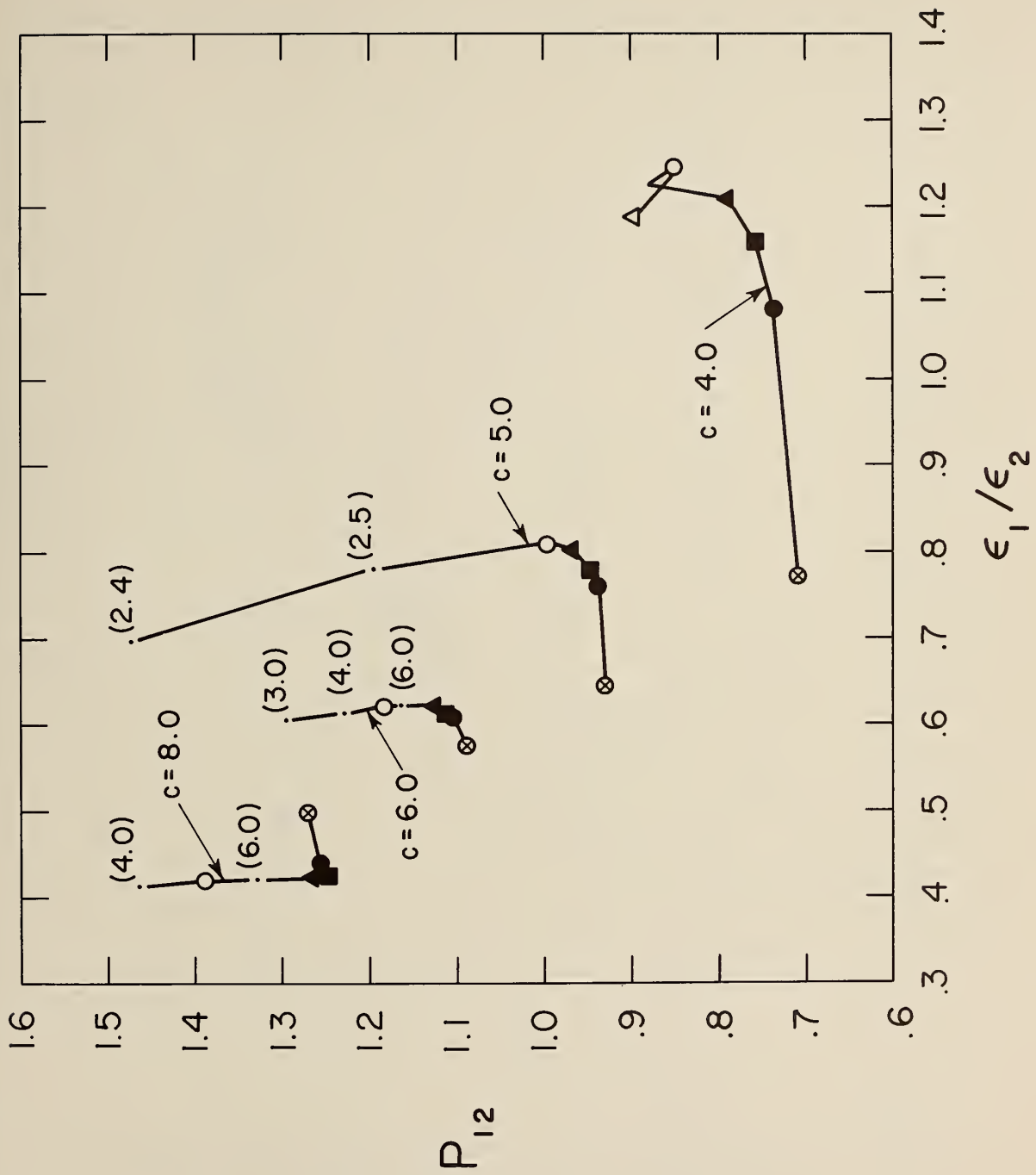

Fig. 21. ϵ ratios versus P_{12} ratios for the replacement of the zero density Joule-Thomson coefficient calculated for the 12-6 potential function by that calculated for the Morse function. Unless otherwise indicated, the key to the temperatures along the curves is as in Fig. 11.

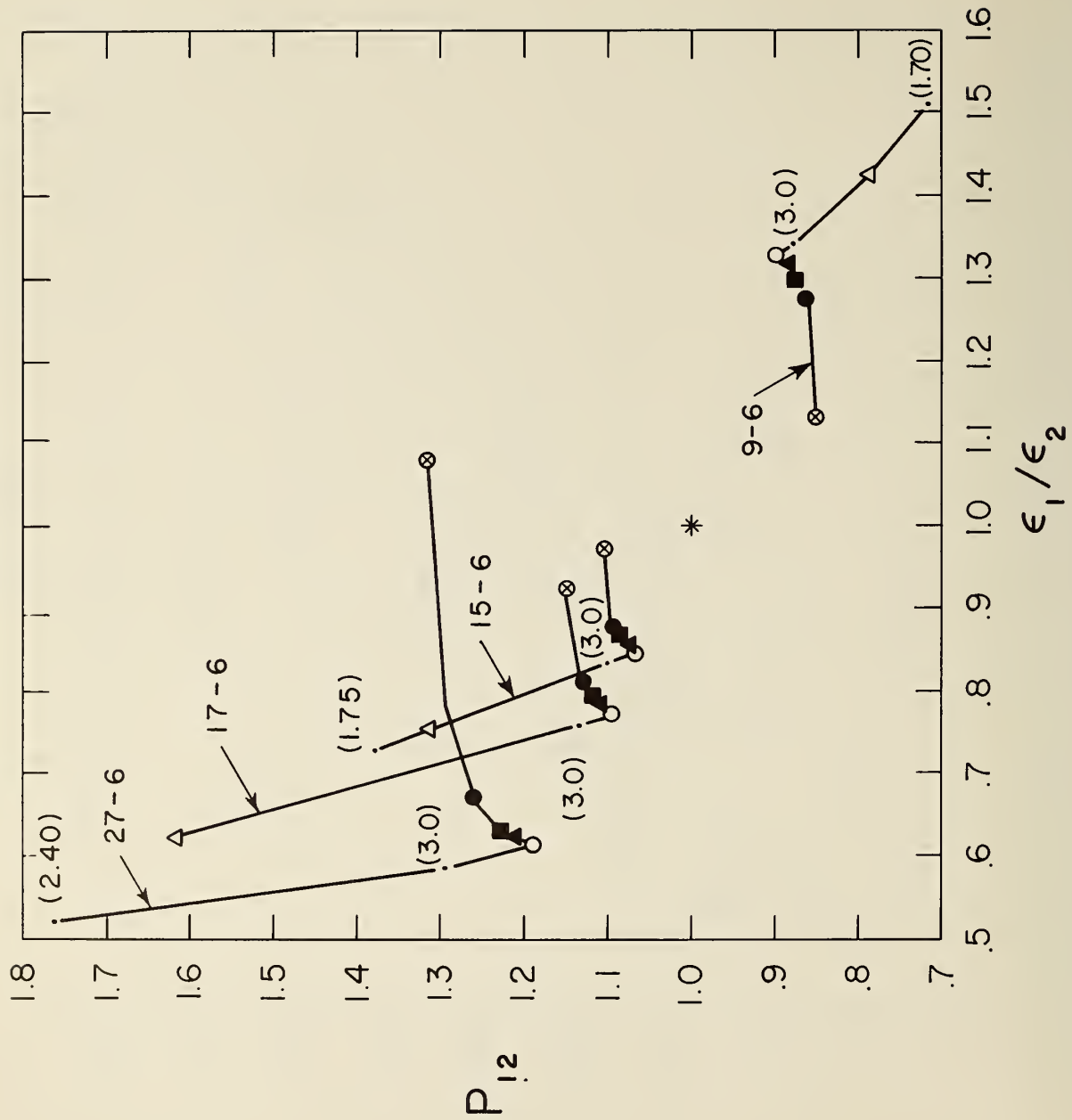

Fig. 22. ϵ ratios versus P_{12} ratios for the replacement of the zero density Joule-Thomson coefficient calculated for the 12-6 potential function by that calculated for the m-6 function. Unless otherwise indicated, the key to the temperatures along the curves is as in Fig. 11.

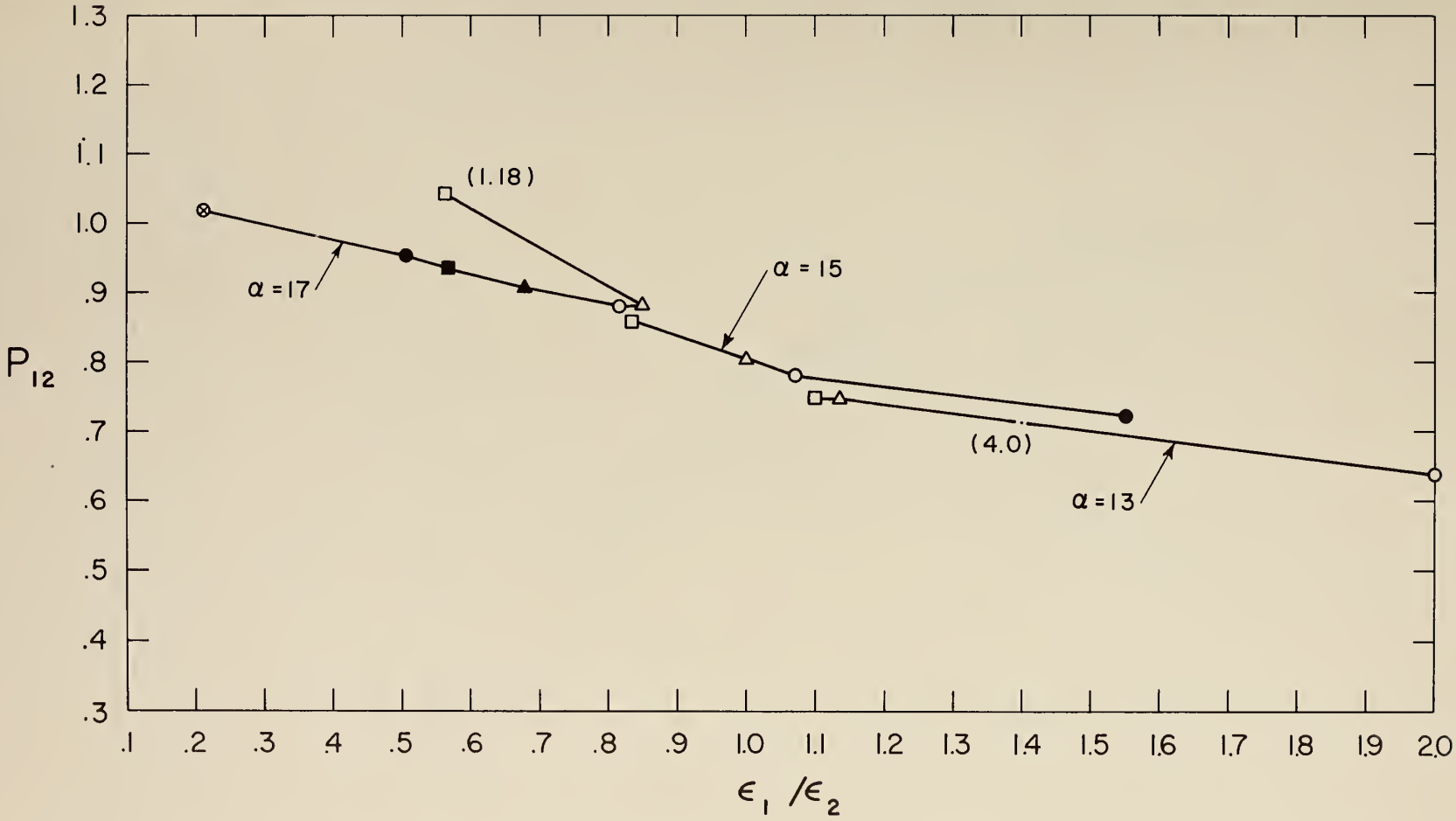

Fig. 23. ε ratios versus P_{12} ratios for the replacement of the diffusion coefficient calculated for the 12-6 potential function by that calculated for the exp:6 function. Unless otherwise indicated, the key to the temperatures along the curves is as in Fig. 11.

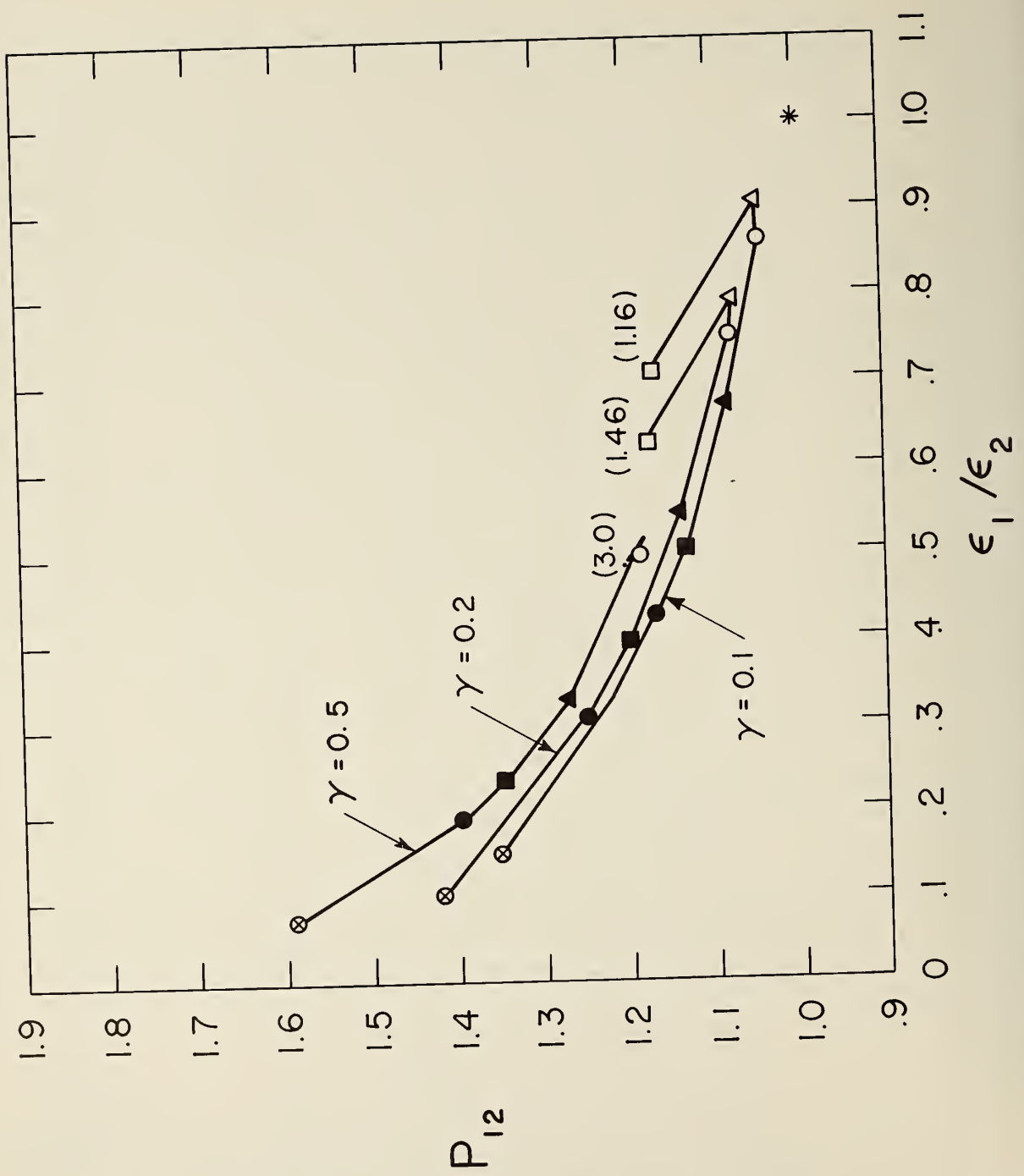

Fig. 24. ϵ ratios versus P_{12} ratios for the replacement of the diffusion coefficient calculated for the 12-6 potential function by that calculated for the Kihara function. Unless otherwise indicated, the key to the temperatures along the curves is as in Fig. 11.

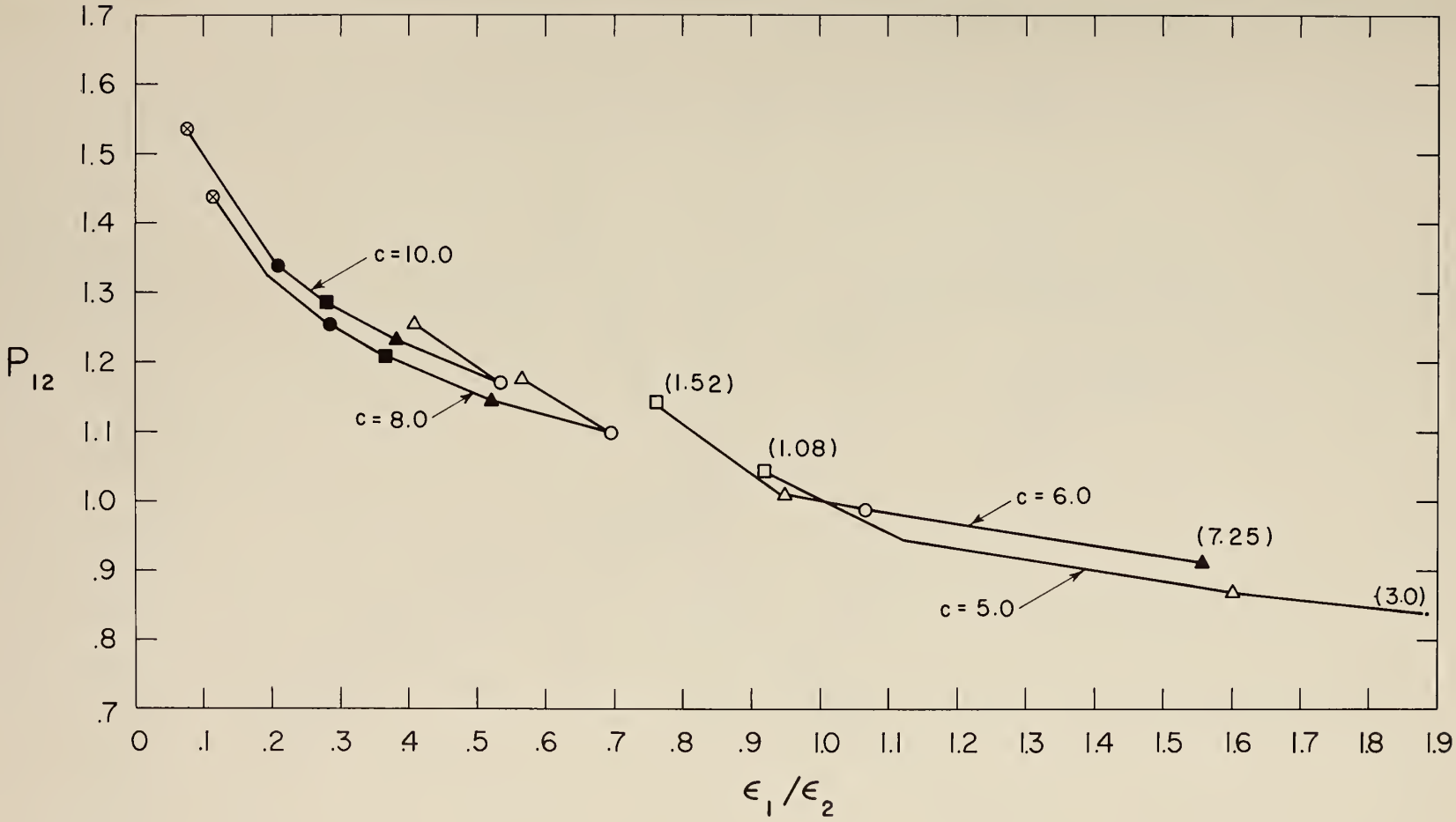

Fig. 25. ϵ ratios versus P_{12} ratios for the replacement of the diffusion coefficient calculated for the 12-6 potential function by that calculated for the Morse function. Unless otherwise indicated, the key to the temperatures along the curves is as in Fig. 11.

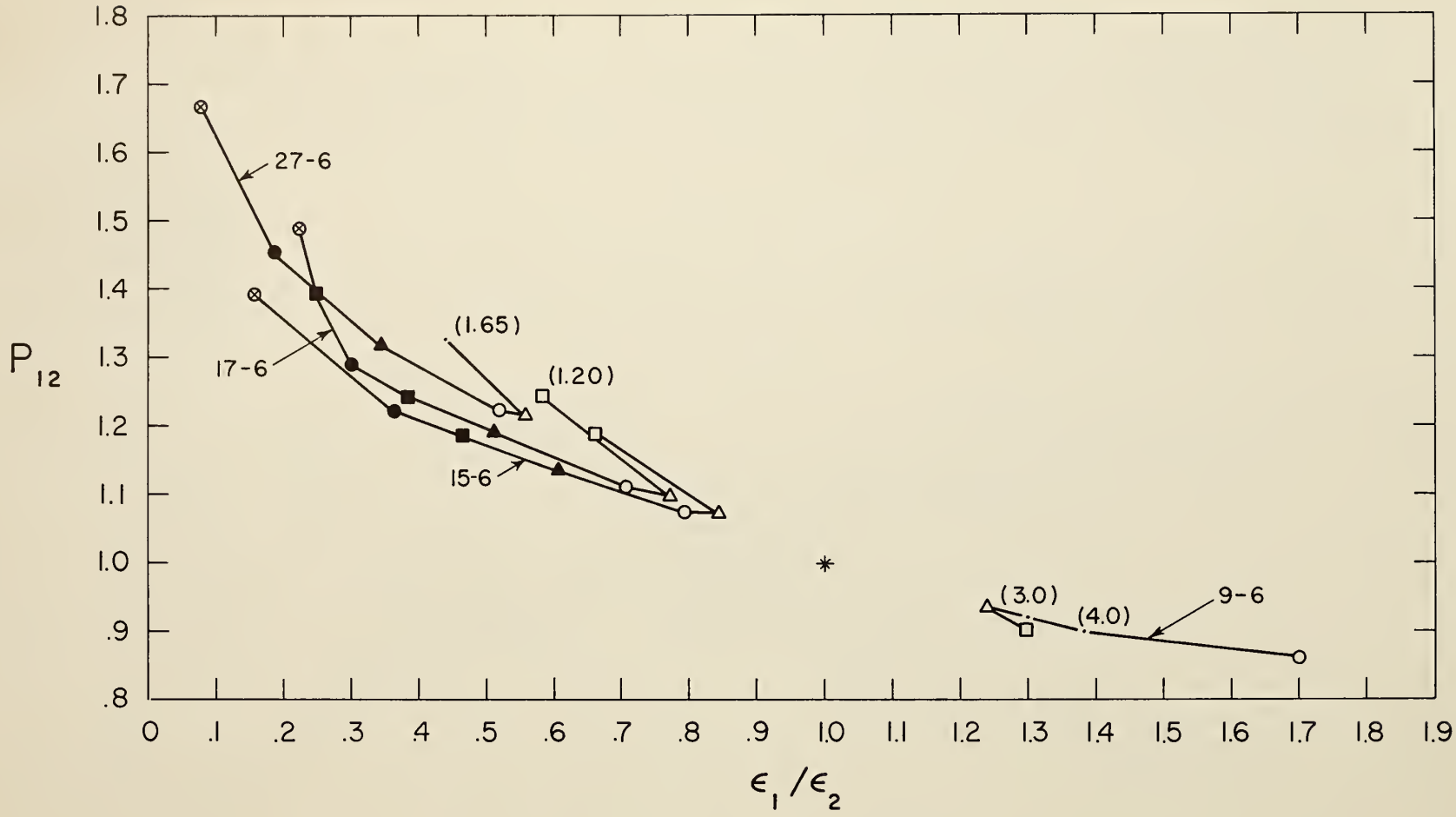

Fig. 26. ϵ ratios versus P_{12} ratios for the replacement of the diffusion coefficient calculated for the 12-6 potential function by that calculated for the Morse function.

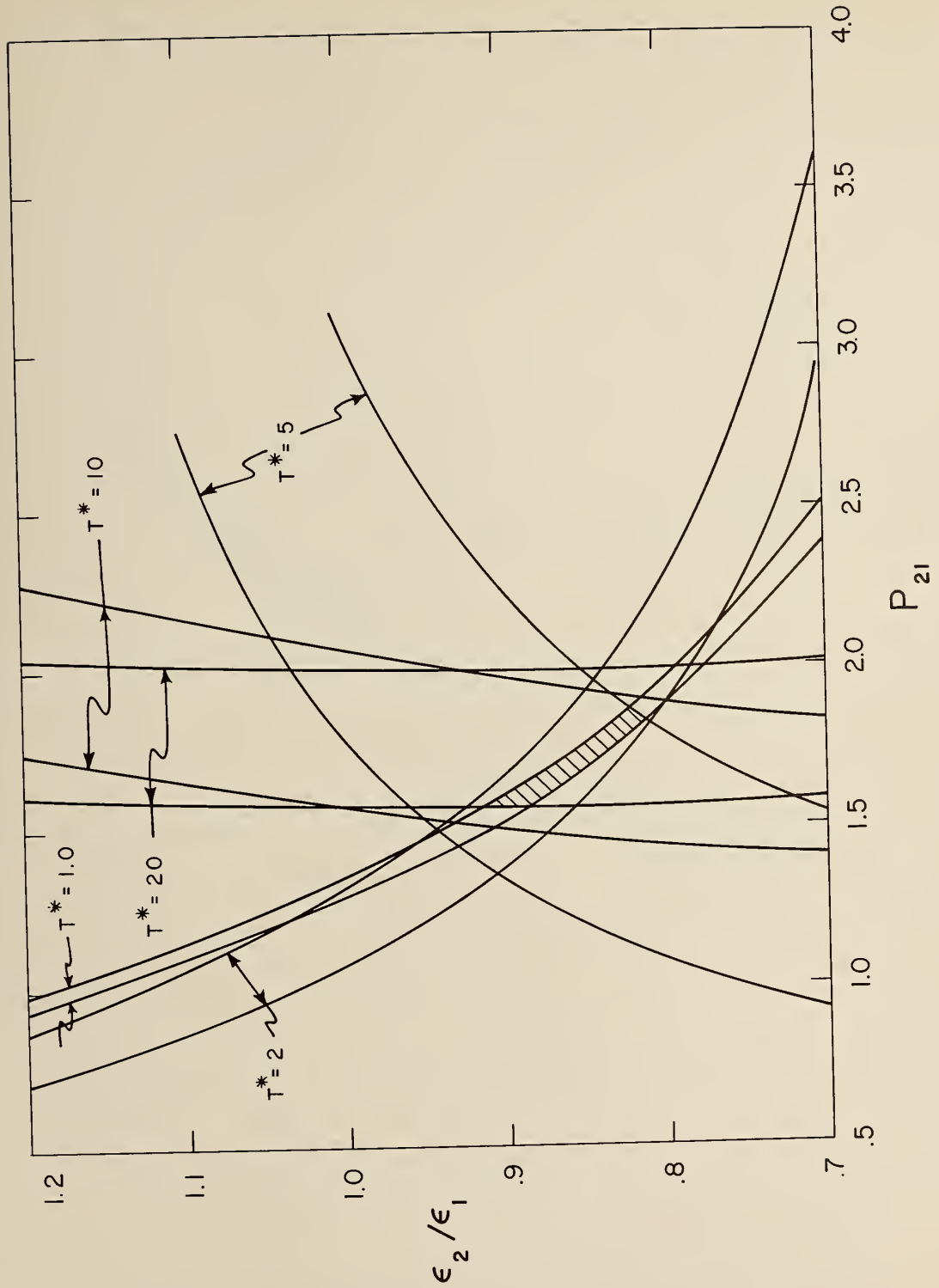

Fig. 27. The loci of potential parameter ratios which convert several values of the second virial coefficient from the 12-6 potential function to the exp:6 function for $\alpha = 12$ within an uncertainty given by 10% of the value of the second virial coefficient at $T^*_{12-6} = 2.0$. The common area of overlap is the loci of all pairs which simultaneously fit all the values within the assigned tolerance.

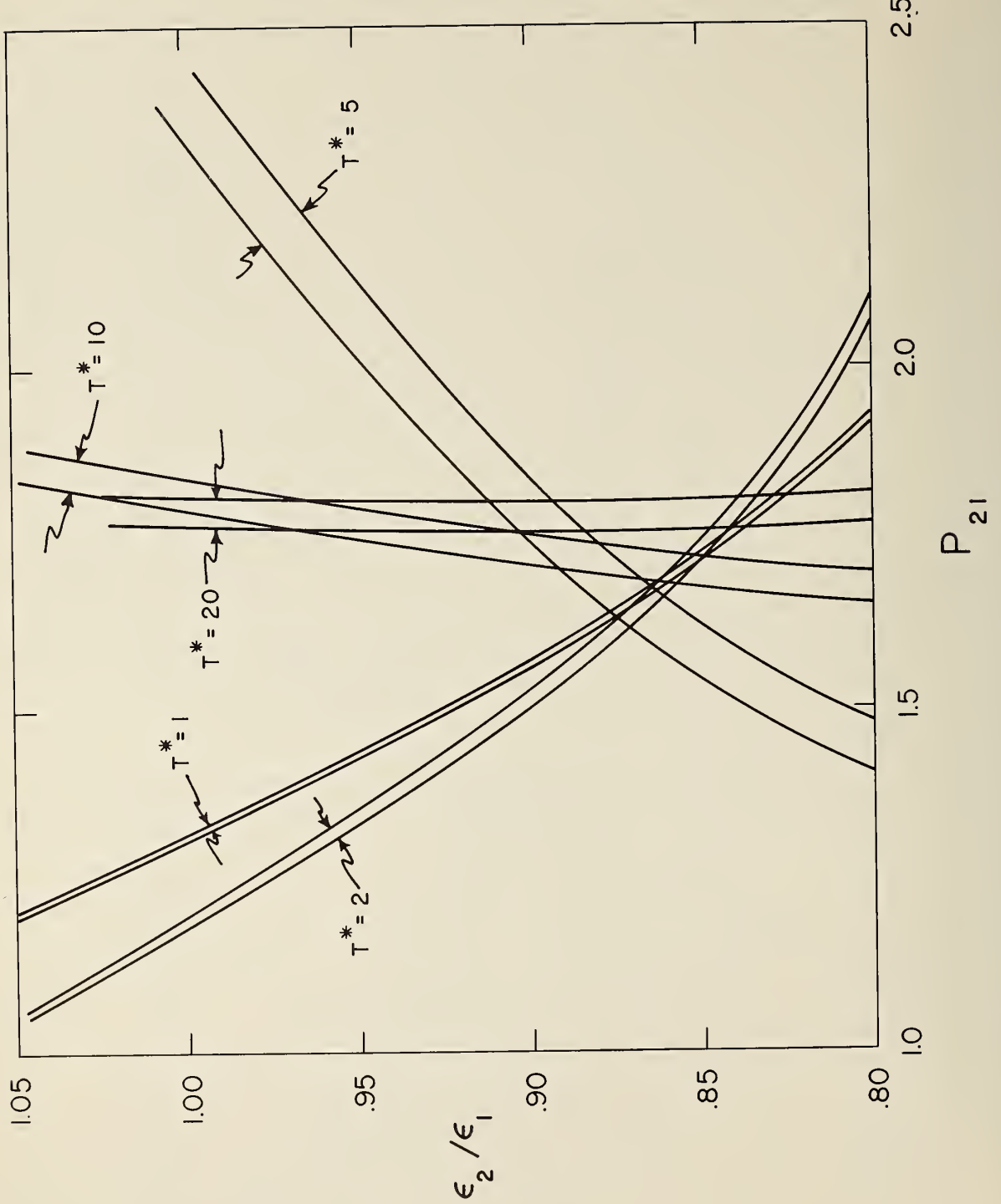

Fig. 28. The loci of potential parameter ratios which convert several values of the second virial coefficient from the 12-6 potential function to the exp:6 function for $\alpha = 12$ within an uncertainty of 1% of the value of the second virial coefficient at $T^*_{12-8} = 2.0$. The absence of a net area of overlap shows that the two potentials are not equivalent within this tolerance over the temperature range included.

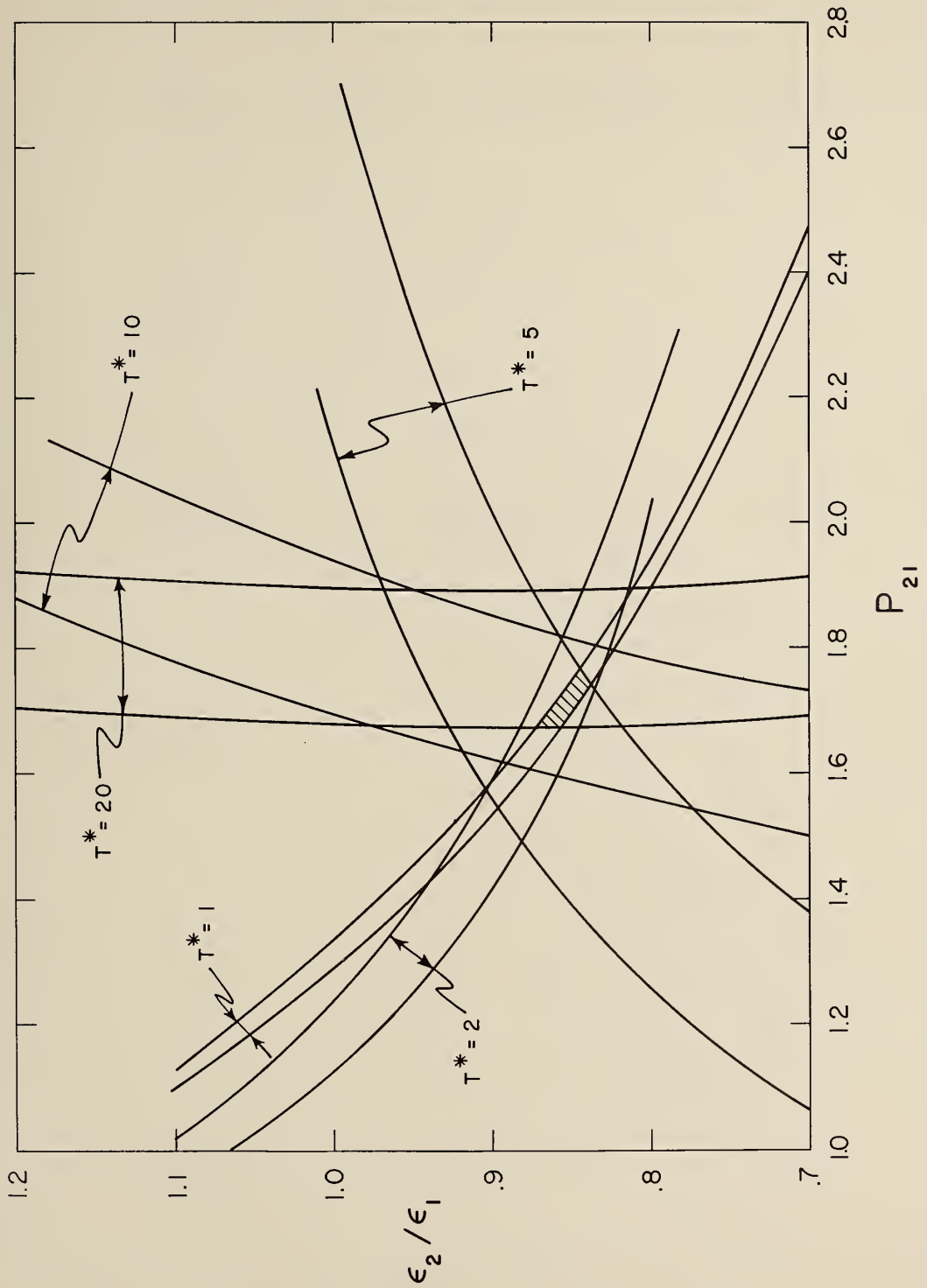

Fig. 29. The loci of potential parameter ratios which convert several values of the second virial coefficient from the 12-6 potential function to the exp:6 function for $\alpha = 12$ within an uncertainty of 5% of the value of the second virial coefficient at $T^*_{12-6} = 2.0$. The small size of the area of overlap indicates that 5% is close to the minimum uncertainty allowed for a simultaneous fit to all temperatures.

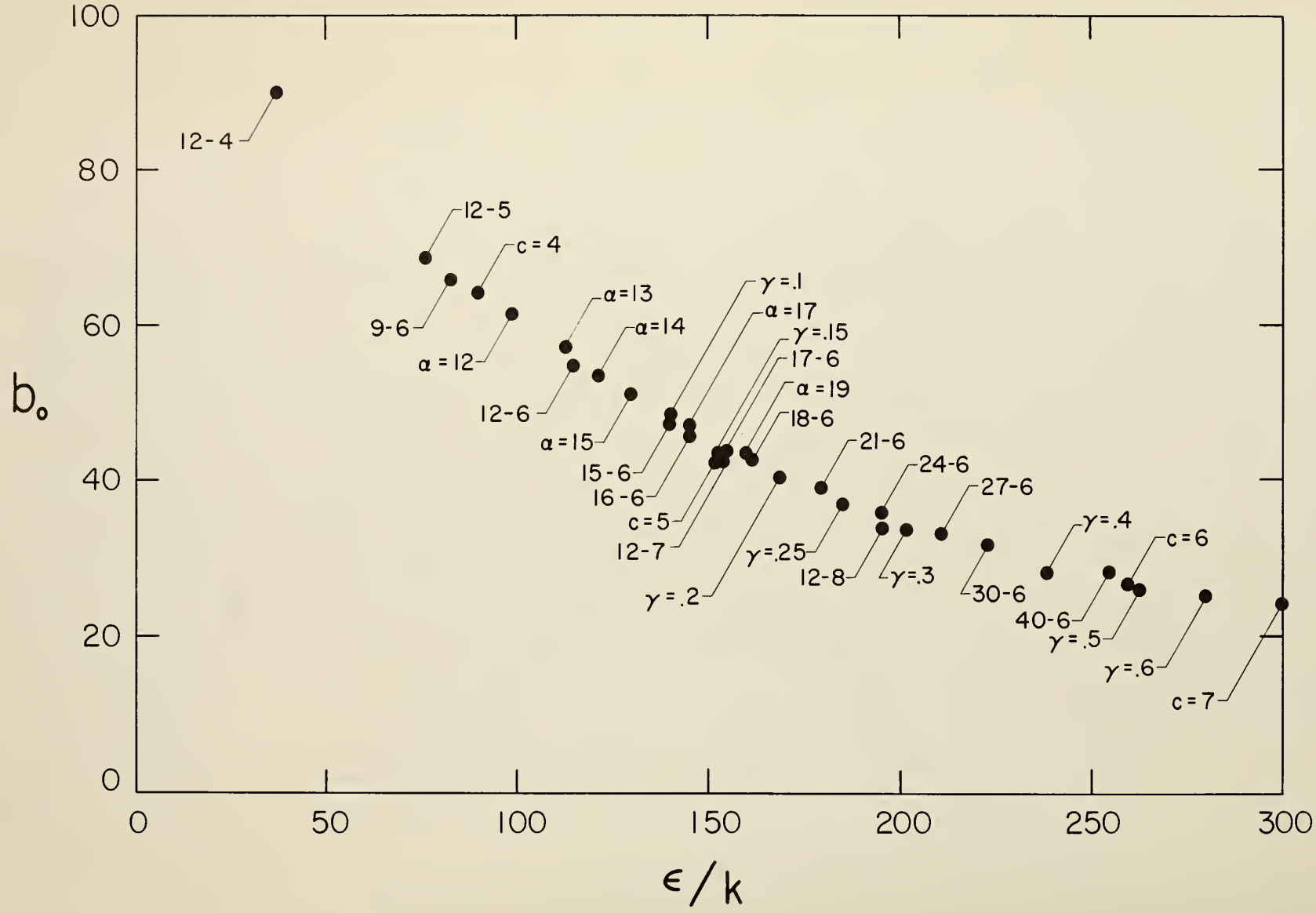

Fig. 30. ϵ/k and b_o values corresponding to the best fits of the second virial coefficients of argon [13] to those calculated for the members of five families of potential functions. Note that all families fall on essentially the same curve.

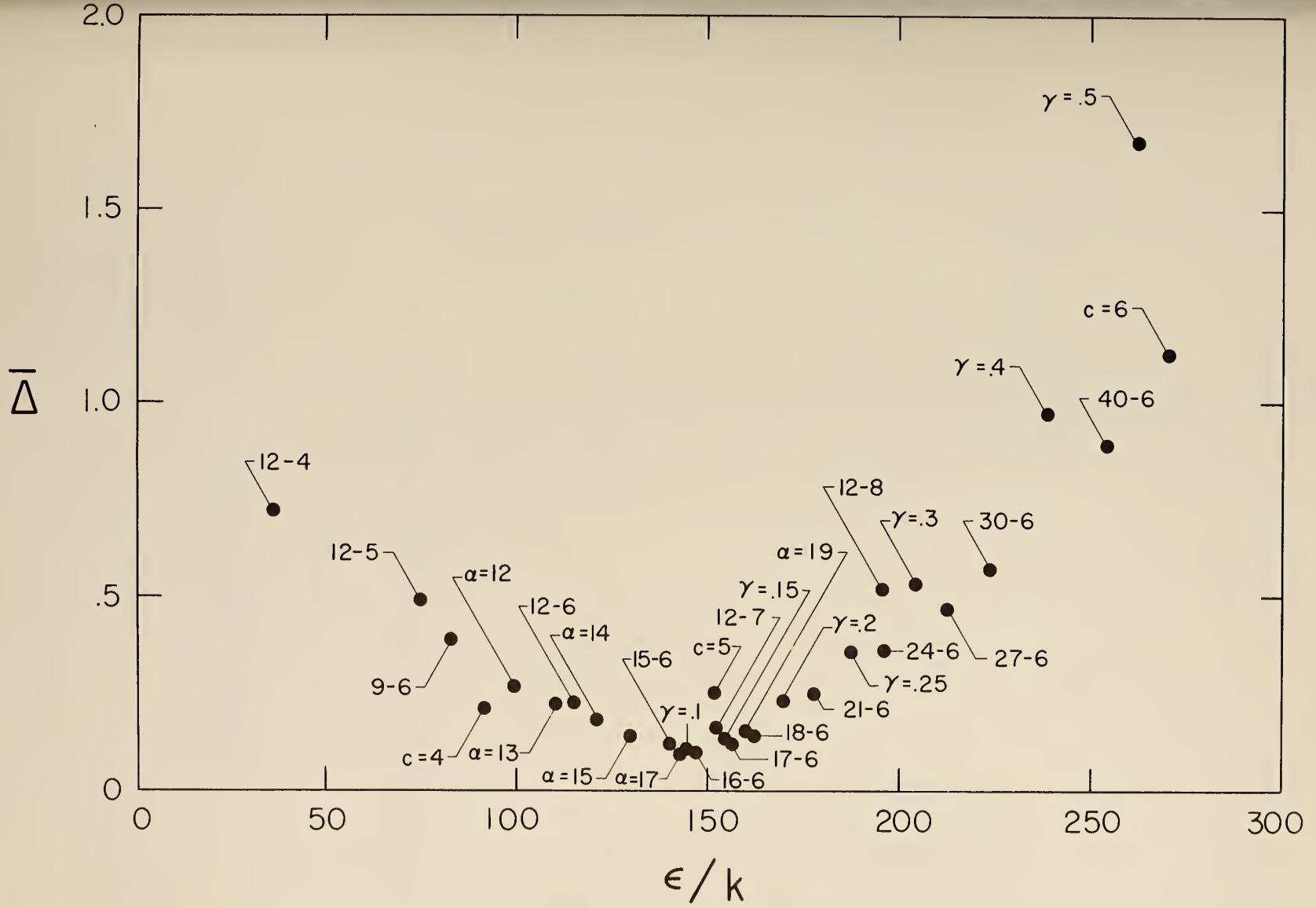

Fig. 31. Standard deviation of the best fit of the second virial coefficient of argon [13] to those calculated for the members of five families of potential functions. The similarity in behavior among the families (with the exception of the Morse function) is of particular relevance.

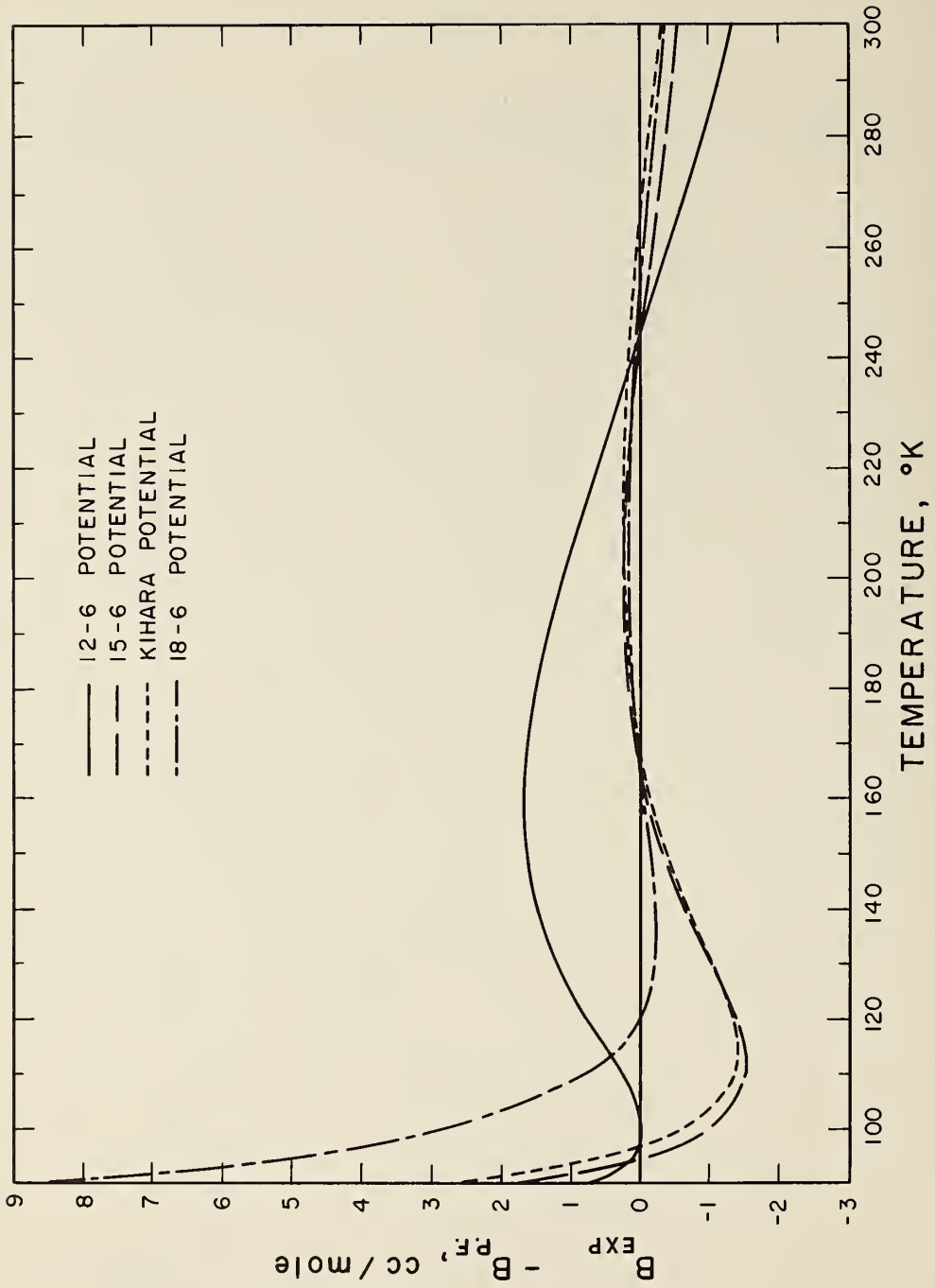

Fig. 32. The equivalence of the second virial coefficients calculated for the m = 15 member of the m-6 family and the $\gamma = 0.1$ member of the Kihara family. The experimental data are taken from [14]. Note that there is essentially a point by point equivalence over the entire temperature range. The deviation plots for the m = 12 and 18 members of the m-6 family are also included to illustrate the sensitivity of the plot. Parameters: m = 15, $\sigma = 3.37$Å, $\epsilon/k = 138.5$°K; $\gamma = 0.1$, $\sigma = 3.35$Å, $\epsilon/k = 139.8$°K.

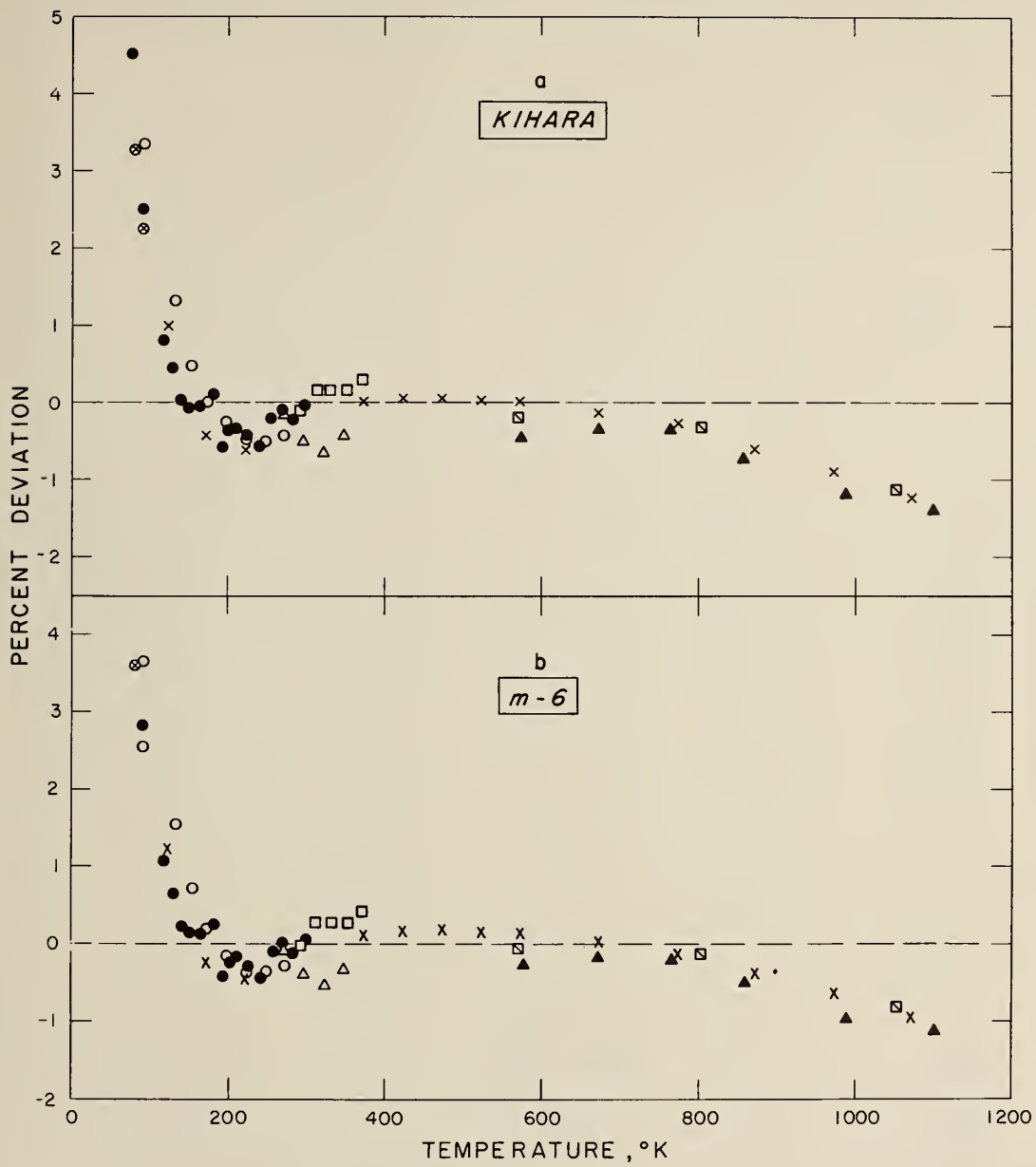

Fig. 33. Deviation curve, $\left[\frac{\eta_{exp} - \eta_{calc}}{\eta_{calc}} \right] \times 100$, for the viscosity of argon for two functions: a) The Kihara with $\gamma = 0.1$, b) The m-6 with $m = 15$. In both cases $\sigma = 3.35$ Å, $\epsilon/k = 139.8°K$. Curves (a) and (b) clearly indicate the equivalence between these two functions. Experimental data points were taken from Ref. 11, and Refs. 15 - 21.

Key:

●	[11]	▲	[17]	□	[20]
△	[15]	⧅	[18]	×	[21]
⊗	[16]	○	[19]		

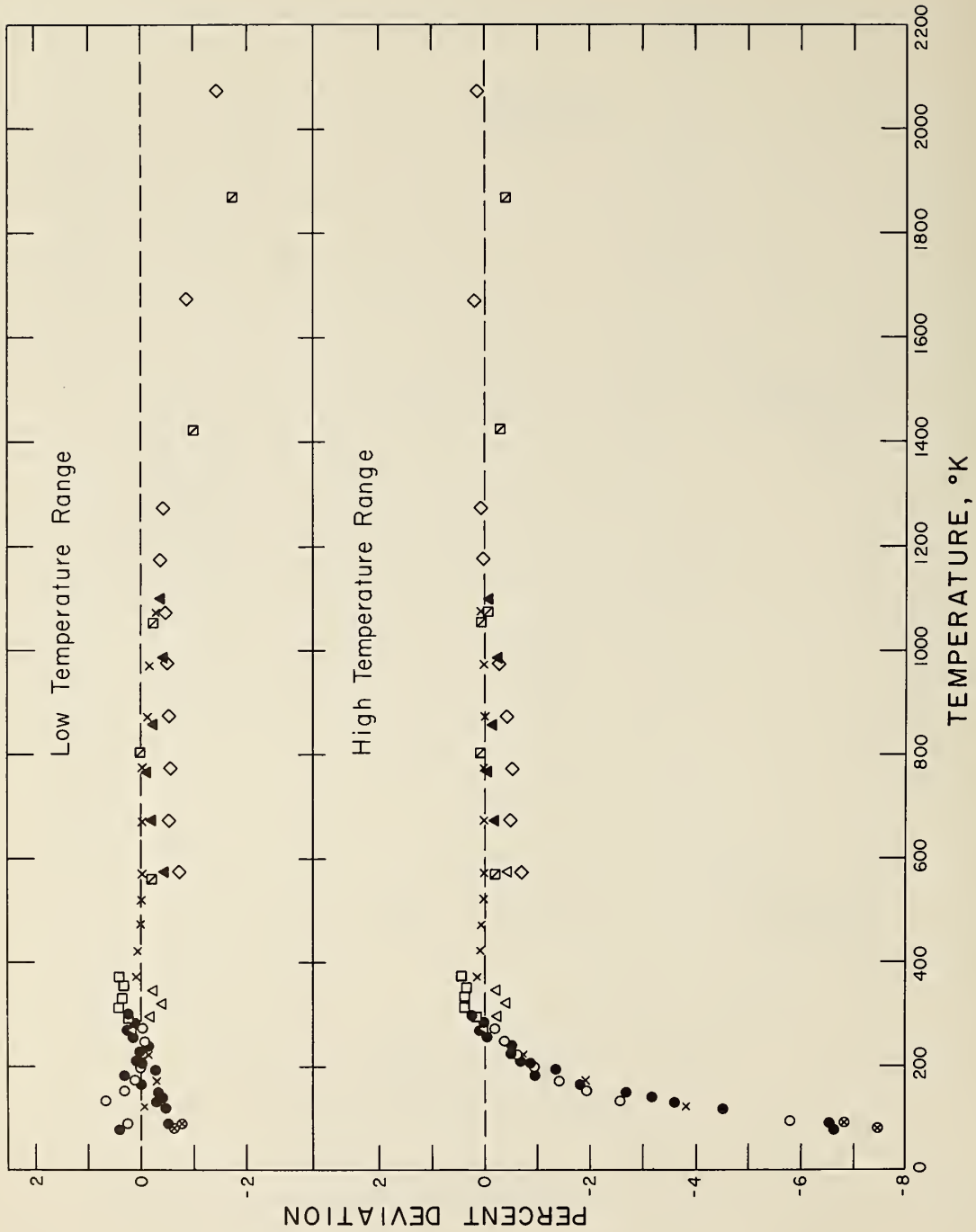

Fig. 34. Deviation curves for argon with the parameter values of Table III. The key for the data is given in Fig. 33 except for the addition of ◇ [23]. Note that the high temperature points are not fit properly if the potential appropriate to the low temperature data is used [curve (a)] and that the low temperature points are very poorly fit when the potential appropriate to the high temperature data is used [curve (b)]. The fact that the intermediate temperature points, 250°K < T < 1000°K (i.e., $2.0 < T^*_{12-6} < 8.0$), are properly fit in either case is of considerable importance.

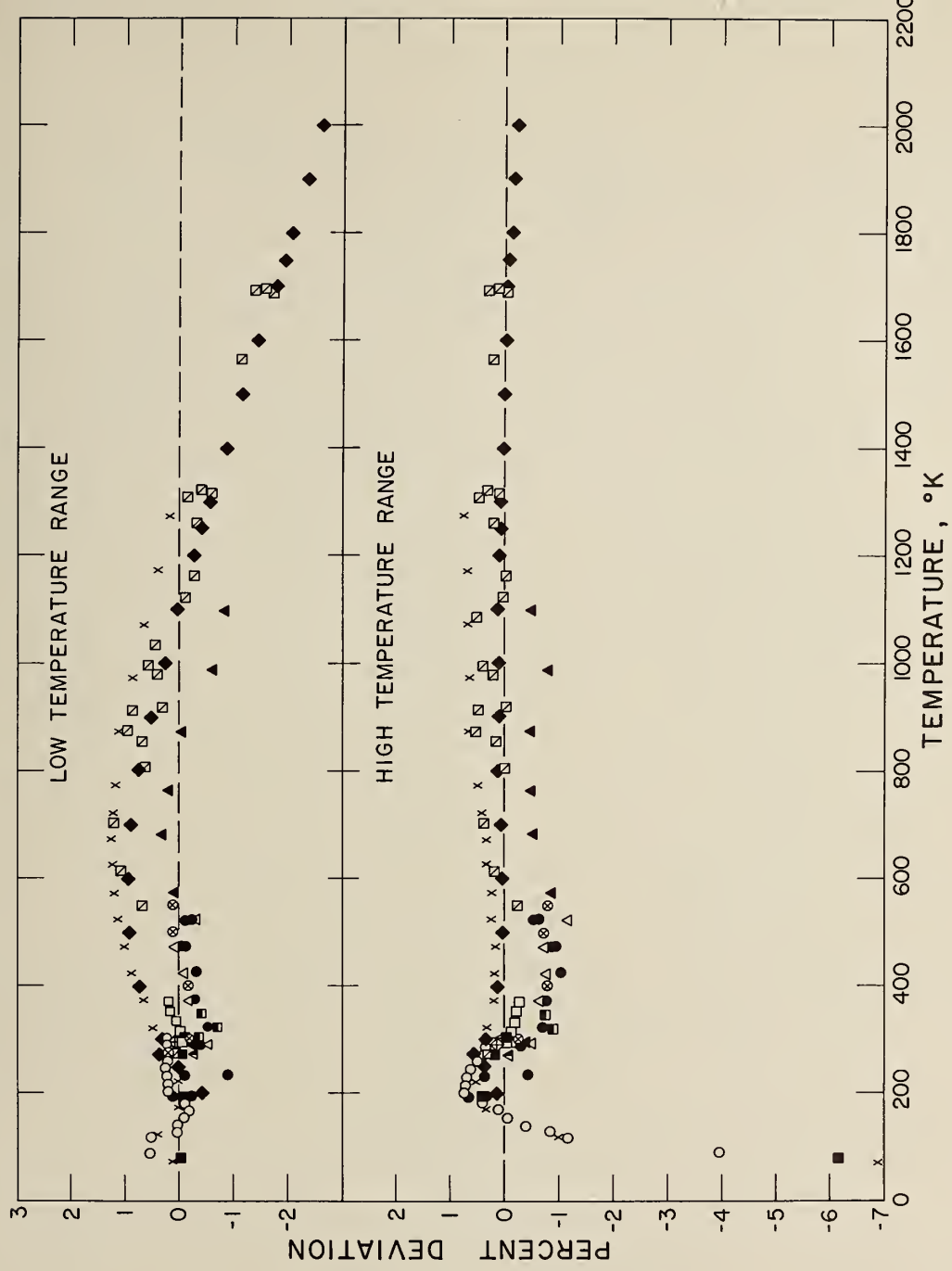

Fig. 35. Deviation curves for nitrogen in the manner of Fig. 34 for argon. The data are taken from Refs. 17, 18, 21 and 24-33. The results are essentially as for argon.

Key:

▲ [17]	● [25]	
▨ [18]	⊗ [26]	■ [30]
□ [20]	△ [27]	◆ [31]
× [21]	⊕ [28]	◭ [32]
◭ [24]	○ [29]	◨ [33]

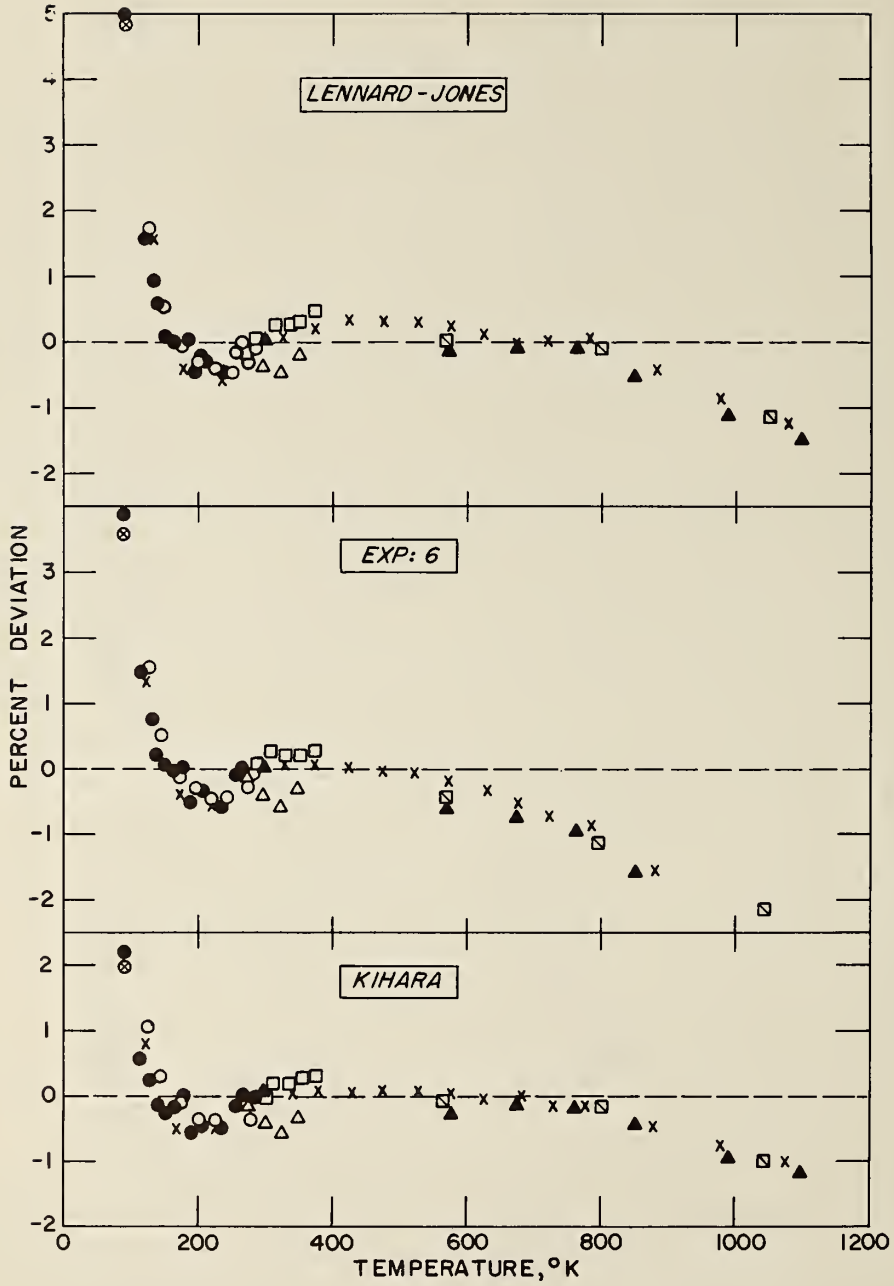

Fig. 36. Deviation plots for the viscosity coefficients for three families of function. These are taken from [34]. The key for the data is given in Fig. 33. Note that the intermediate temperature region is fit equally well by each function.

GPO 840-626

NBS TECHNICAL PUBLICATIONS

PERIODICALS

JOURNAL OF RESEARCH reports National Bureau of Standards research and development in physics, mathematics, chemistry, and engineering. Comprehensive scientific papers give complete details of the work, including laboratory data, experimental procedures, and theoretical and mathematical analyses. Illustrated with photographs, drawings, and charts.

Published in three sections, available separately:

- **Physics and Chemistry**

Papers of interest primarily to scientists working in these fields. This section covers a broad range of physical and chemical research, with major emphasis on standards of physical measurement, fundamental constants, and properties of matter. Issued six times a year. Annual subscription: Domestic, $5.00; foreign, $6.00*.

- **Mathematical Sciences**

Studies and compilations designed mainly for the mathematician and theoretical physicist. Topics in mathematical statistics, theory of experiment design, numerical analysis, theoretical physics and chemistry, logical design and programming of computers and computer systems. Short numerical tables. Issued quarterly. Annual subscription: Domestic, $2.25; foreign, $2.75*.

- **Engineering and Instrumentation**

Reporting results of interest chiefly to the engineer and the applied scientist. This section includes many of the new developments in instrumentation resulting from the Bureau's work in physical measurement, data processing, and development of test methods. It will also cover some of the work in acoustics, applied mechanics, building research, and cryogenic engineering. Issued quarterly. Annual subscription: Domestic, $2.75; foreign, $3.50*.

TECHNICAL NEWS BULLETIN

The best single source of information concerning the Bureau's research, developmental, cooperative and publication activities, this monthly publication is designed for the industry-oriented individual whose daily work involves intimate contact with science and technology—*for engineers, chemists, physicists, research managers, product-development managers, and company executives.* Annual subscription: Domestic, $1.50; foreign, $2.25*.

*Difference in price is due to extra cost of foreign mailing.

NONPERIODICALS

Applied Mathematics Series. Mathematical tables, manuals, and studies.

Building Science Series. Research results, test methods, and performance criteria of building materials, components, systems, and structures.

Handbooks. Recommended codes of engineering and industrial practice (including safety codes) developed in cooperation with interested industries, professional organizations, and regulatory bodies.

Special Publications. Proceedings of NBS conferences, bibliographies, annual reports, wall charts, pamphlets, etc.

Monographs. Major contributions to the technical literature on various subjects related to the Bureau's scientific and technical activities.

National Standard Reference Data Series. NSRDS provides quantitative data on the physical and chemical properties of materials, compiled from the world's literature and critically evaluated.

Product Standards. Provide requirements for sizes, types, quality and methods for testing various industrial products. These standards are developed cooperatively with interested Government and industry groups and provide the basis for common understanding of product characteristics for both buyers and sellers. Their use is voluntary.

Technical Notes. This series consists of communications and reports (covering both other agency and NBS-sponsored work) of limited or transitory interest.

CLEARINGHOUSE

The Clearinghouse for Federal Scientific and Technical Information, operated by NBS, supplies unclassified information related to Government-generated science and technology in defense, space, atomic energy, and other national programs. For further information on Clearinghouse services, write:

Clearinghouse
U.S. Department of Commerce
Springfield, Virginia 22151

Order NBS publications from:
Superintendent of Documents
Government Printing Office
Washington, D.C. 20402

U.S. DEPARTMENT OF COMMERCE
WASHINGTON, D.C. 20230

OFFICIAL BUSINESS

POSTAGE AND FEES PAID
U.S. DEPARTMENT OF COMMERCE